

ULTRAFILTRATION OF BLOOD BETWEEN TWO
PARALLEL MEMBRANES

A THESIS

Presented to

The Faculty of the Graduate Division

by

Nan Wei

In Partial Fulfillment
of the Requirements for the Degree
Doctor of Philosophy
in the School of Chemical Engineering

Georgia Institute of Technology

June, 1976

ULTRAFILTRATION OF BLOOD BETWEEN TWO
PARALLEL MEMBRANES

Approved:

Henderson C. Ward, Chairman

Homer V. Grubb

Joseph J. Smrefar

Date approved by Chairman: 6/2/76

ACKNOWLEDGMENTS

The author wishes to express his sincere appreciation for the constant encouragement and guidance of his thesis advisor, Dr. Henderson C. Ward, whose advice and help have made this work possible. He is also grateful to Dr. Homer V. Grubb and Dr. Joseph J. Smrekar for serving on the Reading Committee and for their many constructive criticisms and valuable suggestions.

Particular appreciation is expressed to Dr. G. Leon Bridger for his advice and guidance in pilot plant research projects and for providing many years of financial support. The fellowship provided by Allied Chemical Corporation during the winter and spring quarters of 1976 is gratefully acknowledged.

Appreciation is also extended to Dr. Waldemar T. Ziegler for his valuable guidance and advice.

Special appreciation is also due to Drs. Elbert P. Tuttle and Edwin J. Macon of Grady Memorial Hospital, for their advice and guidance in the medical aspect of this work.

The help and instructions of the Georgia Institute of Technology Rich Electronic Computer Center is acknowledged.

Sincere appreciation is acknowledged for the friendly encouragement and support of many friends, especially Dr. J. F. Shiau, Dr. T. Y. Fang and Dr. M. G. Klett.

The author wishes to thank his parents for their many years of patience and encouragement.

TABLE OF CONTENTS

	Page
ACKNOWLEDGMENTS	ii
LIST OF TABLES	v
LIST OF ILLUSTRATIONS	vi
NOMENCLATURE	x
SUMMARY	xi
Chapter	
I. INTRODUCTION	1
Artificial Kidneys and the Significance of this Study Rheology of Blood Two-Dimensional Blood Flow	
II. MATHEMATICAL DESCRIPTION OF THE PROBLEM	5
Statement of the Problem Development of Casson's Model for Two- Dimensional Flow Fluid Flow Equations and Boundary Conditions Dimensionless Fluid Flow Equations and Boundary Conditions Equations in Terms of Dimensionless Stream Functions and Stresses	
III. NUMERICAL TECHNIQUE	21
Mathematical Derivation of Finite Difference Differentiation and Graphical Interpretations System of Grid Points and Two-Dimensional Partial Derivatives Finite Difference Flow Equations Computational Procedures	
IV. RESULTS AND DISCUSSION	39
Comparison of Iterative and Analytical Results in Limiting Cases	

Chapter	Page
Effect of Finite Yield Stress (τ_0) Effect of Wall Suction Rate (R_w) ⁰ Some Mutually Related Variables	
V. CONCLUSIONS AND RECOMMENDATIONS	107
APPENDICES	
A. CASSONIAN FLOW BETWEEN TWO PARALLEL NON-PERMEABLE PLATES	110
B. COMPUTER PROGRAM	114
BIBLIOGRAPHY	139
VITA	142

LIST OF TABLES

Table	Page
1. Values of Variables Studied in Cassonian Flow	41
2. Values of Variables Studied in Newtonian Flow	42
3. Comparison of Iterative and Analytical Values of ψ Case 1: Reduced to Newtonian Flow	43
4. Comparison of Iterative and Analytical Values of ψ Case 2: Reduced to One-Dimensional Flow	45

LIST OF ILLUSTRATIONS

Figure	Page
1. Schematic Drawing of the System	6
2. Graphical Interpretation of Finite Difference Differentiation	23
3. System of Grid Points	26
4. Newton-Raphson Iteration	33
5. Newton-Raphson Iteration Fails to Converge	34
6. The Method of False Position	35
7. Contours of Stream Function (ψ) and Shear Stress (T_{yx}) Cassonian: $H = 0.01$; $\tau_0 = 0$; $R_x = 1.0$; $R_y = 0.001$	47
7a. Contours of Stream Function (ψ) and Shear Stress (T_{yx}) Newtonian: $H = 0.01$; $R_x = 1.0$; $R_y = 0.001$	48
8. Contours of Stream Function (ψ) and Shear Stress (T_{yx}) Cassonian: $H = 0.01$; $\tau_0 = 0.01$; $R_x = 1.0$; $R_y = 0.001$	49
9. Contours of Stream Function (ψ) and Shear Stress (T_{yx}) Cassonian: $H = 0.01$; $\tau_0 = 0.04$; $R_x = 1.0$; $R_y = 0.001$	50
10. Contours of Stream Function (ψ) and Shear Stress (T_{yx}) Cassonian: $H = 0.01$; $\tau_0 = 0.08$; $R_x = 1.0$; $R_y = 0.001$	51
11. Contours of Stream Function (ψ) and Shear Stress (T_{yx}) Cassonian: $H = 0.01$; $\tau_0 = 0.2$; $R_x = 1.0$; $R_y = 0.001$	52
12. Stream Function (ψ) and Shear Stress (T_{yx}) vs Y Cassonian: $H = 0.01$; $\tau_0 = 0$; $R_x = 1.0$; $R_y = 0.001$	53
13. Stream Function (ψ) and Shear Stress (T_{yx}) vs Y Cassonian: $H = 0.01$; $\tau_0 = 0.01$; $R_x = 1.0$; $R_y = 0.001$	54
14. Stream Function (ψ) and Shear Stress (T_{yx}) vs Y Cassonian: $H = 0.01$; $\tau_0 = 0.04$; $R_x = 1.0$; $R_y = 0.001$	55
15. Stream Function (ψ) and Shear Stress (T_{yx}) vs Y Cassonian: $H = 0.01$; $\tau_0 = 0.08$; $R_x = 1.0$; $R_y = 0.001$	56

	Page
16. Stream Function (ψ) and Shear Stress (T_{yx}) vs Y Cassonian: $H = 0.01$; $\tau_0 = 0.2$; $R_x = 1.0$; $R_y = 0.001$. . .	57
17. Velocity Profiles (V_x) Cassonian: $H = 0.01$; $\tau_0 = 0$; $R_x = 1.0$; $R_y = 0.001$	59
18. Velocity Profiles (V_x) Cassonian: $H = 0.01$; $\tau_0 = 0.01$; $R_x = 1.0$; $R_y = 0.001$. .	60
19. Velocity Profiles (V_x) Cassonian: $H = 0.01$; $\tau_0 = 0.04$; $R_x = 1.0$; $R_y = 0.001$. .	61
20. Velocity Profiles (V_x) Cassonian: $H = 0.01$; $\tau_0 = 0.08$; $R_x = 1.0$; $R_y = 0.001$. .	62
21. Velocity Profiles (V_x) Cassonian: $H = 0.01$; $\tau_0 = 0.2$; $R_x = 1.0$; $R_y = 0.01$. . .	63
22. Pressure on the Central Plane vs X $H = 0.01$; $R_x = 0.001$; $R_y = 0.001$	64
23. Contours of Stream Function (ψ) and Shear Stress (T_{yx}) Cassonian: $H = 0.01$; $\tau_0 = 0.04$; $R_x = 1.0$; $R_y = 0$	65
24. Contours of Stream Function (ψ) and Shear Stress (T_{yx}) Cassonian: $H = 0.01$; $\tau_0 = 0.04$; $R_x = 1.0$; $R_y = 0.00025$. .	66
25. Contours of Stream Function (ψ) and Shear Stress (T_{yx}) Cassonian: $H = 0.01$; $\tau_0 = 0.04$; $R_x = 1.0$; $R_y = 0.0005$. .	67
26. Contours of Stream Function (ψ) and Shear Stress (T_{yx}) Cassonian: $H = 0.01$; $\tau_0 = 0.04$; $R_x = 1.0$; $R_y = 0.00075$	68
27. Contours of Stream Function (ψ) and Shear Stress (T_{yx}) Cassonian: $H = 0.01$; $\tau_0 = 0.04$; $R_x = 1.0$; $R_y = 0.001$	69
28. Contours of Stream Function (ψ) and Shear Stress (T_{yx}) Cassonian: $H = 0.01$; $\tau_0 = 0.04$; $R_x = 1.0$; $R_y = 0.0015$. .	70
29. Contours of Stream Function (ψ) and Shear Stress (T_{yx}) Cassonian: $H = 0.01$; $\tau_0 = 0.04$; $R_x = 1.0$; $R_y = 0.002$	71
30. Stream Function (ψ) and Shear Stress (T_{yx}) vs Y Cassonian: $H = 0.01$; $\tau_0 = 0.04$; $R_x = 1.0$; $R_y = 0$	73
31. Stream Function (ψ) and Shear Stress (T_{yx}) vs Y Cassonian: $H = 0.01$; $\tau_0 = 0.04$; $R_x = 1.0$; $R_y = 0.005$. .	74

	Page
32. Stream Function (ψ) and Shear Stress (T_{yx}) vs Y Cassonian: $H = 0.01$; $\tau_0 = 0.04$; $R_x = 1.0$; $R_y = 0.001$. . .	75
33. Stream Function (ψ) and Shear Stress (T_{yx}) vs Y Cassonian: $H = 0.01$; $\tau_0 = 0.04$; $R_x = 1.0$; $R_y = 0.002$. . .	76
34. Stream Function (ψ) and Shear Stress (T_{yx}) vs Y Newtonian: $H = 0.01$; $R_x = 1.0$; $R_y = 0.$	77
35. Stream Function (ψ) and Shear Stress (T_{yx}) vs Y Newtonian: $H = 0.01$; $R_x = 1.0$; $R_y = 0.0005$	78
36. Stream Function (ψ) and Shear Stress (T_{yx}) vs Y Newtonian: $H = 0.01$; $R_x = 1.0$; $R_y = 0.001$	79
37. Stream Function (ψ) and Shear Stress (T_{yx}) vs Y Newtonian: $H = 0.01$; $R_x = 1.0$; $R_y = 0.002$	80
38. Velocity Profiles (V_x) Cassonian: $H = 0.01$; $\tau_0 = 0.04$; $R_x = 1.0$; $R_y = 0$	81
39. Velocity Profiles (V_x) Cassonian: $H = 0.01$; $\tau_0 = 0.04$; $R_x = 1.0$; $R_y = 0.0005$. .	82
40. Velocity Profiles (V_x) Cassonian: $H = 0.01$; $\tau_0 = 0.04$; $R_x = 1.0$; $R_y = 0.001$. . .	83
41. Velocity Profiles (V_x) Cassonian: $H = 0.01$; $\tau_0 = 0.04$; $R_x = 1.0$; $R_y = 0.002$. . .	84
42. Velocity Profiles (V_y) Cassonian: $H = 0.01$; $\tau_0 = 0.04$; $R_x = 1.0$; $R_y = 0.0005$. .	85
43. Velocity Profiles (V_y) Cassonian: $H = 0.01$; $\tau_0 = 0.04$; $R_x = 1.0$; $R_y = 0.001$. . .	86
44. Velocity Profiles (V_y) Cassonian: $H = 0.01$; $\tau_0 = 0.04$; $R_x = 1.0$; $R_y = 0.002$. . .	87
45. Pressure on the Central Plane vs X Cassonian: $H = 0.01$; $\tau_0 = 0.04$; $R_x = 1.0$	88
46. Pressure on the Central Plane vs X Comparison: $H = 0.01$; $\tau_0 = 0.04$; $R_x = 1.0$	90
47. Stream Function (ψ) and Shear Stress (T_{yx}) vs Y Newtonian: $H = 0.01$; $R_x = 1.0$; $R_y = 0.001$	92

	Page
48. Stream Function (ψ) and Shear Stress (T_{yx}) vs Y Newtonian: $H = 0.05$; $R_x = 1.0$; $R_y = 0.001$	93
49. Stream Function (ψ) and Shear Stress (T_{yx}) vs Y Newtonian: $H = 0.005$; $R_x = 1.0$; $R_y = 0.001$	94
50. Stream Function (ψ) and Shear Stress (T_{yx}) vs Y Newtonian: $H = 0.01$; $R_x = 25$; $R_y = 0.025$	95
51. Stream Function (ψ) and Shear Stress (T_{yx})(R_x) vs Y Newtonian: $H = 0.01$; $R_x = 25$; $R_y = 0.025$	96
52. Stream Function (ψ) and Shear Stress (T_{yx}) vs Y Newtonian: $H = 0.01$; $R_x = 0.25$; $R_y = 0.00025$	97
53. Stream Function (ψ) and Shear Stress (T_{yx})(R_x) vs Y Newtonian: $H = 0.01$; $R_x = 0.25$; $R_y = 0.00025$	98
54. Stream Function (ψ) and Shear Stress (T_{yx}) vs Y Cassonian: $H = 0.05$; $\tau_0 = 0.0016$; $R_x = 1.0$; $R_y = 0.001$	100
55. Stream Function (ψ) and Shear Stress (T_{yx}) vs Y Cassonian: $H = 0.005$; $\tau_0 = 0.16$; $R_x = 1.0$; $R_y = 0.001$	101
56. Stream Function (ψ) and Shear Stress (T_{yx}) vs Y Cassonian: $H = 0.01$; $\tau_0 = 1.0$; $R_x = 25$; $R_y = 0.025$	102
57. Stream Function (ψ) and Shear Stress (T_{yx})(R_x) vs Y Cassonian: $H = 0.01$; $\tau_0 = 1.0$; $R_x = 25$; $R_y = 0.025$	103
58. Stream Function (ψ) and Shear Stress (T_{yx}) vs Y Cassonian: $H = 0.01$; $\tau_0 = 0.01$; $R_x = 0.25$; $R_y = 0.00025$	104
59. Stream Function (ψ) and Shear Stress (T_{yx})(R_x) vs Y Cassonian: $H = 0.01$; $\tau_0 = 0.01$; $R_x = 0.25$; $R_y = 0.00025$	105

NOMENCLATURE

F	a function of ψ defined in equation (3-19)
F'	$\partial F / \partial \psi$
g	gravitational acceleration, cm/sec^2
h	grid step size in x-direction, cm
H	half-distance between the two parallel membranes, cm
I	positive integer in x-direction
J	positive integer in y-direction
k	1. grid step size in y-direction, cm. 2. square root of ultimate viscosity coefficient, $(\text{gm}/\text{cm-sec})^{1/2}$
K	$k/\rho U_0^2$, dimensionless viscosity coefficient
L	length of the flow channel, cm
p	pressure of fluid, dyne/cm^2
P_f	pressure factor defined in equation (A-6), dyne/cm^3
P	dimensionless pressure
P_f	dimensionless pressure factor
Q_0	entrance volumetric flow rate, cm^3/sec
R_x	entrance Reynolds number, $4U_0 H \rho / k^2$
R_y	wall Reynolds number, $v_0 H \rho / k^2$
s	step size ratio, h/k
T_0	dimensionless yield stress of fluid
T_{yx}, T_{xx}, T_{yy}	dimensionless stress components

U_0	entrance average velocity, cm/sec
v_x	velocity component in x-direction, cm/sec
v_y	velocity component in y-direction, cm/sec
v_0	wall suction velocity, cm/sec
V_0	dimensionless wall suction velocity
V_x	dimensionless velocity component in x-direction
V_y	dimensionless velocity component in y-direction
W	width of the flow channel, cm
x	distance in x-direction, cm
X	dimensionless distance in x-direction
y	distance in y-direction, cm
Y	dimensionless distance in y-direction
α	relaxation factor in stream-function equation
β	relaxation factor in shear-stress equation
γ	shear-stress correlation factor defined in equation (2-35)
μ	Newtonian viscosity coefficient, g/cm-sec
ρ	fluid density, gm/cm ³
τ	shear stress tensor, dyne/cm ²
τ_0	yield stress of fluid, dyne/cm ²
$\tau_{yx}, \tau_{xx}, \tau_{yy}$	stress components, dyne/cm ²
ψ	dimensionless stream function
ψ'	conventional stream function defined in equation (4-1)

Subscript

x	components in x-direction
y	components in y-direction
I	positive integer, denotes a grid point at $x = I\Delta x$
J	positive integer, denotes a grid point at $y = J\Delta y$

SUMMARY

Ultrafiltration of blood between two parallel membranes was studied in this work. The blood was considered as a non-Newtonian fluid with rheological properties that follow the Casson equation. Creeping flow, constant physical properties and constant wall suction rates were assumed.

The system was studied as a two-dimensional Cassonian flow. The well known Casson equation for one-dimensional flow was expanded into multi-dimensional flow form as a function of the second invariant of Δ , the symmetrical rate of deformation tensor. The flow equations were first reduced to dimensionless form. A dimensionless stream function and dimensionless shear stresses were defined and the flow equations were reduced to two equations in terms of these variables. Relations between the shear stress components were developed to reduce the four shear stresses to one shear stress.

The stream function equation and the shear stress equation were then rewritten with finite difference approximations for the derivative terms. A successive relaxation procedure was used to obtain numerical values of the stream function and the shear stress. The stream function equation had to be solved iteratively within each relaxation cycle.

Since there was no similar study or experimental data for comparison, the accuracy of the numerical technique used was checked in limiting cases with the results obtained from analytical solutions. The agreement of the iterative results with the analytical results were excellent.

The half distances between membranes were set at 0.005, 0.01 and 0.05 cm. The blood yield stress was taken to be the normal average value of 0.04 dyne/cm² in most cases but other values were also used to study the effect this yield stress term had on the flow. The entrance Reynolds number covered a range from 0.25 to 25. The wall Reynolds number covered a range from zero to 0.025.

It was found that increasing yield stress values caused an increase in shear stress and pressure drop. With wall suction, the shear stress of the fluid and the pressure drop became smaller than those without wall suction. Larger suction rates resulted in smaller shear stress and less pressure drop.

Some relationships between the variables studied were developed to help predict the flow behavior at other flow conditions from the results of known flow conditions.

CHAPTER I

INTRODUCTION

Artificial Kidneys and the Significance of this Study

It has been reported [1] that about 20% of the up to 50,000 people who die each year from kidney disease are suited to artificial kidney treatment or kidney transplantation. The artificial kidney is capable of postponing death from irreversible kidney failure for a few years or even indefinitely in some cases. The artificial kidney is also used routinely to sustain a patient who is waiting for a suitable donor kidney to become available for transplantation.

Ever since Kolff's [2] pioneering treatment in 1943 of the first uremic patient by means of hemodialysis, use of the artificial kidney has increased steadily for the correction of biochemical abnormalities associated with endogenous or exogenous intoxication. Scribner [3] in 1960 demonstrated a permanent cannulation technique which allowed relatively easy access to the blood stream for connection to the artificial kidney on a regular basis. In the following years, the attention of researchers turned to the task of optimizing and simplifying the equipment to increase its reliability and to reduce capital and operating costs. Especially notable were the engineering improvement efforts of Babb and Grimsrud [4], Esmond [5], Stewart [6] and Oja [7].

Although significant improvements have been made by the above-mentioned investigators, the basic means of mass transfer of all the

present day clinical units is still dialysis, which requires a large quantity of specially formulated dialysate and a precise delivery system to carefully control the flow condition of the dialysate. Regardless of how small and efficient the blood-dialysis fluid transfer unit is made, there still remains the cumbersome delivery system requirements of pumping, conductivity control, heat exchange, pressure control, precise stream mixing and safety. Therefore, the patients are literally immobilized for treatment two or three times a week. A portable or wearable treatment unit which can be moved along by the patient is much desired. The only way to achieve this kind of portability is to eliminate the handling of the large quantity of dialysate. This requires a different concept of an artificial kidney. One such concept is the selective ultrafiltration and returning of water and perhaps some necessary electrolytes back to the blood stream while leaving behind the toxic substances such as urea, creatinine, etc. This process would be more analogous to the function of the living kidney than the dialysis process. Preliminary work toward the development of a blood ultrafiltration unit has been done by a few investigators [8-16] but the recovery of water has not yet been attempted.

Because of the many advantages of the ultrafiltration artificial kidney, it is believed that ultrafiltration will ultimately replace dialysis in artificial kidneys.

Very few theoretical studies can be found in the literature on blood ultrafiltration because it has only recently gained importance. The fact that blood is a non-Newtonian fluid and that blood ultrafiltration processes involve two dimensional flow make the mathematical study of this problem very complicated.

It is the object of this work to pioneer into the task of solving such a blood ultrafiltration problem to obtain the flow patterns and velocity-pressure relations which will assist the design of an ultrafiltration artificial kidney and the prediction of its performance.

Rheology of Blood

It has been mentioned previously that blood is a non-Newtonian fluid. Normal human blood possesses a distinctive yield stress. When the yield stress is exceeded, the same blood has a shear-stress shear-rate function closely following Casson's model, which implies reversible aggregation of red cells in rouleaux and flow dominated by movement of rouleaux [16]. Casson's equation [17] was first developed for pigment-oil suspensions and relates the rheological properties of a suspension composed of particles which are capable of aggregating into rodlike clusters.

$$\tau_{yx}^{1/2} = \tau_0^{1/2} + k \left(-\frac{dV_y}{dx} \right)^{1/2} \quad (1-1)$$

Because of the formation of rouleaux by red blood cells [18], good correlation has been found between the rheological data taken on human blood with the Casson equation [19,20,21,22]. For banked-type O blood (containing ethylene-diamine tetraacetic acid as anticoagulant) the following empirical relations have been proposed [23]:

$$\tau_0^{1/2} = (H - 0.017)^{1/2} (1.55 C_f + 0.76) \quad (1-2)$$

$$k = \left[\frac{\mu_0}{(1 - H)^{2j}} \right]^{1/2} \quad (1-3)$$

where τ_0 = yield stress, dyne/cm²

H = hematocrit (volume percent of red cells in whole blood)

C_F = fibrinogen concentration, g/100 ml

μ_0 = viscosity of the suspending plasma, centipoise

j = a dimensionless constant of the order of unity,

varying with the concentrations of the other plasma proteins.

For normal human blood at a hematocrit of 40, the average value of τ_0 is 0.04 dyne/cm² and the average value of k is 0.18 (g/sec-cm)^{1/2} [22,24].

Two-Dimensional Blood Flow

It has been pointed out that blood ultrafiltration involves two-dimensional flow of a non-Newtonian fluid. Because of the complexities involved, most analytical studies of blood flow have been greatly simplified. Blood flow in dialysis artificial kidneys has been treated as one-dimensional Newtonian flow in many papers [25,26,27]. Merrill [24], Aroesty [28], Kosijman [29], Shay [30] and Oka [34] used Casson's model in their blood flow analysis but their studies were limited to one-dimensional flow. Although there are many papers on the ultrafiltration of Newtonian flow between parallel plates and cylindrical pipes [31,32,33] no article on the ultrafiltration of non-Newtonian flow could be found in the literature.

The scope of this work will be confined to the simplest case of two-dimensional Cassonian flow, namely the ultrafiltration of blood between two parallel membranes with constant wall suction.

CHAPTER II

MATHEMATICAL DESCRIPTION OF THE PROBLEM

Statement of the Problem

The system under consideration, Figure 1, consists of a Cassonian fluid flowing downward between two parallel walls. At a certain point in the channel the walls become permeable. The flow is laminar and fully developed before the fluid contacts the walls that are permeable, and the dimensions of the channel are such that it can be considered semi-infinite.

Additional assumptions are:

- (1) The fluid is Cassonian with constant physical properties.
- (2) The flow is steady, isothermal and two-dimensional with velocity components in the x- and y-directions only.
- (3) The wall suction rate is uniform and constant at each wall.
- (4) There is no wall slip.
- (5) The flow is symmetrical about the middle plane between the walls.

The purpose of this study is to establish for such a system velocity and pressure profiles at various mass flowrates, wall suction rates and yield stresses.

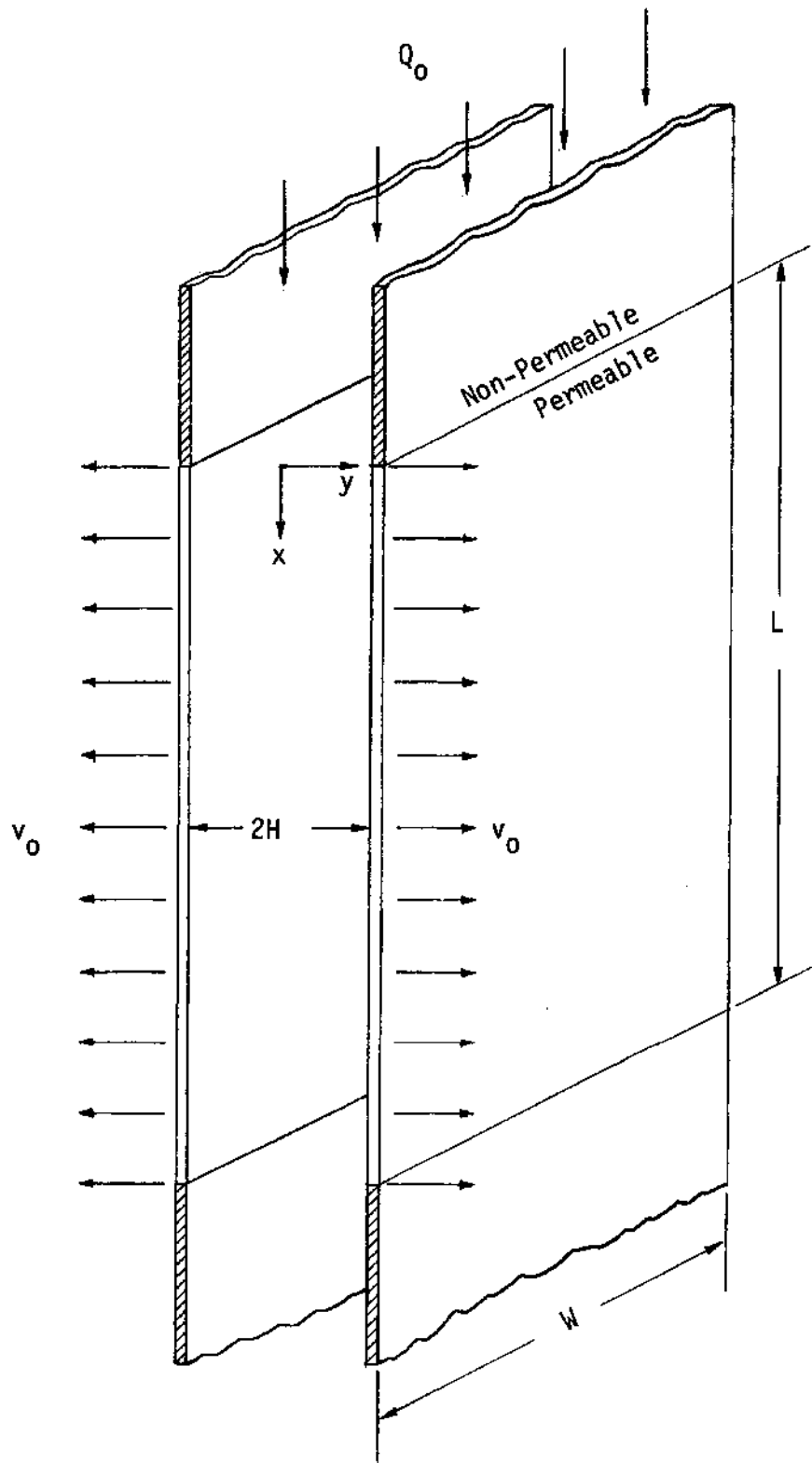


Figure 1. Schematic Drawing of the System.

Development of Casson's Model for Two-Dimensional Flow

For multidimensional, incompressible flow, Newton's law of viscosity is

$$\tau = -\mu\Delta \quad (2-1)$$

where Δ is the symmetrical rate of deformation tensor with cartesian components $\Delta_{ij} = (\partial v_i / \partial x_j) + (\partial v_j / \partial x_i)$. The coefficient of viscosity μ is independent of τ or Δ for a Newtonian fluid.

For a non-Newtonian fluid, the relation between τ and Δ is

$$\tau = -\eta\Delta \quad (2-2)$$

where the non-Newtonian viscosity η is a scalar function of Δ or τ . Consequently η must depend only on the invariants of Δ . The three invariants of Δ are

$$I_1 = (\Delta:\delta) = \sum_i \Delta_{ii} \quad (2-3)$$

$$I_2 = (\Delta:\Delta) = \sum_i \sum_j \Delta_{ij} \Delta_{ji} \quad (2-4)$$

$$I_3 = \det\Delta = \sum_i \sum_j \sum_k \epsilon_{ijk} \Delta_{1i} \Delta_{2j} \Delta_{3k} \quad (2-5)$$

From the equation of continuity it can be shown that I_1 is always zero for incompressible fluids

$$\begin{aligned}
 I_1 &= \Sigma_i \Delta_{ii} \\
 &= \Sigma_i \left(\frac{\partial v_i}{\partial x_i} \right) + \left(\frac{\partial v_i}{\partial x_i} \right) \\
 &= \Sigma_i 2 \left(\frac{\partial v_i}{\partial x_i} \right) \\
 &= 2 (\Delta \cdot v)
 \end{aligned}$$

But $(\Delta \cdot v) = 0$ for incompressible fluids, therefore

$$I_1 = 0$$

For many simple flows, the third invariant I_3 either vanishes identically or can be assumed not very important. Therefore it is customary to assume [35,36,37] that η can be taken to be a function of the second invariant I_2 .

The Casson equation for one-dimensional flow has been introduced in Chapter I;

$$\tau_{yx}^{1/2} = \tau_0^{1/2} + k \left(-\frac{dv}{dx} \right)^{1/2} \quad (2-6)$$

Squaring the above equation:

$$\tau_{yx} = \tau_0 + 2\tau_0^{1/2} k \left(-\frac{dv}{dx} \right)^{1/2} + k^2 \left(-\frac{dv}{dx} \right) \quad (2-7)$$

According to Hohenemser [35], the above equation can be written in the following tensor form for multidimensional flow:

$$\begin{aligned} \tau = & -[\tau_0 + 2\tau_0^{1/2} k | \sqrt{\frac{1}{2} (\Delta:\Delta)} |]^{1/2} \\ & + k^2 \{ \sqrt{\frac{1}{2} (\Delta:\Delta)} | \} \frac{\Delta}{\sqrt{\frac{1}{2} (\Delta:\Delta)} |} \end{aligned} \quad (2-8)$$

For two dimensional flow in the x- and y-directions:

$$\frac{1}{2} (\Delta:\Delta) = [(\frac{\partial v_x}{\partial x})^2 + (\frac{\partial v_y}{\partial y})^2] + [\frac{\partial v_y}{\partial x} + \frac{\partial v_x}{\partial y}]^2 \quad (2-9)$$

Since this quantity will always be positive, substituting (2-9) into (2-8) gives

$$\begin{aligned} \tau = & -\{\tau_0 (2[(\frac{\partial v_x}{\partial x})^2 + (\frac{\partial v_y}{\partial y})^2] \\ & + [\frac{\partial v_y}{\partial x} + \frac{\partial v_x}{\partial y}]^2)^{-1/2} \\ & + 2\tau_0^{1/2} k (2[(\frac{\partial v_x}{\partial x})^2 + (\frac{\partial v_y}{\partial y})^2] \\ & + [\frac{\partial v_y}{\partial x} + \frac{\partial v_x}{\partial y}]^2)^{-1/2} + k^2 \} \Delta \end{aligned} \quad (2-10)$$

For two-dimensional flow, the following stress components exist:

$$\begin{aligned} \tau_{xx} = & -\{\tau_0 (2[(\frac{\partial v_x}{\partial x})^2 + (\frac{\partial v_y}{\partial y})^2] + [\frac{\partial v_y}{\partial x} + \frac{\partial v_x}{\partial y}]^2)^{-1/2} \\ & + 2\tau_0^{1/2} k (2[(\frac{\partial v_x}{\partial x})^2 + (\frac{\partial v_y}{\partial y})^2] + [\frac{\partial v_y}{\partial x} + \frac{\partial v_x}{\partial y}]^2)^{-1/2} \\ & + k^2 \} (2 \frac{\partial v_x}{\partial x}) \end{aligned} \quad (2-11)$$

$$\begin{aligned} \tau_{yy} = & -\{\tau_0 (2[(\frac{\partial v_x}{\partial x})^2 + (\frac{\partial v_y}{\partial y})^2] + [\frac{\partial v_y}{\partial x} + \frac{\partial v_x}{\partial y}]^2)^{-\frac{1}{2}} \\ & + 2\tau_0^{\frac{1}{2}} k(2[(\frac{\partial v_x}{\partial x})^2 + (\frac{\partial v_y}{\partial y})^2] + [\frac{\partial v_y}{\partial x} + \frac{\partial v_x}{\partial y}]^2)^{-\frac{1}{2}} \\ & + k^2\} (2 \frac{\partial v_y}{\partial y}) \end{aligned} \quad (2-12)$$

$$\begin{aligned} \tau_{xy} = \tau_{yx} = & -\{\tau_0 (2[(\frac{\partial v_x}{\partial x})^2 + (\frac{\partial v_y}{\partial y})^2] + [\frac{\partial v_y}{\partial x} + \frac{\partial v_x}{\partial y}]^2)^{-\frac{1}{2}} \\ & + 2\tau_0^{\frac{1}{2}} k(2[(\frac{\partial v_x}{\partial x})^2 + (\frac{\partial v_y}{\partial y})^2] + [\frac{\partial v_y}{\partial x} + \frac{\partial v_x}{\partial y}]^2)^{-\frac{1}{2}} \\ & + k^2\} (\frac{\partial v_x}{\partial y} + \frac{\partial v_y}{\partial x}) \end{aligned} \quad (2-13)$$

Fluid Flow Equations and Boundary Conditions

The system to be studied is represented in Figure 1. A Cassonian fluid with density ρ , yield stress τ_0 and Casson viscosity k^2 is flowing downward between two parallel walls which change from non-permeable to permeable at a certain point down the stream. The rectangular coordinate system is used with x measured from the initial end of the permeable walls down along the direction of the flow, and y measured from the medium plane between the two parallel walls out toward the wall on the right. The distance between the two walls is $2H$ and the width is W . The initial volumetric flowrate is Q_0 and the initial pressure is p_0 .

The governing equations for a multidimensional Cassonian flow are

Equation of Continuity

$$(\nabla \cdot v) = 0 \quad (2-14)$$

Equation of Motion

$$\rho \frac{Dv}{Dt} = -\nabla P - [\nabla \cdot \tau] + \rho g \quad (2-15)$$

$$\tau = - \left\{ \frac{\tau_0}{\left| \sqrt{\frac{1}{2}} (\Delta : \Delta) \right|} + \frac{2\tau_0^{\frac{1}{2}} k}{\left| \sqrt{\frac{1}{2}} (\Delta : \Delta) \right|^{\frac{1}{2}} + k^2} \right\} \Delta \quad (2-16)$$

For steady two-dimensional Cassonian flow in the system described, the governing equations reduce to

Equation of Continuity

$$\frac{\partial v_x}{\partial x} + \frac{\partial v_y}{\partial y} = 0 \quad (2-17)$$

Equations of Motion

$$\rho \left(v_x \frac{\partial v_x}{\partial x} + v_y \frac{\partial v_x}{\partial y} \right) = -\frac{\partial p}{\partial x} - \left(\frac{\partial \tau_{xx}}{\partial x} + \frac{\partial \tau_{yx}}{\partial y} \right) + \rho g_x \quad (2-18)$$

$$\rho \left(v_x \frac{\partial v_y}{\partial x} + v_y \frac{\partial v_y}{\partial y} \right) = -\frac{\partial p}{\partial y} - \left(\frac{\partial \tau_{xy}}{\partial x} + \frac{\partial \tau_{yy}}{\partial y} \right) + \rho g_y \quad (2-19)$$

where as derived in (2-11), (2-12) and (2-13)

$$\begin{aligned} \tau_{xx} = & - \left\{ \tau_0 \left(2 \left[\left(\frac{\partial v_x}{\partial x} \right)^2 + \left(\frac{\partial v_y}{\partial y} \right)^2 \right] + \left[\frac{\partial v_y}{\partial x} + \frac{\partial v_x}{\partial y} \right]^2 \right)^{-\frac{1}{2}} \right. \\ & + 2\tau_0^{\frac{1}{2}} k \left(2 \left[\left(\frac{\partial v_x}{\partial x} \right)^2 + \left(\frac{\partial v_y}{\partial y} \right)^2 \right] + \left[\frac{\partial v_y}{\partial x} + \frac{\partial v_x}{\partial y} \right]^2 \right)^{-\frac{1}{4}} \\ & \left. + k^2 \right\} \left(2 \frac{\partial v_x}{\partial x} \right) \end{aligned}$$

$$\begin{aligned} \tau_{yy} = & - \left\{ \tau_0 \left(2 \left[\left(\frac{\partial v_x}{\partial x} \right)^2 + \left(\frac{\partial v_y}{\partial y} \right)^2 \right] + \left[\frac{\partial v_y}{\partial x} + \frac{\partial v_x}{\partial y} \right]^2 \right)^{-\frac{1}{2}} \right. \\ & + 2\tau_0^{\frac{1}{2}} k \left(2 \left[\left(\frac{\partial v_x}{\partial x} \right)^2 + \left(\frac{\partial v_y}{\partial y} \right)^2 \right] + \left[\frac{\partial v_y}{\partial x} + \frac{\partial v_x}{\partial y} \right]^2 \right)^{-\frac{1}{4}} \\ & \left. + k^2 \right\} \left(2 \frac{\partial v_y}{\partial y} \right) \end{aligned}$$

$$\begin{aligned} \tau_{yx} = \tau_{xy} = & - \left\{ \tau_0 \left(2 \left[\left(\frac{\partial v_x}{\partial x} \right)^2 + \left(\frac{\partial v_y}{\partial y} \right)^2 \right] + \left[\frac{\partial v_y}{\partial x} + \frac{\partial v_x}{\partial y} \right]^2 \right)^{-\frac{1}{2}} \right. \\ & + 2\tau_0^{\frac{1}{2}} k \left(2 \left[\left(\frac{\partial v_x}{\partial x} \right)^2 + \left(\frac{\partial v_y}{\partial y} \right)^2 \right] + \left[\frac{\partial v_y}{\partial x} + \frac{\partial v_x}{\partial y} \right]^2 \right)^{-\frac{1}{4}} \\ & \left. + k^2 \right\} \left(\frac{\partial v_x}{\partial y} + \frac{\partial v_y}{\partial x} \right) \end{aligned}$$

Boundary Conditions

$$\begin{aligned} \text{at } y = 0, \quad y = 0 \\ \frac{\partial v_x}{\partial y} = 0 \end{aligned}$$

$$\text{and } \tau_{yx} = \tau_{xy} = 0$$

$$\text{at } y = \pm H, \quad v_y = \pm v_0 \text{ (constant)}$$

$$v_x = 0$$

$$\text{and } \tau_{xx} = 0$$

$$\text{at } x = 0, \quad p = p_0$$

$$\text{and } 2W \int_0^H v_x dy = Q_0$$

$$\text{at } x = x, \quad 2W \int_0^H v_x dy = Q_0 - 2W \int_0^x v_0 dx$$

Dimensionless Fluid Flow Equation and Boundary Conditions

To rewrite the flow equations and boundary conditions in dimensionless quantities, the average initial velocity $U_0 = Q_0/2WH$ and the half distance H between the two parallel walls were chosen as reference quantities. The dimensionless variables are defined as follows

$$T_0 = \tau_0/\rho U_0^2 \quad K = k/(\rho U_0 H)^{1/2} \quad V_0 = v_0/U_0$$

$$X = x/H \quad Y = y/H$$

$$T_{xx} = \tau_{xx}/\rho U_0^2 \quad T_{yy} = \tau_{yy}/\rho U_0^2$$

$$T_{xy} = \tau_{xy}/\rho U_0^2 \quad T_{yx} = \tau_{yx}/\rho U_0^2$$

$$P = [p - \rho(g_x x + g_y y)]/\rho U_0^2$$

Substituting the above dimensionless variables into the previous equations and boundary conditions gives the following dimensionless flow equations and boundary conditions:

Equation of Continuity

$$\frac{\partial V_x}{\partial X} + \frac{\partial V_y}{\partial Y} = 0 \quad (2-20)$$

Equation of Motion

$$V_x \frac{\partial V_x}{\partial X} + V_y \frac{\partial V_x}{\partial Y} = - \frac{\partial P}{\partial X} - \left(\frac{\partial T_{xx}}{\partial X} + \frac{\partial T_{yx}}{\partial Y} \right) \quad (2-21)$$

$$V_x \frac{\partial V_y}{\partial X} + V_y \frac{\partial V_y}{\partial Y} = - \frac{\partial P}{\partial Y} - \left(\frac{\partial T_{xy}}{\partial X} + \frac{\partial T_{yy}}{\partial Y} \right) \quad (2-22)$$

where

$$\begin{aligned} T_{xx} = & - \left\{ T_0 \left(2 \left[\left(\frac{\partial V_x}{\partial X} \right)^2 + \left(\frac{\partial V_y}{\partial Y} \right)^2 \right] + \left[\frac{\partial V_x}{\partial Y} + \frac{\partial V_y}{\partial X} \right]^2 \right)^{-\frac{1}{2}} \right. \\ & + 2T_0^{\frac{1}{2}} K \left(2 \left[\left(\frac{\partial V_x}{\partial X} \right)^2 + \left(\frac{\partial V_y}{\partial Y} \right)^2 \right] + \left[\frac{\partial V_x}{\partial Y} + \frac{\partial V_y}{\partial X} \right]^2 \right)^{-\frac{1}{4}} \\ & \left. + K^2 \right\} \left(2 \frac{\partial V_x}{\partial X} \right) \end{aligned} \quad (2-23)$$

$$\begin{aligned} T_{yy} = & - \left\{ T_0 \left(2 \left[\left(\frac{\partial V_x}{\partial X} \right)^2 + \left(\frac{\partial V_y}{\partial Y} \right)^2 \right] + \left[\frac{\partial V_x}{\partial Y} + \frac{\partial V_y}{\partial X} \right]^2 \right)^{-\frac{1}{2}} \right. \\ & + 2T_0^{\frac{1}{2}} K \left(2 \left[\left(\frac{\partial V_x}{\partial X} \right)^2 + \left(\frac{\partial V_y}{\partial Y} \right)^2 \right] + \left[\frac{\partial V_x}{\partial Y} + \frac{\partial V_y}{\partial X} \right]^2 \right)^{-\frac{1}{4}} \\ & \left. + K^2 \right\} \left(2 \frac{\partial V_y}{\partial Y} \right) \end{aligned} \quad (2-24)$$

$$\begin{aligned}
 T_{yx} = T_{xy} = & - \{ T_0 (2 [(\frac{\partial V_x}{\partial X})^2 + (\frac{\partial V_y}{\partial Y})^2] + [\frac{\partial V_x}{\partial Y} + \frac{\partial V_y}{\partial X}]^2)^{-\frac{1}{2}} \\
 & + 2T_0^{\frac{1}{2}} K (2 [(\frac{\partial V_x}{\partial X})^2 + (\frac{\partial V_y}{\partial Y})^2] + [\frac{\partial V_x}{\partial Y} + \frac{\partial V_y}{\partial X}]^2)^{-\frac{1}{4}} \\
 & + K^2 \} (\frac{\partial V_x}{\partial Y} + \frac{\partial V_y}{\partial X})
 \end{aligned} \tag{2-25}$$

Boundary Conditions

$$\text{at } Y = 0, \quad V_y = 0$$

$$\frac{\partial V_x}{\partial Y} = 0$$

$$\text{and} \quad T_{yx} = T_{xy} = 0$$

$$\text{at } Y = \pm 1, \quad V_y = \pm V_0,$$

$$V_x = 0$$

$$\text{and} \quad T_{xx} = 0$$

$$\text{at } X = 0, \quad P = P_0$$

$$\text{and} \quad \int_0^1 V_x dY = 1$$

$$\text{at } X = X, \quad \int_0^1 V_x dY = 1 - \int_0^X V_0 dX$$

Equations in Terms of a Modified Dimensionless Stream
Function and Stresses

Differentiating (2-21) with respect to Y, differentiating (2-22) with respect to X and combining the two resulting equations to eliminate the pressure terms gives

$$\begin{aligned} \frac{\partial}{\partial Y} (v_x \frac{\partial v_x}{\partial X} + v_y \frac{\partial v_x}{\partial Y}) - \frac{\partial}{\partial X} (v_x \frac{\partial v_y}{\partial X} + v_y \frac{\partial v_y}{\partial Y}) & \quad (2-26) \\ = \frac{\partial}{\partial X} (\frac{\partial T_{xy}}{\partial X} + \frac{\partial T_{yy}}{\partial Y}) - \frac{\partial}{\partial Y} (\frac{\partial T_{xx}}{\partial X} + \frac{\partial T_{yx}}{\partial Y}) \end{aligned}$$

Now assume a modified dimensionless stream function ψ which is defined by the following relations:

$$v_x = \frac{\partial \psi}{\partial Y} \quad v_y = - \frac{\partial \psi}{\partial X}$$

With the above definition, v_x and v_y automatically satisfy the equation of continuity (2-20).

Introducing the stream function ψ into (2-26) gives

$$\begin{aligned} (\frac{\partial \psi}{\partial Y}) [\frac{\partial}{\partial X} (\frac{\partial^2 \psi}{\partial Y^2} + \frac{\partial^2 \psi}{\partial X^2})] - (\frac{\partial \psi}{\partial X}) [\frac{\partial}{\partial Y} (\frac{\partial^2 \psi}{\partial Y^2} + \frac{\partial^2 \psi}{\partial X^2})] & \quad (2-27) \\ = \frac{\partial}{\partial X} (\frac{\partial T_{xy}}{\partial X} + \frac{\partial T_{yy}}{\partial Y}) - \frac{\partial}{\partial Y} (\frac{\partial T_{xx}}{\partial X} + \frac{\partial T_{yx}}{\partial Y}) \end{aligned}$$

The left side of (2-26) can be written in a more conventional form

$$\frac{\partial(\psi, \nabla^2 \psi)}{\partial(X, Y)} = \frac{\partial}{\partial X} (\frac{\partial T_{xy}}{\partial X} + \frac{\partial T_{yy}}{\partial Y}) - \frac{\partial}{\partial Y} (\frac{\partial T_{xx}}{\partial X} + \frac{\partial T_{yx}}{\partial Y}) \quad (2-28)$$

where

$$\frac{\partial(\psi, \nabla^2 \psi)}{\partial(X, Y)} = \begin{vmatrix} \frac{\partial \psi}{\partial X} & \frac{\partial \psi}{\partial Y} \\ \frac{\partial}{\partial X} (\nabla^2 \psi) & \frac{\partial}{\partial Y} (\nabla^2 \psi) \end{vmatrix}$$

and
$$\nabla^2 \psi = \frac{\partial^2 \psi}{\partial X^2} + \frac{\partial^2 \psi}{\partial Y^2}$$

Introducing the stream function ψ into (2-23), (2-24) and (2-25) gives

$$\begin{aligned} T_{xx} = & - \{ T_0 [4 \left(\frac{\partial^2 \psi}{\partial X \partial Y} \right)^2 + \left(\frac{\partial^2 \psi}{\partial Y^2} - \frac{\partial^2 \psi}{\partial X^2} \right)^2]^{-\frac{1}{2}} \\ & + 2T_0^{\frac{1}{2}} K [4 \left(\frac{\partial^2 \psi}{\partial X \partial Y} \right)^2 + \left(\frac{\partial^2 \psi}{\partial Y^2} - \frac{\partial^2 \psi}{\partial X^2} \right)^2]^{-\frac{1}{4}} \\ & + K^2 \} \left(2 \frac{\partial^2 \psi}{\partial X \partial Y} \right) \end{aligned} \quad (2-29)$$

$$\begin{aligned} T_{yy} = & - \{ T_0 [4 \left(\frac{\partial^2 \psi}{\partial X \partial Y} \right)^2 + \left(\frac{\partial^2 \psi}{\partial Y^2} - \frac{\partial^2 \psi}{\partial X^2} \right)^2]^{-\frac{1}{2}} \\ & + 2T_0^{\frac{1}{2}} K [4 \left(\frac{\partial^2 \psi}{\partial X \partial Y} \right)^2 + \left(\frac{\partial^2 \psi}{\partial Y^2} - \frac{\partial^2 \psi}{\partial X^2} \right)^2]^{-\frac{1}{4}} \\ & + K^2 \} \left(-2 \frac{\partial^2 \psi}{\partial X \partial Y} \right) \end{aligned} \quad (2-30)$$

$$\begin{aligned} T_{yx} = T_{xy} = & - \{ T_0 [4 \left(\frac{\partial^2 \psi}{\partial X \partial Y} \right)^2 + \left(\frac{\partial^2 \psi}{\partial Y^2} - \frac{\partial^2 \psi}{\partial X^2} \right)^2]^{-\frac{1}{2}} \\ & + 2T_0^{\frac{1}{2}} K [4 \left(\frac{\partial^2 \psi}{\partial X \partial Y} \right)^2 + \left(\frac{\partial^2 \psi}{\partial Y^2} - \frac{\partial^2 \psi}{\partial X^2} \right)^2]^{-\frac{1}{4}} \\ & + K^2 \} \left(\frac{\partial^2 \psi}{\partial Y^2} - \frac{\partial^2 \psi}{\partial X^2} \right) \end{aligned} \quad (2-31)$$

By (2-29) and (2-30)

$$T_{xx} = -T_{yy} \quad (2-32)$$

This relation can also be proved with stress equations (2-23), (2-24), and the equation of continuity (2-20) in terms of velocity components. Substituting (2-32) into (2-28) gives

$$\frac{\partial(\psi, \nabla^2 \psi)}{\partial(X, Y)} = \frac{\partial^2 T_{yx}}{\partial Y^2} - \frac{\partial^2 T_{yx}}{\partial X^2} + 2 \frac{\partial^2 T_{xx}}{\partial X \partial Y} \quad (2-33)$$

The assumption of creeping flow greatly simplifies the above equation without seriously restricting the utility of the results [38]. By assuming creeping flow, the left side of (2-33) may be neglected. After rearranging

$$\frac{\partial^2 T_{yx}}{\partial Y^2} - \frac{\partial^2 T_{yx}}{\partial X^2} + 2 \frac{\partial^2 T_{xx}}{\partial X \partial Y} = 0 \quad (2-34)$$

Dividing (2-29) by (2-30) gives

$$\begin{aligned} \frac{T_{xx}}{T_{yx}} &= \frac{2 \frac{\partial^2 \psi}{\partial X \partial Y}}{\frac{\partial^2 \psi}{\partial Y^2} - \frac{\partial^2 \psi}{\partial X^2}} \\ &= \frac{2F^2 \psi}{D^2 \psi} = 2\gamma \end{aligned}$$

where

$$F^2 = \frac{\partial^2}{\partial X \partial Y}, \quad D^2 = \frac{\partial^2}{\partial Y^2} - \frac{\partial^2}{\partial X^2}, \quad \gamma = \frac{F^2 \psi}{D^2 \psi} \quad (2-35)$$

$$T_{xx} = \left(\frac{2F^2 \psi}{D^2 \psi} \right) T_{yx} = 2\gamma T_{yx}$$

Substituting (2-35) into (2-34) gives

$$2F^2 (\gamma T_{yx}) + D^2 T_{yx} = 0 \quad (2-36)$$

where

$$\begin{aligned} T_{yx} = & - \{ T_0 [4(F^2 \psi)^2 + (D^2 \psi)^2]^{-1/2} \\ & + 2T_0^{1/2} K [4(F^2 \psi)^2 + (D^2 \psi)^2]^{-1/4} \\ & + K^2 \} (D^2 \psi) \end{aligned} \quad (2-37)$$

Equations (2-36) and (2-37) are to be solved with the following boundary conditions:

$$\text{at } Y = 0, \quad \psi = 0,$$

$$\frac{\partial^2 \psi}{\partial Y^2} = 0$$

$$\text{and} \quad T_{yx} = 0$$

$$\text{at } Y = 1, \quad \psi = 1 - V_0 X,$$

$$\frac{\partial \psi}{\partial Y} = 0$$

$$\text{and} \quad T_{yx} = F(\psi) |_{Y=1}$$

at $X = 0$,

$$\psi = \frac{Y}{K^2} \left\{ \frac{1}{2} P_f \left(1 - \frac{Y^2}{3}\right) - \frac{4}{3} T_0^{1/2} P_f^{1/2} \left(1 - \frac{2}{5} Y^{3/2}\right) + T_0 \left(1 - \frac{Y}{2}\right) \right\} \quad (2-38)$$

and $T_{yx} = P_f Y \quad (2-39)$

where $P_f^{1/2} = \frac{6}{5} T_0^{1/2} + \left(3K^2 - \frac{3}{50} T_0\right)^{1/2*} \quad (2-40)$

* Derivations of equations (2-38), (2-39) and (2-40) are presented in Appendix A.

CHAPTER III

NUMERICAL TECHNIQUE

It is often very difficult or even impossible to obtain analytical solutions for fluid flow problems that involve complicated partial differential equations such as those developed in this study. However, the numerical approximation method coupled with the high-speed electronic computer can in many cases give numerical solutions at predetermined points in the domain of interest which are sufficient for engineering design and analysis. The numerical techniques used in this study are "finite difference approximations," "the relaxation method," "Newton-Raphson iteration" and "the method of false position" [39,40, 41,42].

Mathematical Derivation of Finite Difference
Differentiation and Graphical Interpretations

Finite difference approximation converts differential equations into algebraic equations which correlate the functional values of the neighboring points. In doing this, each differential term in the differential equation is replaced with a corresponding finite difference approximation. Such finite difference approximations can be obtained from Taylor's series.

Referring to Figure 2, $y = f(x)$ is a function represented by the curve ABC whose first derivative we wish to approximate. Dividing the x coordinate into equal increments of Δx

$$x_I = I\Delta x,$$

$$f_I = f(x_I) = f(I\Delta x) \quad \text{and}$$

$$f_{I+1} = f(x_{I+1}) = f(I\Delta x + \Delta x)$$

From Taylor's series expansion

$$f_{I-1} = f_I - \Delta x \left. \frac{df}{dx} \right|_I + \frac{\Delta x^2}{2!} \left. \frac{d^2f}{dx^2} \right|_I - \frac{\Delta x^3}{3!} \left. \frac{d^3f}{dx^3} \right|_I + \frac{\Delta x^4}{4!} \left. \frac{d^4f}{dx^4} \right|_I - \dots \quad (3-1)$$

$$f_{I+1} = f_I + \Delta x \left. \frac{df}{dx} \right|_I + \frac{\Delta x^2}{2!} \left. \frac{d^2f}{dx^2} \right|_I + \frac{\Delta x^3}{3!} \left. \frac{d^3f}{dx^3} \right|_I + \frac{\Delta x^4}{4!} \left. \frac{d^4f}{dx^4} \right|_I + \dots \quad (3-2)$$

As long as Δx is sufficiently small, terms of the order of Δx^2 and higher may be neglected. Then from equation (3-1), we get the following approximation

$$\left. \frac{df}{dx} \right|_I = \frac{f_I - f_{I-1}}{\Delta x} + O(\Delta x) \quad (3-3)$$

or from equation (3-2)

$$\left. \frac{df}{dx} \right|_I = \frac{f_{I+1} - f_I}{\Delta x} + O(\Delta x) \quad (3-4)$$

If equation (3-2) is subtracted from equation (3-1) and neglecting the Δx^3 and higher order terms, we get a better approximation because we do not have to neglect the Δx^2 terms

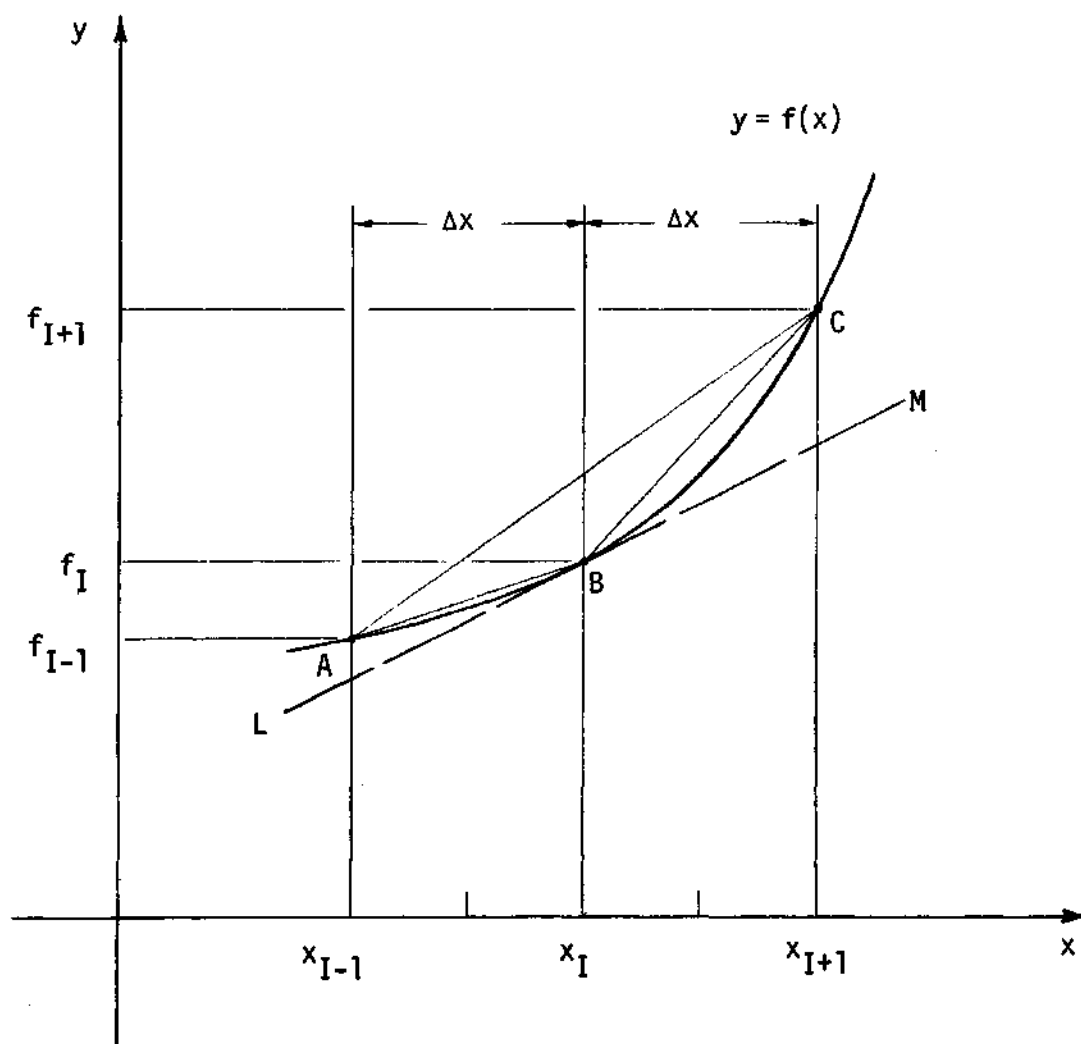


Figure 2. Graphical Interpretation of Finite Difference Differentiation.

$$\left. \frac{df}{dx} \right|_I = \frac{f_{I+1} - f_{I-1}}{2\Delta x} + O(\Delta x^n) \quad (3-5)$$

where $O(\Delta x^n)$ is the truncation error involved in neglecting the terms of the order of Δx^{n+1} and higher. $O(\Delta x^n)$ can usually be neglected when Δx is sufficiently small.

The approximations in equations (3-3), (3-4) and (3-5) can also be obtained graphically (Figure 2). By definition, $df/dx|_I$ is the slope of the tangent line LM. This slope can be approximated by the slope of line AB or line BC and best by the slope of line AC. When Δx becomes smaller, these slopes approach the true slope of the tangent line LM. These slopes are

$$\text{for AB} \quad \left. \frac{df}{dx} \right|_I = \frac{f_I - f_{I-1}}{\Delta x} \quad (3-3A)$$

$$\text{for BC} \quad \left. \frac{df}{dx} \right|_I = \frac{f_{I+1} - f_I}{\Delta x} \quad (3-4A)$$

$$\text{for AC} \quad \left. \frac{df}{dx} \right|_I = \frac{f_{I+1} - f_{I-1}}{2\Delta x} \quad (3-5A)$$

Equations (3-3A), (3-4A) and (3-5A) are equivalent to equations (3-3), (3-4) and (3-5) with the truncation terms $O(\Delta x^n)$ neglected.

Adding equations (3-1) and (3-2) and neglecting Δx^3 and higher order terms we get

$$\left. \frac{d^2f}{dx^2} \right|_I = \frac{f_{I+1} - 2f_I + f_{I-1}}{\Delta x^2} + O(\Delta x^2) \quad (3-6)$$

Graphically this approximation can also be derived from the slopes.

$$\left. \frac{d^2f}{dx^2} \right|_I = \left. \frac{df'}{dx} \right|_I = \frac{f'_{I+1/2} - f'_{I-1/2}}{\Delta x} \quad (3-7)$$

where $f'_{I+1/2}$ and $f'_{I-1/2}$ are the slopes of the curve at $x_{I+1/2}$ and $x_{I-1/2}$ which can be approximated by the slopes of BC and AB.

$$f'_{I+1/2} = \left. \frac{df}{dx} \right|_{I+1/2} = \frac{f_{I+1} - f_I}{\Delta x} \quad (3-8)$$

$$f'_{I-1/2} = \left. \frac{df}{dx} \right|_{I-1/2} = \frac{f_I - f_{I-1}}{\Delta x} \quad (3-9)$$

Substituting equations (3-8) and (3-9) into equation (3-7) we get

$$\left. \frac{d^2f}{dx^2} \right|_I = \frac{f_{I+1} - 2f_I + f_{I-1}}{\Delta x^2} \quad (3-6A)$$

Again (3-6A) is equivalent to (3-6) with the truncation term $O(\Delta x^2)$ neglected.

The derivation procedure used in equations (3-7), (3-8), (3-9) and (3-6A) will be used in deriving approximations to partial derivatives with respect to two independent variables in the next section.

System of Grid Points and Two-Dimensional Partial Derivatives

Consider a function $f(X,Y)$ which depends on both X and Y . Cover the X - Y plane with a rectangular grid system as shown in Figure 3 so

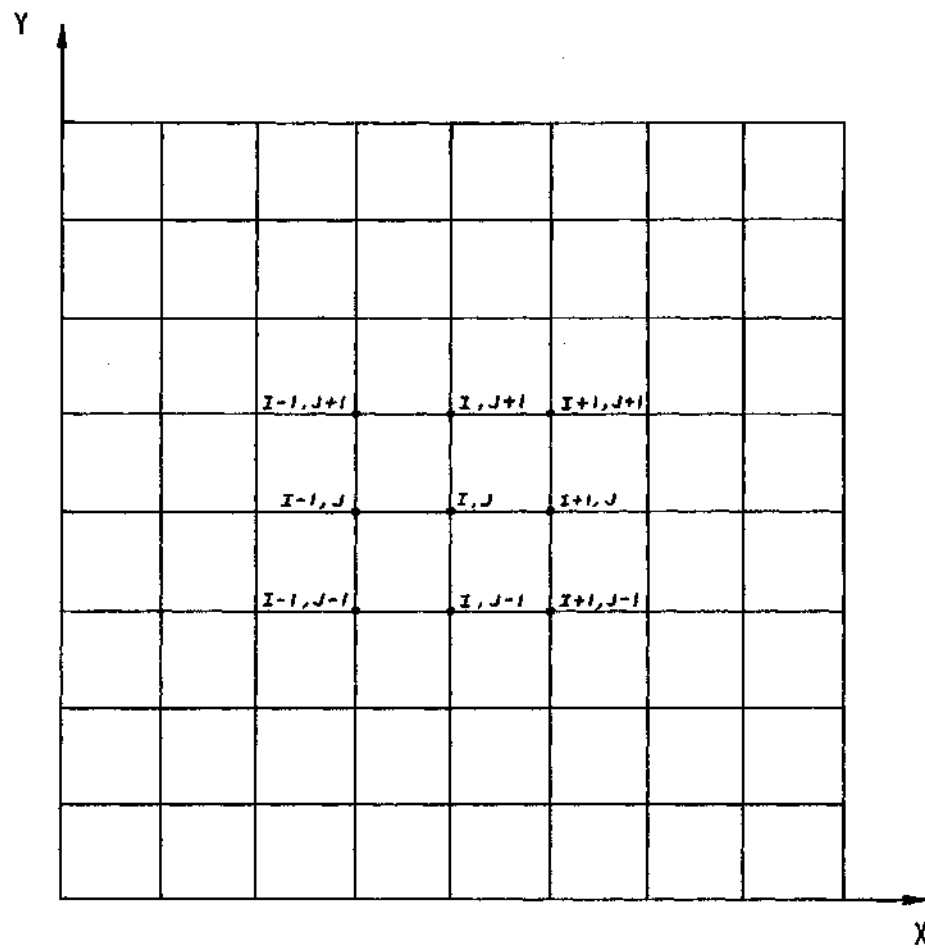


Figure 3. System of Grid Points.

that the grid point (I,J) is equivalent to the space point $(I\Delta X, J\Delta Y)$ and the value of the variable $f(X,Y)$ on this grid point is $f_{I,J} = f(I\Delta X, J\Delta Y)$. The neighboring grid points are labeled $(I+1,J)$, $(I-1,J)$, $(I,J+1)$, $(I,J-1)$, $(I+1,J+1)$, $(I-1,J-1)$, $(I+1,J-1)$ and $(I-1,J+1)$ as shown in Figure 3.

Letting $\Delta X = k$, $\Delta Y = h$ and $k = sh$, the partial derivatives can be approximated according to (3-5A) and (3-6A) as

$$\left. \frac{\partial f}{\partial X} \right|_{I,J} = \frac{f_{I+1,J} - f_{I-1,J}}{2k} = \frac{f_{I+1,J} - f_{I-1,J}}{2sh} \quad (3-7)$$

$$\left. \frac{\partial f}{\partial Y} \right|_{I,J} = \frac{f_{I,J+1} - f_{I,J-1}}{2h} \quad (3-8)$$

$$\begin{aligned} \left. \frac{\partial^2 f}{\partial X^2} \right|_{I,J} &= \frac{f_{I+1,J} - 2f_{I,J} + f_{I-1,J}}{k^2} & (3-9) \\ &= \frac{f_{I+1,J} - 2f_{I,J} + f_{I-1,J}}{s^2 h^2} \end{aligned}$$

$$\left. \frac{\partial^2 f}{\partial Y^2} \right|_{I,J} = \frac{f_{I,J+1} - 2f_{I,J} + f_{I,J-1}}{h^2} \quad (3-10)$$

The derivative $\partial^2 f / \partial X \partial Y$ can be approximated by a procedure similar to the steps taken in deriving (3-6A)

$$\begin{aligned}
\frac{\partial^2 f}{\partial X \partial Y} \Big|_{I,J} &= \frac{\partial}{\partial X} \left(\frac{\partial f}{\partial Y} \right) \Big|_{I,J} \\
&= \frac{\frac{\partial f}{\partial Y} \Big|_{I+1,J} - \frac{\partial f}{\partial Y} \Big|_{I-1,J}}{2sh} \\
&= \frac{1}{2sh} \left(\frac{f_{I+1,J+1} - f_{I+1,J-1}}{2h} - \frac{f_{I-1,J+1} - f_{I-1,J-1}}{2h} \right) \\
\frac{\partial^2 f}{\partial X \partial Y} \Big|_{I,J} &= \frac{1}{4sh^2} (f_{I+1,J+1} + f_{I-1,J-1} - f_{I+1,J-1} - f_{I-1,J+1}) \quad (3-11)
\end{aligned}$$

Finite Difference Flow Equations

From equations (3-7), (3-8), (3-9), (3-10) and (3-11) we can write

$$\begin{aligned}
F^2(\gamma T) \Big|_{I,J} &= \frac{\partial^2}{\partial X \partial Y} (\gamma T) \Big|_{I,J} \quad (3-12) \\
&= \frac{1}{4sh^2} [(\gamma T)_{I+1,J+1} + (\gamma T)_{I-1,J-1} \\
&\quad - (\gamma T)_{I+1,J-1} - (\gamma T)_{I-1,J+1}]
\end{aligned}$$

where $T = T_{yx}$

$$\begin{aligned}
D^2 T \Big|_{I,J} &= \left(\frac{\partial^2}{\partial Y^2} - \frac{\partial^2}{\partial X^2} \right) T \Big|_{I,J} \quad (3-13) \\
&= \frac{1}{s^2 h^2} [s^2 (T_{I,J+1} + T_{I,J-1}) - 2(s^2 - 1)T_{I,J} \\
&\quad - T_{I+1,J} - T_{I-1,J}]
\end{aligned}$$

Substituting (3-12) and (3-13) into (2-36)

$$\begin{aligned}
 & s[(\gamma T)_{I+1,J+1} + (\gamma T)_{I-1,J-1} - (\gamma T)_{I+1,J-1} \\
 & \quad - (\gamma T)_{I-1,J+1}] + s^2(T_{I,J+1} + T_{I,J-1}) \\
 & \quad - 2(s^2 - 1)T_{I,J} - T_{I+1,J} - T_{I-1,J} = 0
 \end{aligned} \tag{3-14}$$

Equation (3-14) can be rewritten in the following form

$$\begin{aligned}
 & s[(\gamma_{I+1,J+1})(T_{I+1,J+1}) + (\gamma_{I-1,J-1})(T_{I-1,J-1}) \\
 & \quad - (\gamma_{I+1,J-1})(T_{I+1,J-1}) - (\gamma_{I-1,J+1})(T_{I-1,J+1})] \\
 & \quad + s^2(T_{I,J+1} + T_{I,J-1}) - 2(s^2 - 1)T_{I,J} \\
 & \quad - T_{I+1,J} - T_{I-1,J} = 0
 \end{aligned} \tag{3-15}$$

where

$$\gamma_{I,J} = \left. \frac{(F^2\psi)}{D^2\psi} \right|_{I,J} = \frac{(F^2\psi)_{I,J}}{(D^2\psi)_{I,J}}$$

and

$$\begin{aligned}
 (F^2\psi)_{I,J} &= \frac{1}{4sh^2} (\psi_{I+1,J+1} + \psi_{I-1,J-1} \\
 & \quad - \psi_{I+1,J-1} - \psi_{I-1,J+1}) \\
 (D^2\psi)_{I,J} &= \frac{1}{s^2h^2} [s^2(\psi_{I,J+1} + \psi_{I,J-1}) - 2(s^2 - 1)\psi_{I,J} \\
 & \quad - \psi_{I+1,J} - \psi_{I-1,J}]
 \end{aligned}$$

Rearranging equation (3-15), we get

$$\begin{aligned}
 T_{I+1,J} = & s^2(T_{I,J+1} + T_{I,J-1}) - 2(s^2 - 1)T_{I,J} & (3-16) \\
 & - T_{I-1,J} - s[(\gamma_{I+1,J+1})(T_{I+1,J+1}) \\
 & + (\gamma_{I-1,J-1})(T_{I-1,J-1}) - (\gamma_{I+1,J-1})(T_{I+1,J-1}) \\
 & - (\gamma_{I-1,J+1})(T_{I-1,J+1})]
 \end{aligned}$$

or

$$\begin{aligned}
 T'_{I+1,J} = & T_{I+1,J} + \alpha\{s^2(T_{I,J+1} + T_{I,J-1}) & (3-17) \\
 & - 2(s^2 - 1)T_{I,J} - T_{I+1,J} - T_{I-1,J} \\
 & - s[(\gamma_{I+1,J+1})(T_{I+1,J+1}) \\
 & + (\gamma_{I-1,J-1})(T_{I-1,J-1}) - (\gamma_{I+1,J-1})(T_{I+1,J-1}) \\
 & - (\gamma_{I-1,J+1})(T_{I-1,J+1})]\}
 \end{aligned}$$

where α is a relaxation factor, found by trial, for faster convergence.

Now rewrite equation (2-37) in the finite difference form

$$\begin{aligned}
 T_{I,J} = & - \{ (T_0 [4(F^2\psi)_{I,J}^2 + (D^2\psi)_{I,J}^2])^{-\frac{1}{2}} & (3-18) \\
 & + 2T_0^{\frac{1}{2}} K [4(F^2\psi)_{I,J}^2 + (D^2\psi)_{I,J}^2]^{-\frac{1}{4}} \\
 & + K^2 \} (D^2\psi)_{I,J}
 \end{aligned}$$

where again

$$(F^2\psi)_{I,J} = \frac{1}{4sh^2} (\psi_{I+1,J+1} + \psi_{I-1,J-1} - \psi_{I+1,J-1} - \psi_{I-1,J+1})$$

$$(D^2\psi)_{I,J} = \frac{1}{s^2h^2} [s^2(\psi_{I,J+1} + \psi_{I,J-1}) - 2(s^2 - 1)\psi_{I,J} - \psi_{I+1,J} - \psi_{I-1,J}]$$

Equation (3-18) cannot be expressed explicitly for $\psi_{I+1,J}$. Iteration methods have to be used.

Newton-Raphson Iteration

Let

$$F(\psi_{I+1,J}) = \{T_0 [4(F^2\psi)_{I,J}^2 + (D^2\psi)_{I,J}^2]^{-\frac{1}{2}} + 2T_0^{\frac{1}{2}} K [4(F^2\psi)_{I,J}^2 + (D^2\psi)_{I,J}^2]^{-\frac{1}{4}} + K^2\} (D^2\psi)_{I,J} + T_{I,J} \quad (3-19)$$

then

$$F'(\psi_{I+1,J}) = \frac{\partial F(\psi_{I+1,J})}{\partial \psi_{I+1,J}} \quad (3-20)$$

$$= \{T_0 [4(F^2\psi)_{I,J}^2 + (D^2\psi)_{I,J}^2]^{-\frac{1}{2}} + 2T_0^{\frac{1}{2}} K [4(F^2\psi)_{I,J}^2 + (D^2\psi)_{I,J}^2]^{-\frac{1}{4}} + K^2\} \left(-\frac{1}{s^2h^2}\right) + \{T_0 [4(F^2\psi)_{I,J}^2 + (D^2\psi)_{I,J}^2]^{-3/2} + T_0^{\frac{1}{2}} K [4(F^2\psi)_{I,J}^2 + (D^2\psi)_{I,J}^2]^{-5/4} \left[\frac{(D^2\psi)_{I,J}^2}{s^2h^2}\right]$$

The value of $F(\psi_{I+1,J})$ approaches zero when $\psi_{I+1,J}$ approaches a value that satisfies equation (3-18). To find this value of $\psi_{I+1,J}$, a first estimation $\psi_{I+1,J}^0$ is made, then the next improved estimation is $\psi_{I+1,J}^1$ where

$$\psi_{I+1,J}^1 = \psi_{I+1,J}^0 - \frac{F(\psi_{I+1,J}^0)}{F'(\psi_{I+1,J}^0)} \quad (3-21)$$

Repeating this process

$$\psi_{I+1,J}^{m+1} = \psi_{I+1,J}^m - \frac{F(\psi_{I+1,J}^m)}{F'(\psi_{I+1,J}^m)} \quad (3-22)$$

$$m = 0, 1, 2, 3 \dots$$

until $|\psi_{I+1,J}^{m+1} - \psi_{I+1,J}^m| < \epsilon$

Where ϵ is a arbitrarily chosen small value. This process is illustrated in Figure 4. While Newton-Raphson iteration usually converges quite fast, it is unstable in some cases as shown in Figure 5.

The Method of False Position

This method is illustrated in Figure 6. The algorithm is contained in the following sequence of steps:

Step 1. Choose two approximations $\psi_{I+1,J}^0$ and $\psi_{I+1,J}^1$ such that

$$(\psi_{I+1,J}^0)(\psi_{I+1,J}^1) < 0$$

Step 2. Find a next approximation from the formula

$$\psi_{I+1,J}^2 = \frac{(\psi_{I+1,J}^0)F(\psi_{I+1,J}^1) - (\psi_{I+1,J}^1)F(\psi_{I+1,J}^0)}{F(\psi_{I+1,J}^1) - F(\psi_{I+1,J}^0)} \quad (3-23)$$

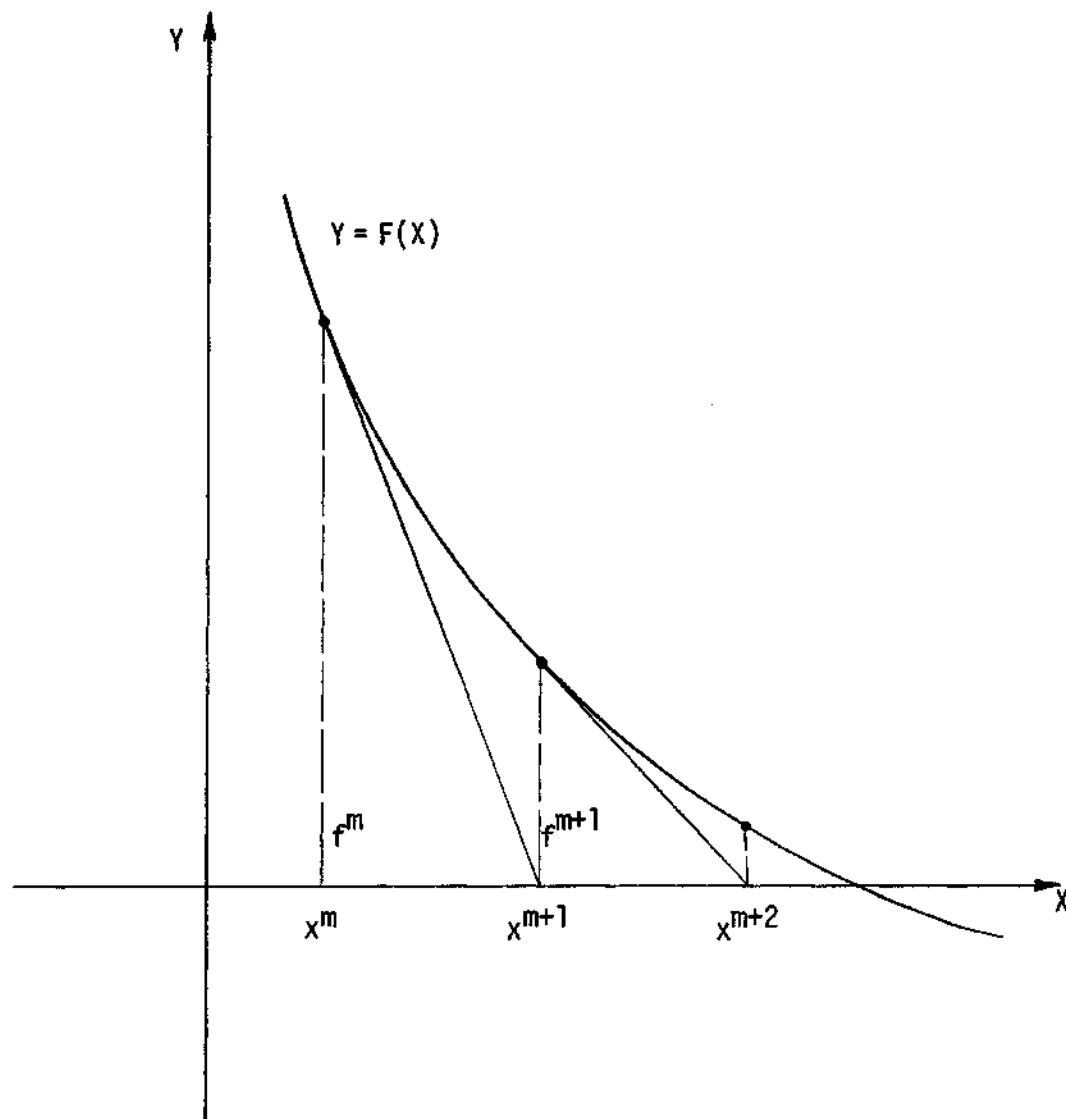


Figure 4. Newton-Raphson Iteration.

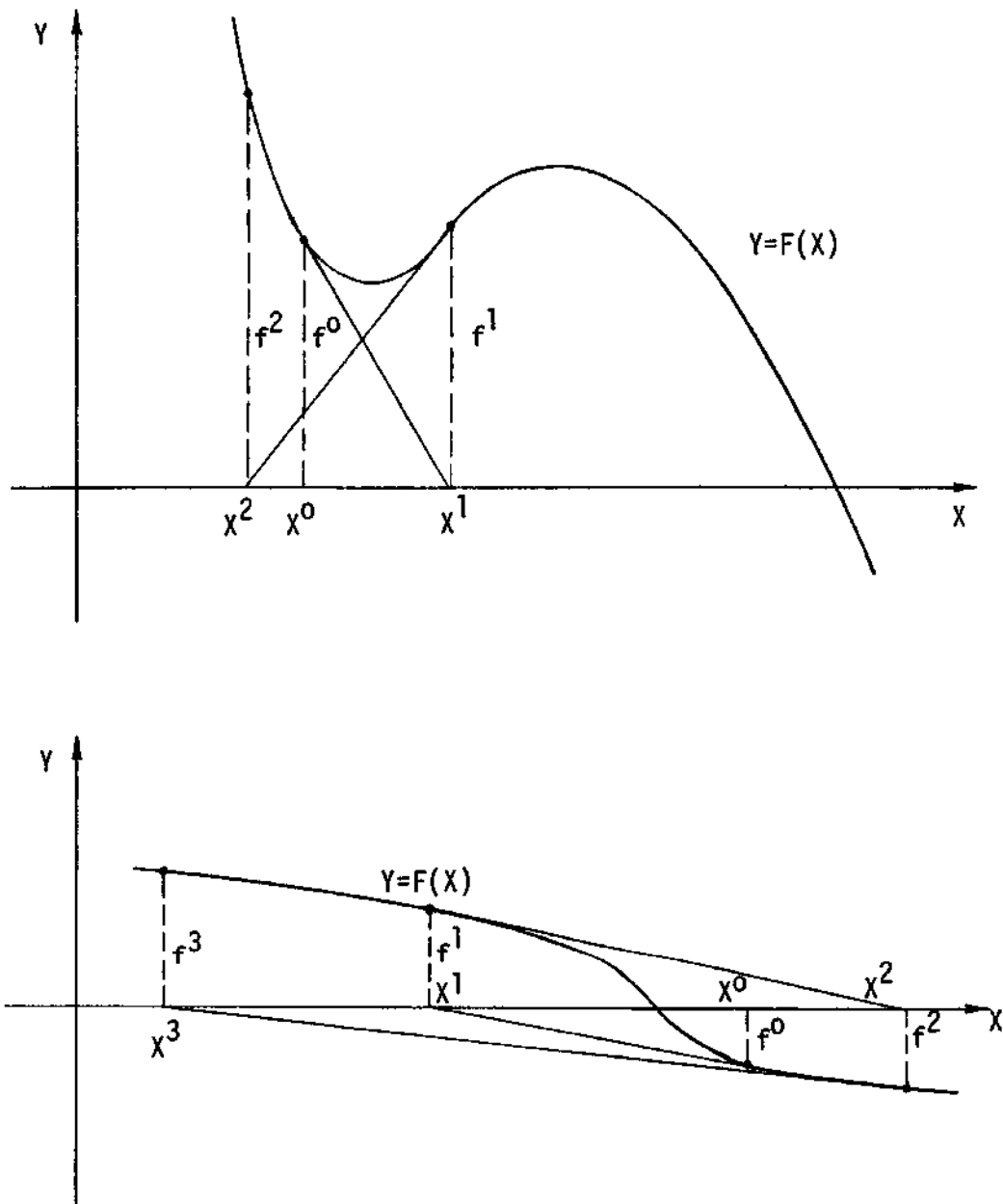


Figure 5. Newton-Raphson Iteration Fails to Converge.

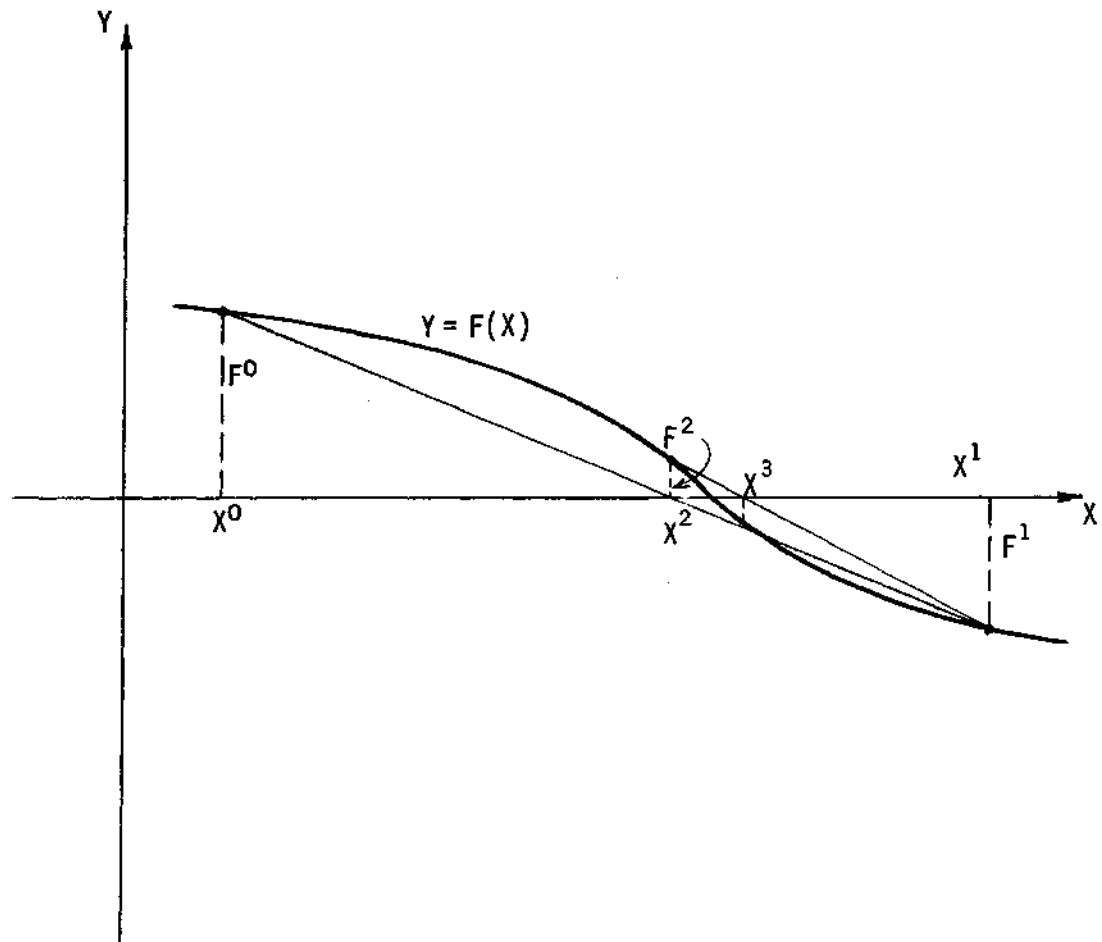


Figure 6. The Method of False Position.

- Step 3. If $|\psi_{I+1,J}^2 - \psi_{I+1,J}^1| < \epsilon$ or if $|\psi_{I+1,J}^2 - \psi_{I+1,J}^0| < \epsilon$ for a prescribed ϵ , $\psi_{I+1,J}^2$ is accepted as the answer. If not, go to Step 4.
- Step 4. If $F(\psi_{I+1,J}^2)F(\psi_{I+1,J}^0) < 0$, replace $\psi_{I+1,J}^1$ by $\psi_{I+1,J}^2$, leave $\psi_{I+1,J}^0$ unchanged and compute the next approximation from equation (3-23). Otherwise replace $\psi_{I+1,J}^0$ by $\psi_{I+1,J}^1$, leave $\psi_{I+1,J}^2$ unchanged and compute the next approximation from (3-23).

Although this method usually does not converge as fast as the Newton-Raphson method, it is more stable and always converges to the solution value if the function changes sign around this value.

If a solution to equation (3-18) is found to be $\psi_{I+1,J}^*$, then it will be used in the following equation to carry out the relaxation process

$$\psi_{I+1,J}^1 = \psi_{I+1,J}^0 + \beta(\psi_{I+1,J}^* - \psi_{I+1,J}^0) \quad (3-24)$$

where β is the relaxation factor. A successive relaxation method [39,42] will be used to calculate the values of $T_{I+1,J}$ and $\psi_{I+1,J}$ from equations (3-17) and (3-24).

Computational Procedures

Most of the calculations were carried out with a Univac-1108 electronic digital computer. The computer programs involved are presented in Appendix B. The following logic steps were taken in computing the desired quantity:

- (1) Calculate initial values of ψ and T with equations (2-38) and (2-39). These are the stream functions and shear stresses of a one-dimensional Cassonian flow between two parallel plates with nonpermeable walls. Mathematical operations in obtaining equations (2-38) and (2-39) are presented in Appendix A.
- (2) The stream function ψ and the shear stress T on the central plane, which is the lower boundary of the flow field to be studied, are set equal to zero.
- (3) The stream function on the upper permeable wall, which is the upper boundary of the flow field to be studied, is calculated according to the boundary condition $\psi = 1 - V_0 X$ on the permeable wall.
- (4) In order to reduce the number of iterations needed, a first estimation of $\psi_{I,J}$ is made by the following relation

$$\psi_{I,J} = \left(\frac{\psi_{I, \text{wall}}}{\psi_{0, \text{wall}}} \right) \psi_{0,J}$$

- (5) New values of ψ on the first line are calculated with iteration equations (3-22) and (3-24) until the difference in the values of ψ between two successive iterative steps is less than ϵ_1 (input data) at each interior point on the first line.
- (6) New values of ψ in the downstream flow field are calculated by iteration equations (3-23) and (3-24).
- (7) New values of T are calculated by equation (3-17).

CHAPTER IV

RESULTS AND DISCUSSION

The present chapter is devoted to the presentation and discussion of numerical experiments on the ultrafiltration of a Cassonian fluid between two parallel membranes. The greatest portion of the numerical calculations was carried out with the aid of a Univac-1108 electronic digital computer at the Georgia Institute of Technology Rich Electronic Computer Center. A small portion of the calculations was made on the CDC CYBER 74 electronic digital computer after the Computer Center made the change from Univac to CDC.

Various rectangular grid steps were used to test the accuracy of the calculations. It was found that 100 grid points in the X-direction and 25 grid points in the Y-direction were sufficiently small to give excellent results. The X to Y grid step ratio, s , used in the calculations was 25, which was close to the maximum value that would not affect the convergence of the iteration process.

The results were plotted with a Calcomp plotter and are presented graphically. Five different types of plots are presented for the easy visualization of the effect of the different variables on the flow. The five types of plots are: (1) streamlines and shear-stress contours in the XY plane, (2) stream function and shear stress in steps of X vs Y, (3) V_x in steps of X vs Y, (4) pressure on the central plane vs X, (5) V_y in steps of X vs Y.

The streamline and shear-stress contours were plotted with the aid of the GPCP (General Purpose Contouring Program) program by California Computer Products [43].

The half distances between the parallel membranes are 0.005 cm, 0.01 cm and 0.05 cm. The entrance Reynolds number R_x ($4U_0 H_0 / k^2$) covers the range from 0.25 to 25. The wall Reynolds number R_y ($v_0 H_0 / k^2$) covers the range from zero to 0.025 (Tables 1, 2).

Results are presented and discussed in four sections: (1) Comparison of iterative and analytical results in limiting cases. (2) Effect of wall suction rate on the flow. (3) Effect of finite yield stress on the flow. (4) Some mutually related variables.

Comparison of Iterative and Analytical Results in Limiting Cases

It is difficult to make a truly comparative evaluation of this study because no experimental or other numerical work could be found on two-dimensional Cassonian flow. However, the logic and validity of the computational procedures can be checked out in two ways.

(1) By setting the finite shear stress τ_0 to zero in the input data, the problem is reduced to a two-dimensional Newtonian flow whose analytical solution can be obtained as the following equation:

$$\psi = \frac{Y}{2} (3 - Y^3)(1 - V_0 X) \quad (3-25)$$

A comparison of the values calculated with the equation above and the values obtained with the iterative procedure at selected grid points is presented in Table 3. It can be seen that the agreement is excellent. Only the last two digits differ from the analytical values

Table 1. Values of Variables Studied in Cassonian Flow

H	τ_0	R_x	R_y
0.01	0.0400	1.00	0.00000
0.01	0.0400	1.00	0.00025
0.01	0.0400	1.00	0.00050
0.01	0.0400	1.00	0.00075
0.01	0.0400	1.00	0.00100
0.01	0.0400	1.00	0.00150
0.01	0.0400	1.00	0.00200
0.01	0.0000	1.00	0.00100
0.01	0.0100	1.00	0.00100
0.01	0.0400	1.00	0.00100
0.01	0.0800	1.00	0.00100
0.01	0.2000	1.00	0.00100
0.01	1.0000	25.00	0.02500
0.01	0.0100	0.25	0.00025
0.05	0.0016	1.00	0.00100
0.005	0.1600	1.00	0.00100
0.05	0.0400	25.00	0.02500

Table 2. Values of Variables Studied in Newtonian Flow

H	R_x	R_y
0.01	1.00	0.00000
0.01	1.00	0.00050
0.01	1.00	0.00100
0.01	1.00	0.00200
0.01	25.00	0.02500
0.01	0.25	0.00025
0.05	1.00	0.00100
0.005	1.00	0.00100

Table 3. Comparison of Iterative and Analytical Values of ψ
 Case 1: Reduced to Newtonian Flow

($\tau_0 = 0$; $H = 0.01$; $R_x = 1.00$; $R_y = 0.001$)

	X	Y						
		0.0	0.2	0.4	0.6	0.8	1.0	
Analytical	0	0.0000000	0.2960000	0.5680000	0.7920000	0.9440000	1.0000000	
Iterative		0.0000000	0.2960000	0.5680000	0.7920000	0.9440000	1.0000000	
A	20	0.0000000	0.2723200	0.5225600	0.7286400	0.8684800	0.9200000	
I		0.0000000	0.2723200	0.5225605	0.7286445	0.8684809	0.9200000	
A	40	0.0000000	0.2486400	0.4771200	0.6652800	0.7929600	0.8400000	
I		0.0000000	0.2486400	0.4771204	0.6652841	0.7929609	0.8400000	
A	60	0.0000000	0.2249600	0.4316800	0.6019200	0.7174400	0.7600000	
I		0.0000000	0.2249600	0.4316804	0.6019237	0.7174408	0.7600000	
A	80	0.0000000	0.2012800	0.3862400	0.5385600	0.6419200	0.6800000	
I		0.0000000	0.2012800	0.3862403	0.5385633	0.6419207	0.6800000	
A	100	0.0000000	0.1776000	0.3408000	0.4752000	0.5664000	0.6000000	
I		0.0000000	0.1776000	0.3408003	0.4752030	0.5664006	0.6000000	

at but a few grid points in the worst cases.

(2) By setting the wall flux velocity v_0 equal to zero ($R_y = 0$) in the input data, the problem is reduced to a one-dimensional Cassonian flow whose analytical solution is derived in Appendix A as:

$$\psi = \frac{Y}{K^2} \left[\frac{1}{2} P_f \left(1 - \frac{Y}{3} \right) - \frac{4}{3} T_0^{1/2} P_f^{1/2} \left(1 - \frac{2}{5} Y^{3/2} \right) + T_0 \left(1 - \frac{Y}{2} \right) \right] \quad (3-26)$$

$$\text{where} \quad P_f = \frac{6}{5} T_0^{1/2} + \left(3K^2 - \frac{3}{50} T_0 \right)^{1/2} \quad (3-27)$$

A comparison of the values calculated with the equation above and the values obtained with the iterative procedure at selected grid points is presented in Table 4. The analytical value is a function of Y only since there is no wall flux. The iterative value did change between $X=0$ and $X=20$ but stabilized with greater X values. The largest deviation of the iterative value from the analytical value is somewhat larger than in the Case 1 comparison but is still less than 0.05% from the analytical value. The agreement can still be considered excellent.

The excellent results of the two comparisons made above indicate that the logic and iterative procedures developed in this study are valid and sound.

Effect of Finite Yield Stress (τ_0)

The finite yield stress τ_0 is a characteristic term in the Casson equation (1-1). The average value of τ_0 is 0.04 dyne/cm² for normal

Table 4. Comparison of Iterative and Analytical Values of ψ
 Case 2: Reduced to One-Dimensional Flow

($\tau_0 = 0.04$; $H = 0.01$; $R_x = 1.00$; $R_y = 0.00$)

	X	Y						
		0.0	0.2	0.4	0.6	0.8	1.0	
Analytical	0	0.000000	0.2916688	0.5626277	0.7881719	0.9426581	1.0000000	
Iterative		0.0000000	0.2916687	0.5626277	0.7881718	0.9426581	1.0000000	
A	20	0.0000000	0.2916688	0.5626277	0.7881719	0.9426581	1.0000000	
I		0.0000000	0.2914968	0.5625684	0.7881460	0.9426412	1.0000000	
A	40	0.0000000	0.2916688	0.5626277	0.7881719	0.9426581	1.0000000	
I		0.0000000	0.2914968	0.5625684	0.7881460	0.9426412	1.0000000	
A	60	0.0000000	0.2916688	0.5626277	0.7881719	0.9426581	1.0000000	
I		0.0000000	0.2914968	0.5625684	0.7881460	0.9426412	1.0000000	
A	80	0.0000000	0.2916688	0.5626277	0.7881719	0.9426581	1.0000000	
I		0.0000000	0.2914968	0.5625684	0.7881460	0.9426412	1.0000000	
A	100	0.0000000	0.2916688	0.5626277	0.7881719	0.9426581	1.0000000	
I		0.0000000	0.2914968	0.5625684	0.7881460	0.9426412	1.0000000	

human blood. To study the effect of this variable on the flow, four other values of τ_0 were assumed. They are 0, 0.01, 0.08 and 0.2. All other variables were kept the same so that the effect of τ_0 could be isolated. The half distance between the two membranes was 0.01 cm. The entrance Reynolds number (R_x) was 1.0 and the wall Reynolds number was 0.001. The results are presented in the following groups of plots:

(1) The contours of stream function (ψ) and shear stress (T_{yx}) in the XY plane are presented in Figures 7 through 11. In Figure 7, τ_0 takes the value of zero and hence the yield stress term no longer exists. This reduces the flow to a Newtonian flow and this plot is essentially identical to the plot in Figure 7a which was made from the analytical solution of a two-dimensional creeping Newtonian flow. As the value of τ_0 increases from zero to 0.2, the changes in stream line contours are too small to be observed in these plots while the shear-stress contours move in from the wall appreciably indicating an increase in shear stress when the value of the finite stress term τ_0 increases.

(2) The stream function (ψ) and shear stress (T_{yx}) at selected values of X are plotted against Y in Figures 12 through 16. It can be observed that both the stream function (ψ) and the shear stress (T_{yx}) decrease with increasing values of X down the stream. The plot in Figure 12 is again reduced to that of a Newtonian flow with τ_0 set equal to zero. This plot is essentially the same as the plot in Figure 36 which was plotted from the analytical solution of a two-dimensional Newtonian flow. It can be seen in Figures 12 through 16 that the shear stress increases with increasing values of τ_0 .

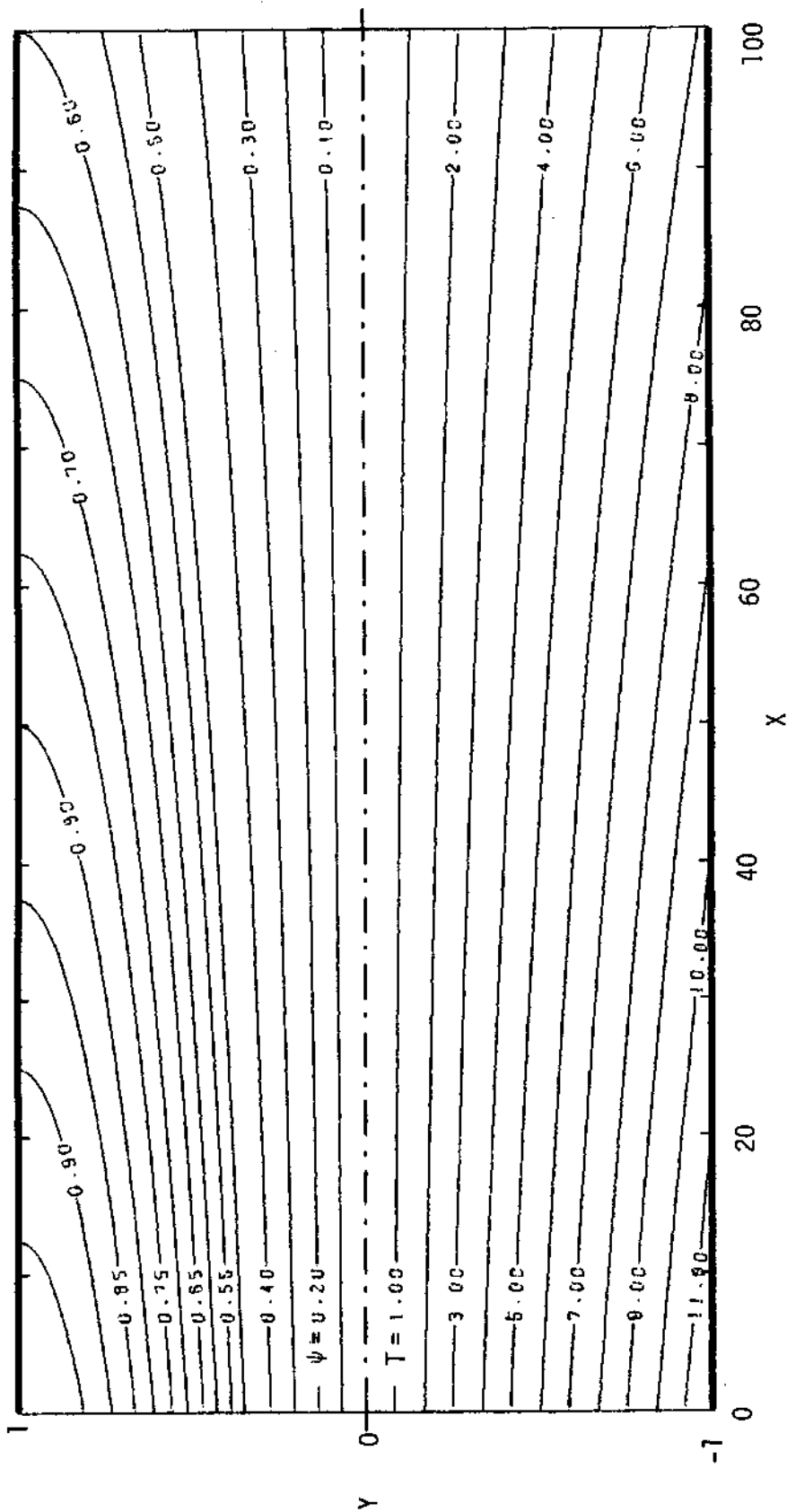


Figure 7. Contours of Stream Function (ψ) and Shear Stress (T_{yx})

Cassonian: $H = 0.01$ $\tau_0 = 0$
 $R_x = 1.0$ $R_y = 0.001$

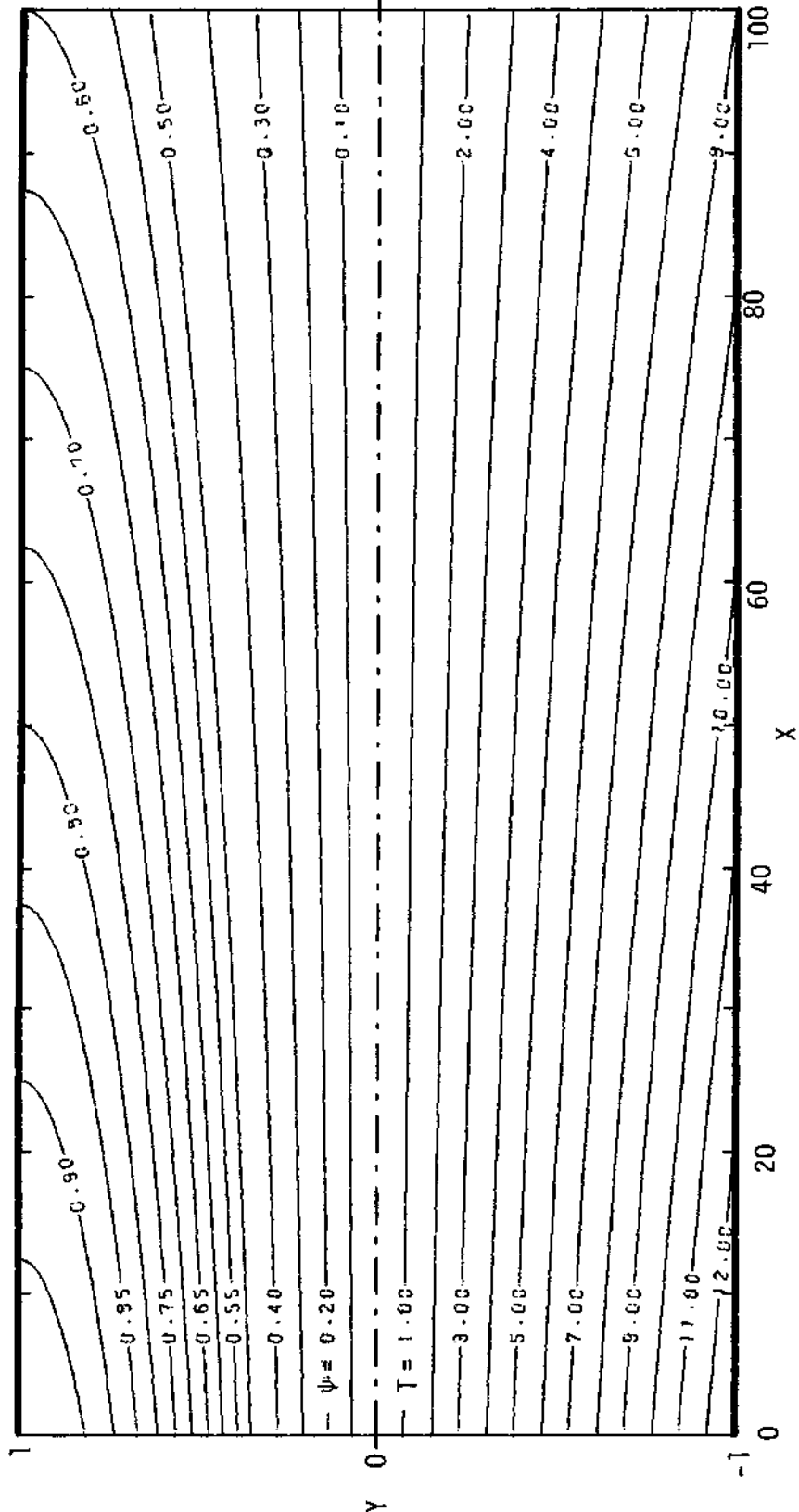


Figure 7a. Contours of Stream Function (ψ) and Shear Stress (T_{yx})

Newtonian: $H = 0.01$ $R_x = 1.0$ $R_y = 0.001$

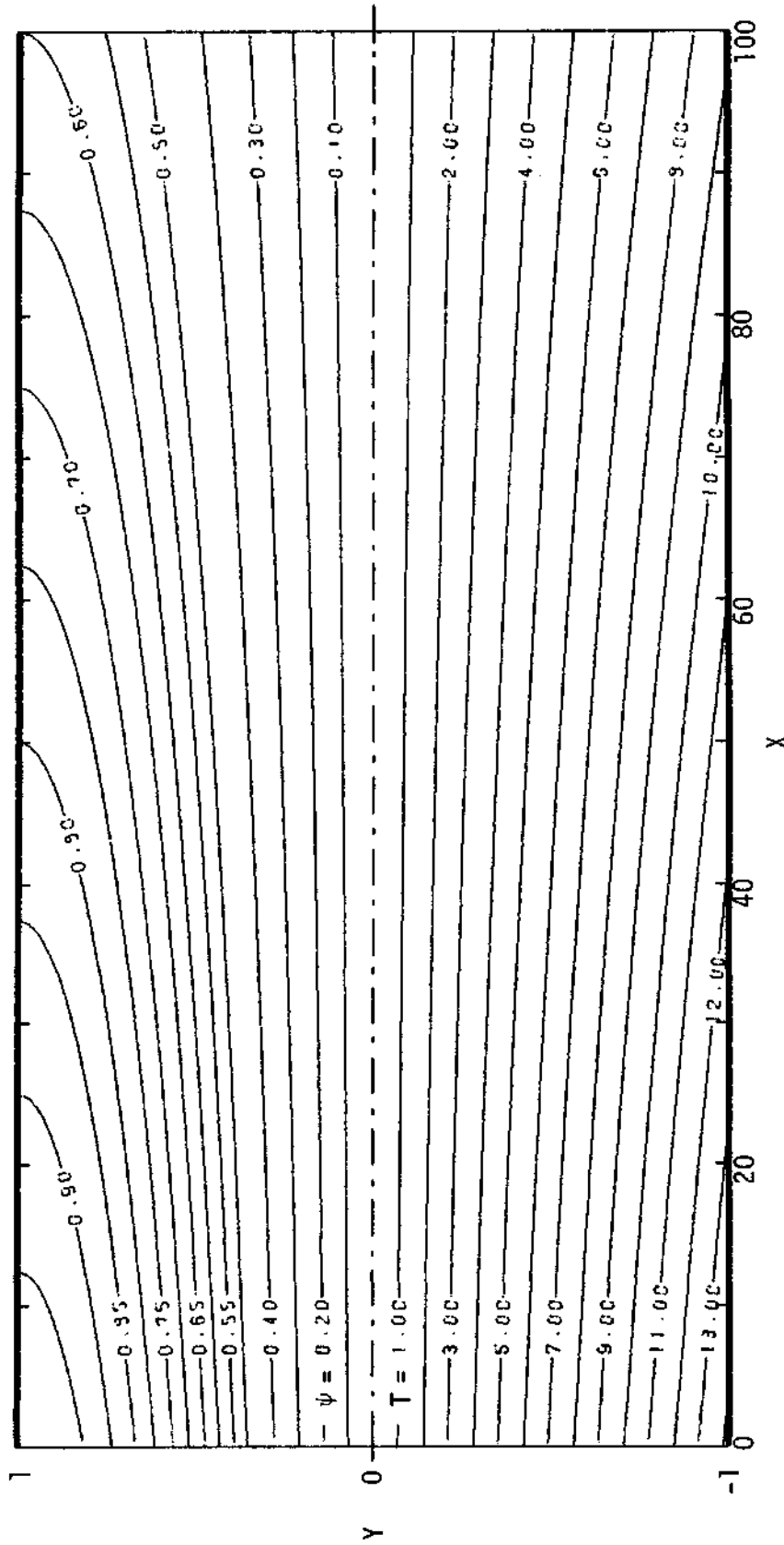


Figure 8. Contours of Stream Function (ψ) and Shear Stress (T_{yx})

Cassonian: $H = 0.01$ $\tau_0 = 0.01$

$R_x = 1.0$ $R_y = 0.001$

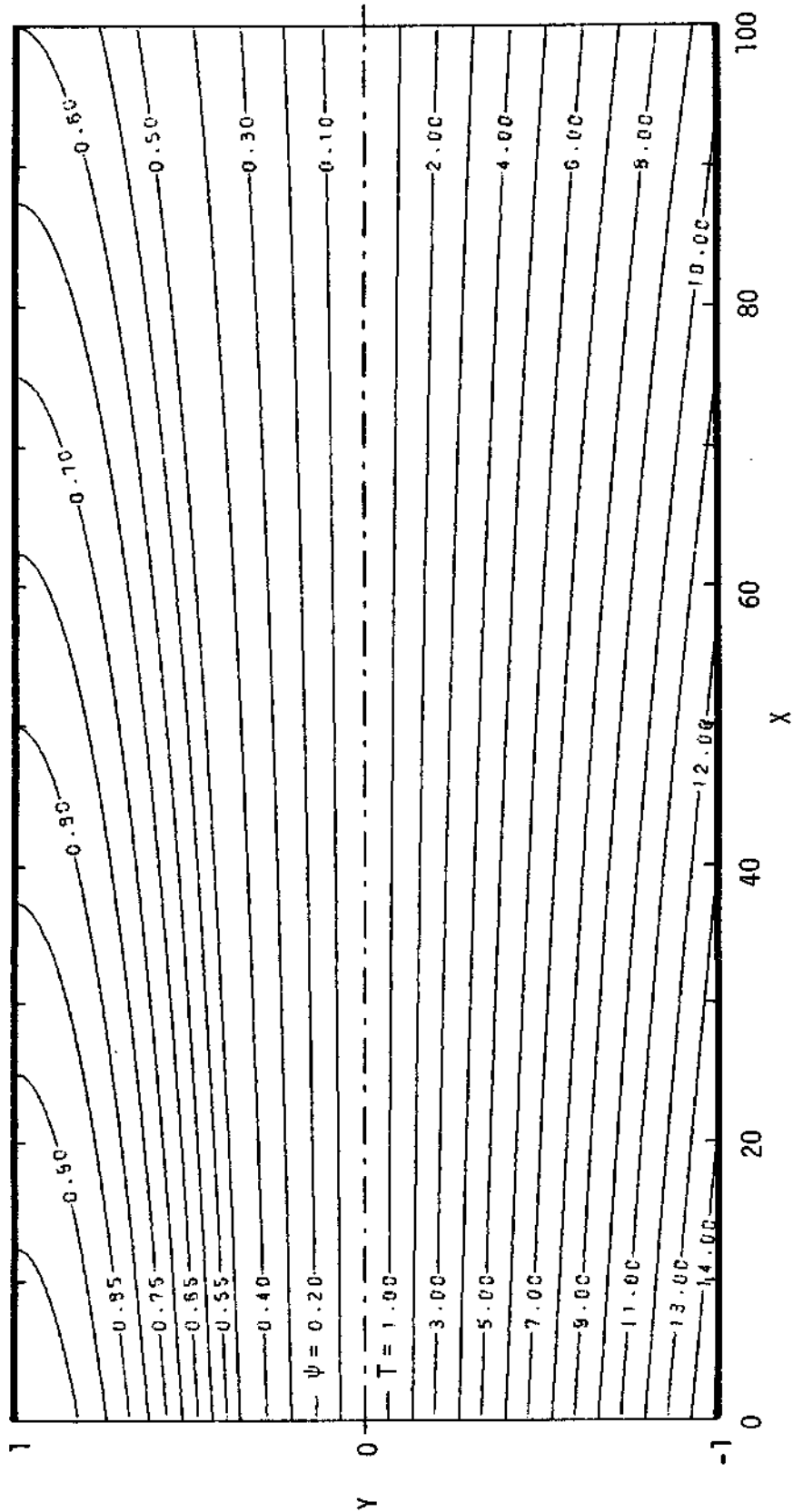


Figure 9. Contours of Stream Function (ψ) and Shear Stress (T_{yx})

Cassonian: $H = 0.01$ $\tau_0 = 0.04$

$R_x = 1.0$ $R_y = 0.01$

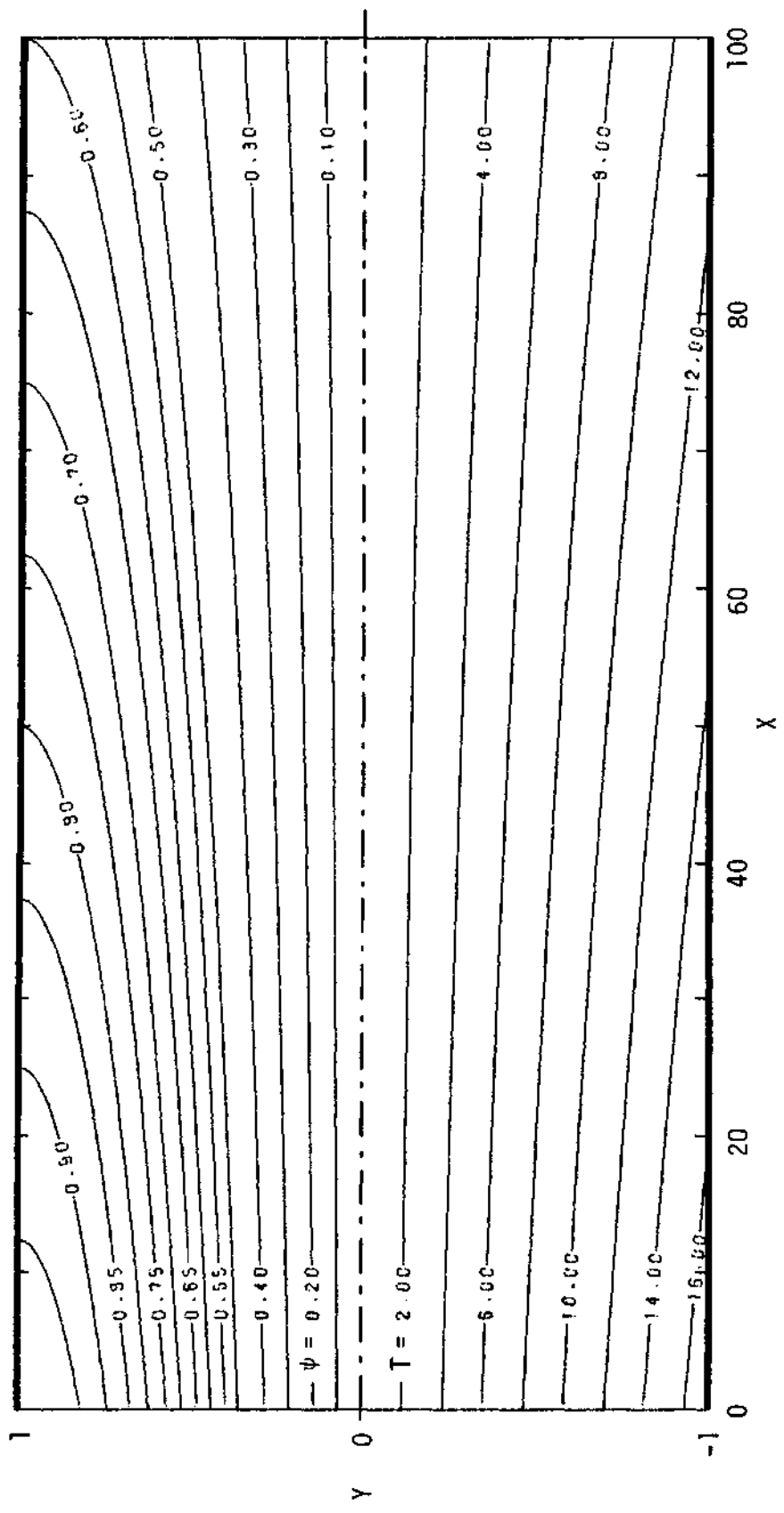


Figure 10. Contours of Stream Function (ψ) and Shear Stress (T_{yx})

Cassonian: $H = 0.01$ $\tau_0 = 0.08$
 $R_x = 1.0$ $R_y = 0.001$

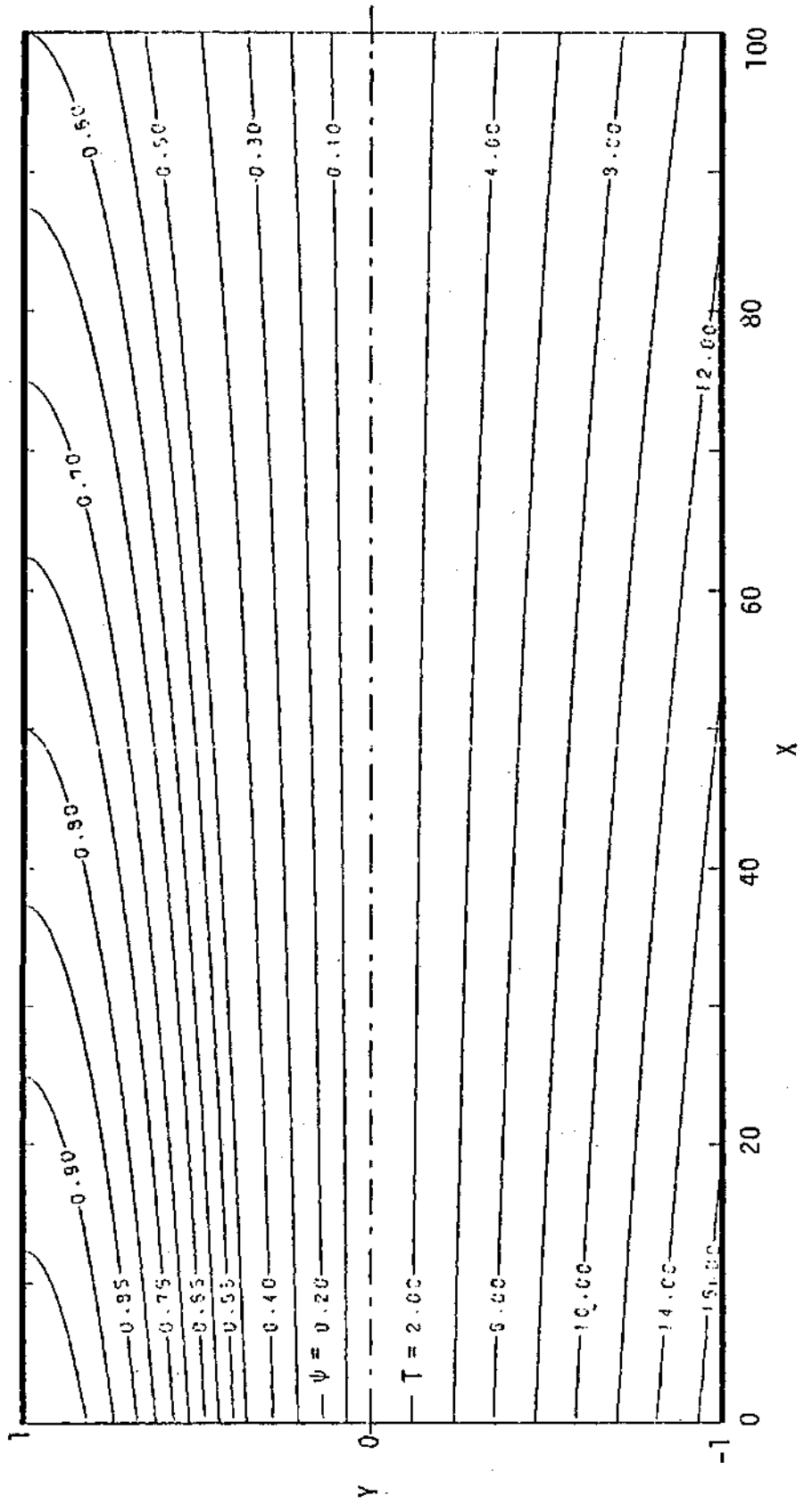


Figure 11. Contours of Stream Function (ψ) and Shear Stress (T_{yx})

Cassonian: $H = 0.01$ $\tau_0 = 0.2$
 $R = 1.0$ $R_y = 0.001$

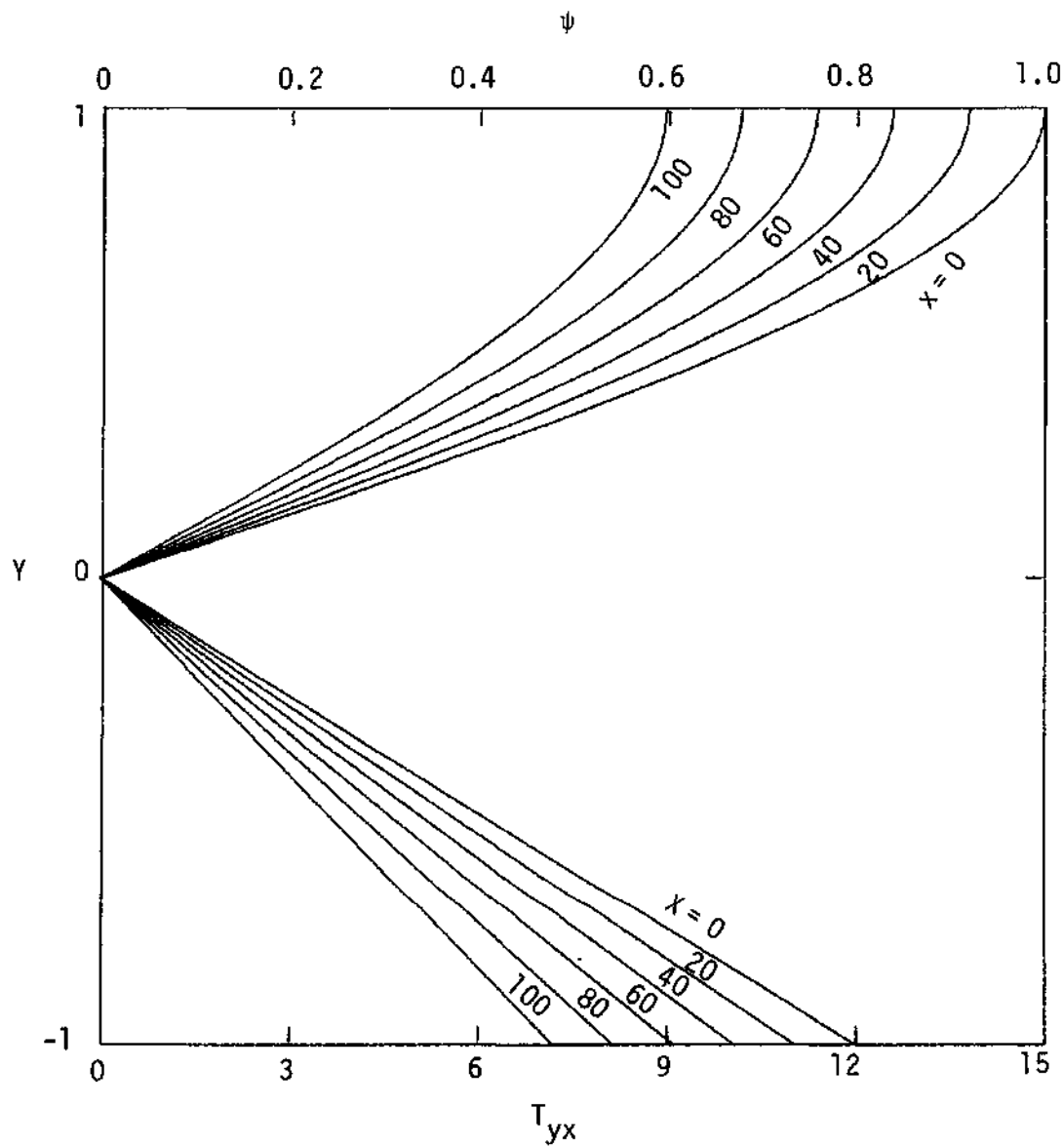


Figure 12. Stream Function (ψ) and Shear Stress (T_{yx}) vs Y

Cassonian: $H = 0.01$ $\tau_0 = 0$
 $R_x = 1.0$ $R_y = 0.001$

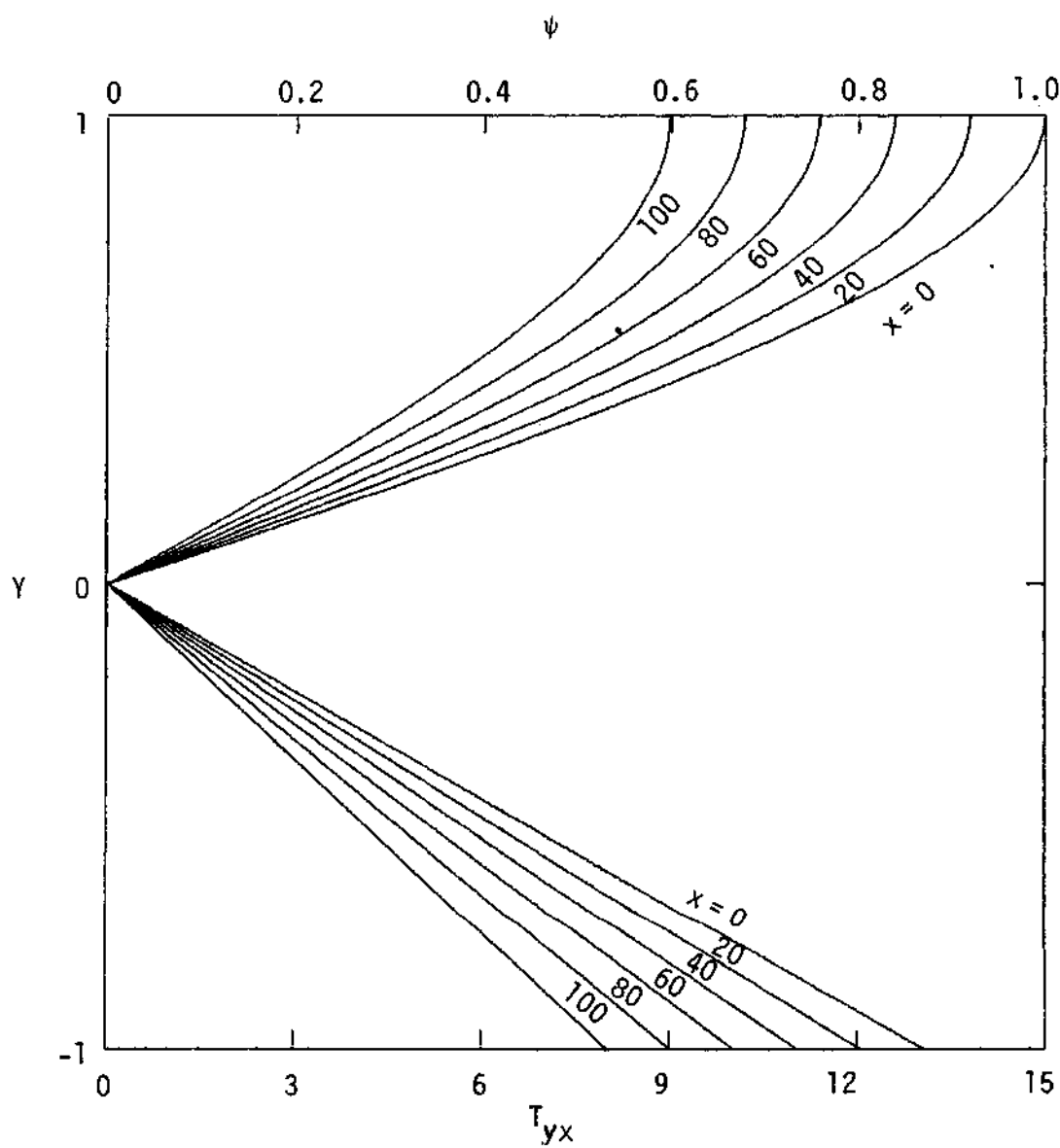


Figure 13. Stream Function (ψ) and Shear Stress (T_{yx}) vs Y

Cassonian: $H = 0.01$ $\tau_0 = 0.01$

$R_x = 1.0$ $R_y = 0.001$

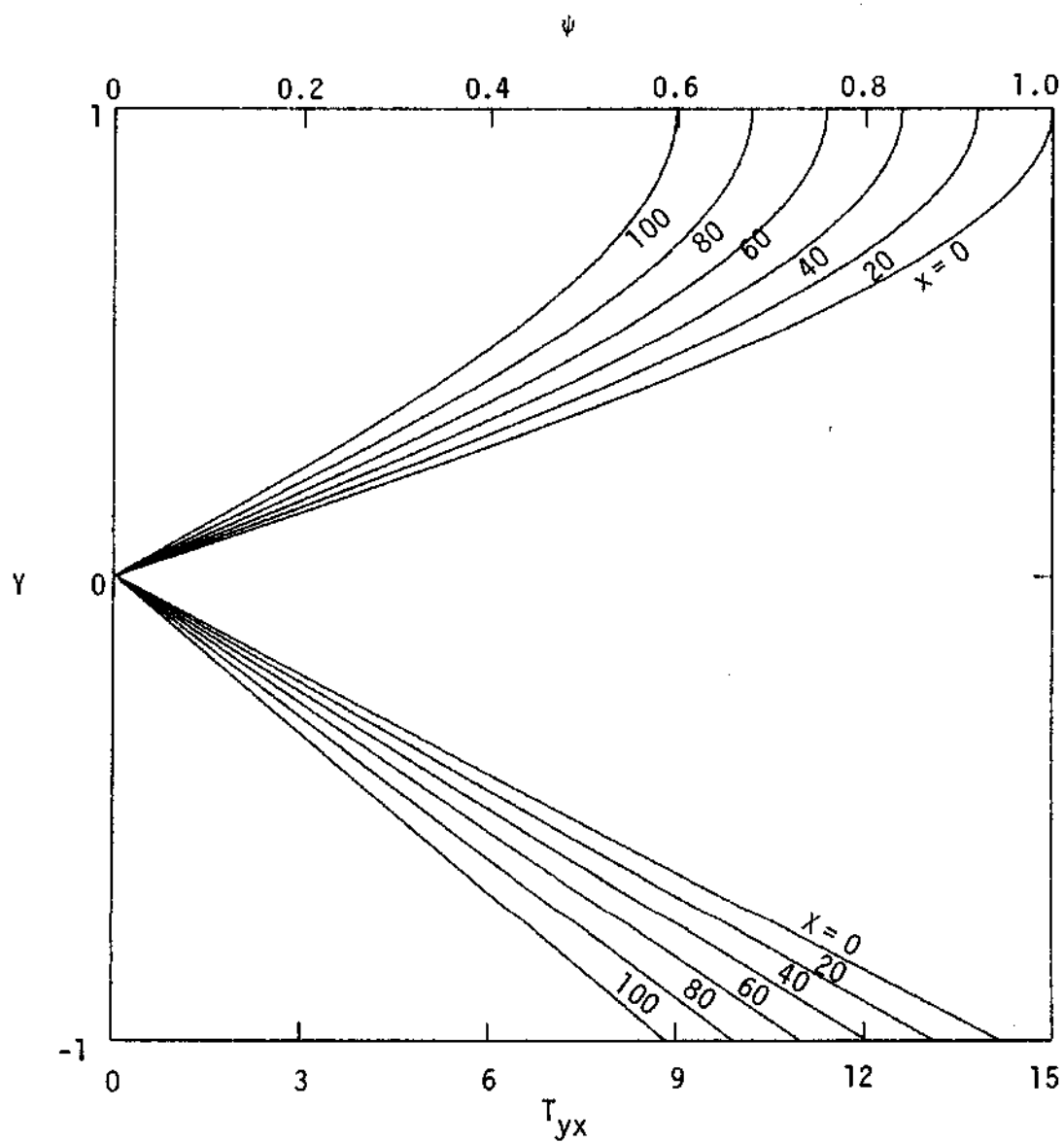


Figure 14. Stream Function (ψ) and Shear Stress (T_{yx}) vs Y .

Cassonian: $H = 0.01$ $\tau_0 = 0.04$

$R_x = 1.0$ $R_y = 0.001$

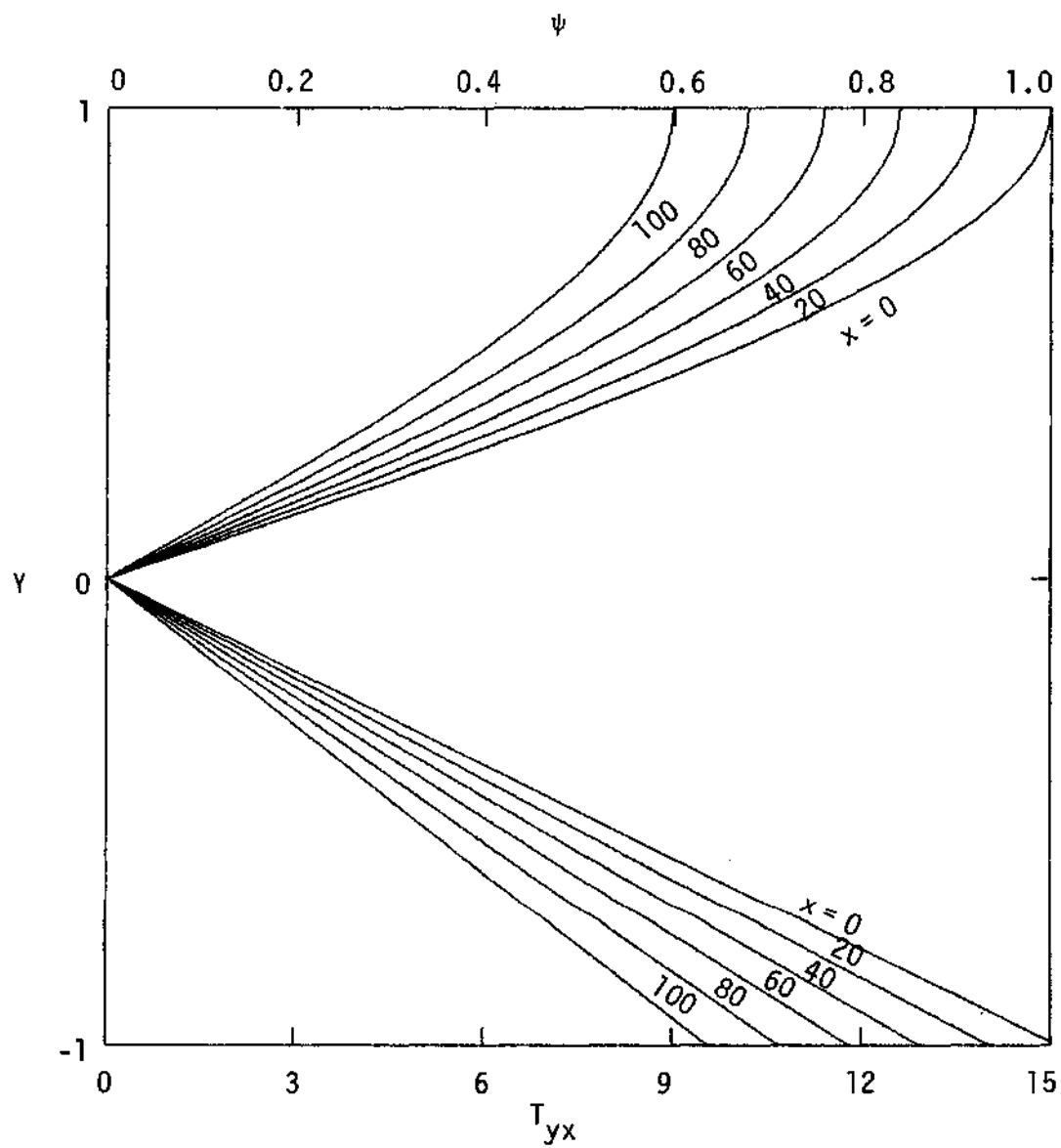


Figure 15. Stream Function (ψ) and Shear Stress (T_{yx}) vs Y .

Cassonian: $H = 0.01$ $\tau_0 = 0.08$
 $R_x = 1.0$ $R_y = 0.001$

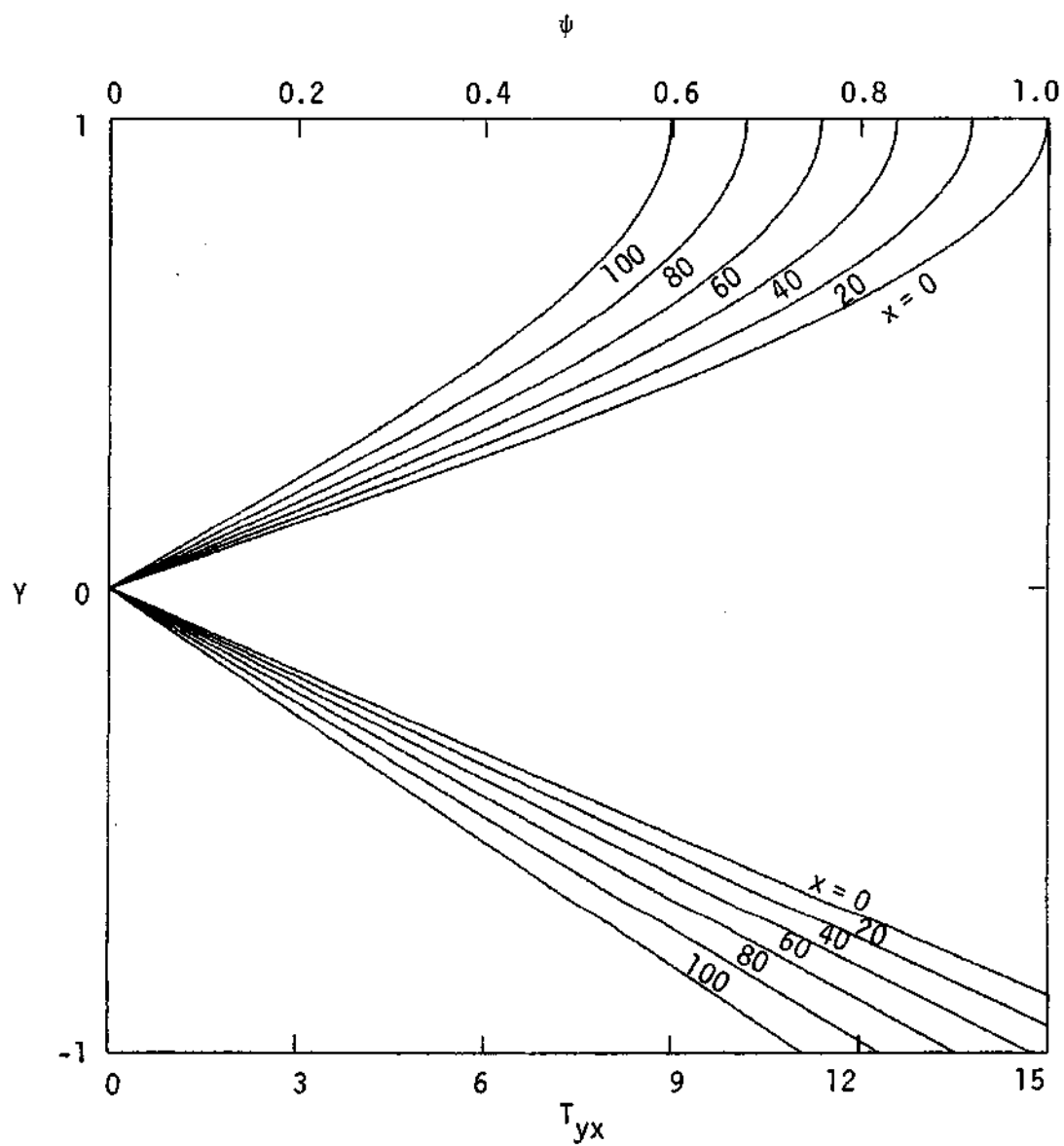


Figure 16. Stream Function (ψ) and Shear Stress (T_{yx}) vs Y .

Cassonian: $H = 0.01$

$\tau_0 = 0.2$

$R_x = 1.0$

$R_y = 0.001$

(3) The velocity component in the X direction (V_x) is plotted against Y in Figures 17 through 21. It can be seen that the plug flow close to the center plane becomes more prominent as the value of the finite yield stress term τ_0 increases. When τ_0 is set equal to zero in Figure 17, the flow becomes Newtonian and there is no plug flow. The maximum dimensionless velocity $(V_x)_{\max}$, which is $(v_x)_{\max}/U_0$, equals 1.5 as predicted for Newtonian flow.

(4) The pressure on the central plane is plotted against X in Figure 22. It can be seen that the existence of a finite yield stress causes greater pressure drop.

Effect of Wall Suction Rate (R_y)

The effect of wall suction on the flow was studied by changing the value of the wall Reynolds number R_y while holding the other variables constant. The half distance between the two parallel membranes was again 0.01 cm. The entrance Reynolds number (R_x) was 1.0 and the yield stress τ_0 was 0.04 dyne/cm². The wall Reynolds numbers were 0, 0.00025, 0.0005, 0.00075, 0.001, 0.0015 and 0.002. The results are presented in the following groups of plots:

(1) The contours of the stream function (ψ) and the shear stress are presented in Figures 23 through 29. When R_y is zero, the flow is reduced to one-dimensional. The stream function (ψ) and shear stress (T_{yx}) are independent of the value of X and the contours of both the stream function (ψ) and the shear stress go straight through the channel. When there is a suction on the wall, both the stream function and the

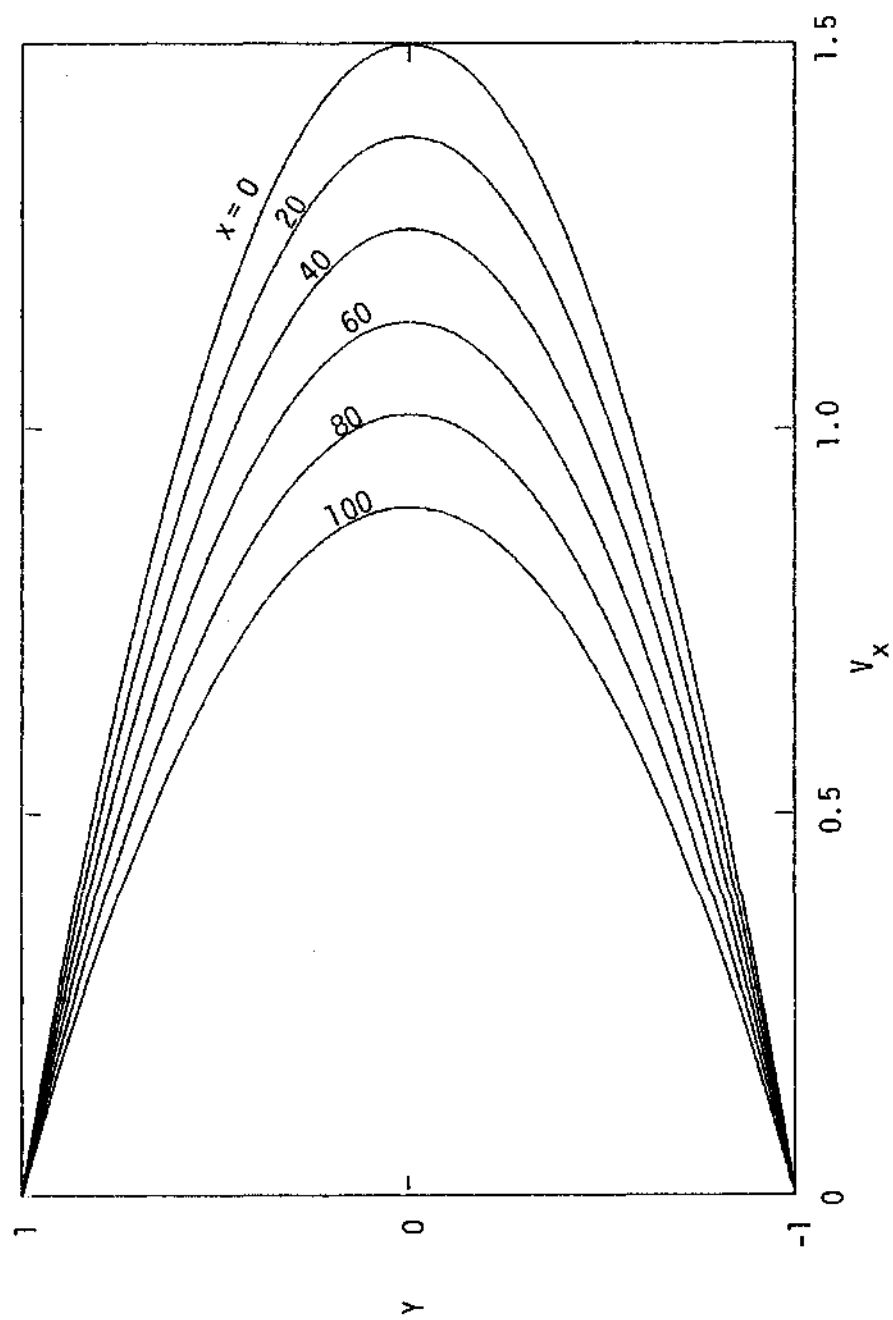


Figure 17. Velocity Profiles (V_x).

Cassonian: $H = 0.01$

$\tau_0 = 0$

$R_x = 1.0$

$R_y = 0.001$

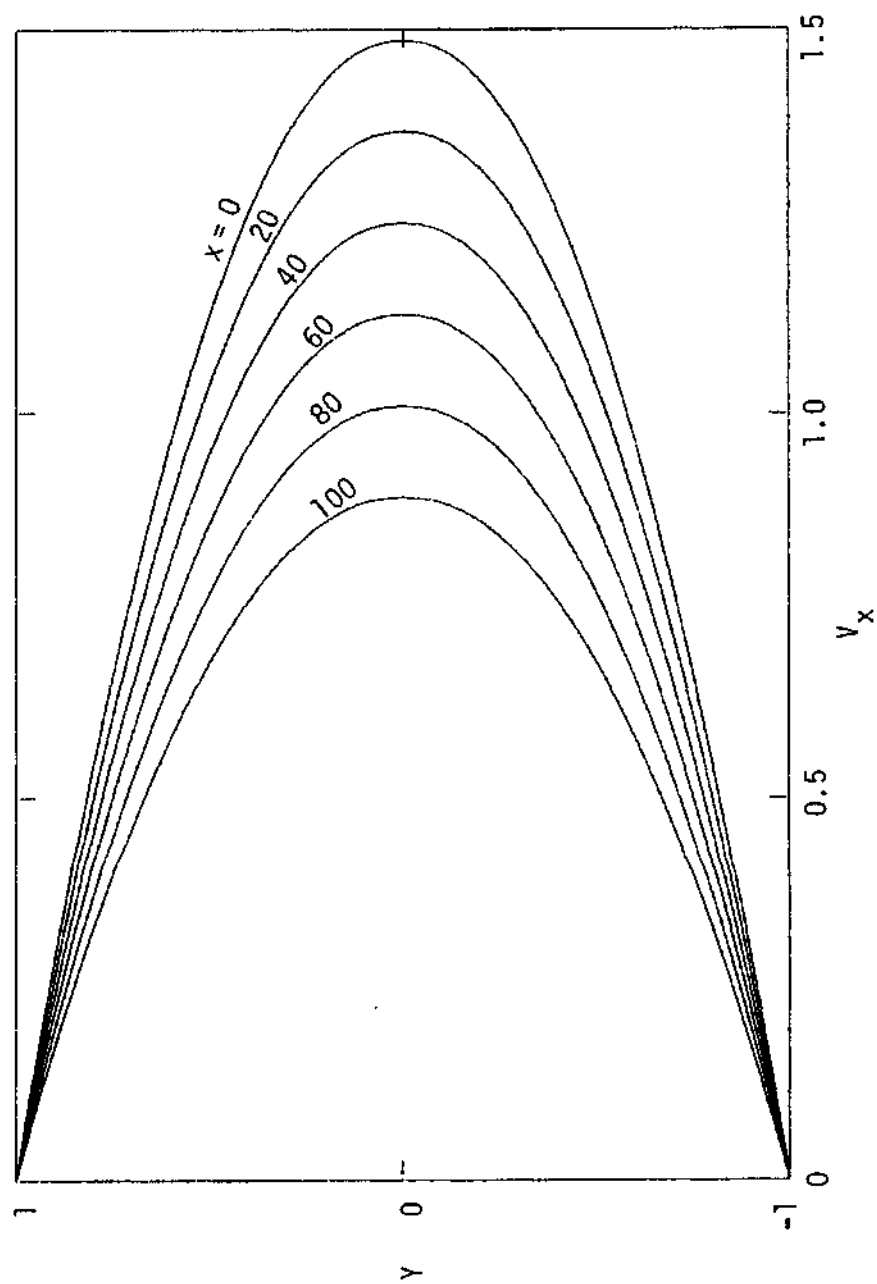


Figure 18. Velocity Profiles (V_x).

Cassonian: $H = 0.01$ $\tau_0 = 0.01$
 $R_x = 1.0$ $R_y = 0.01$

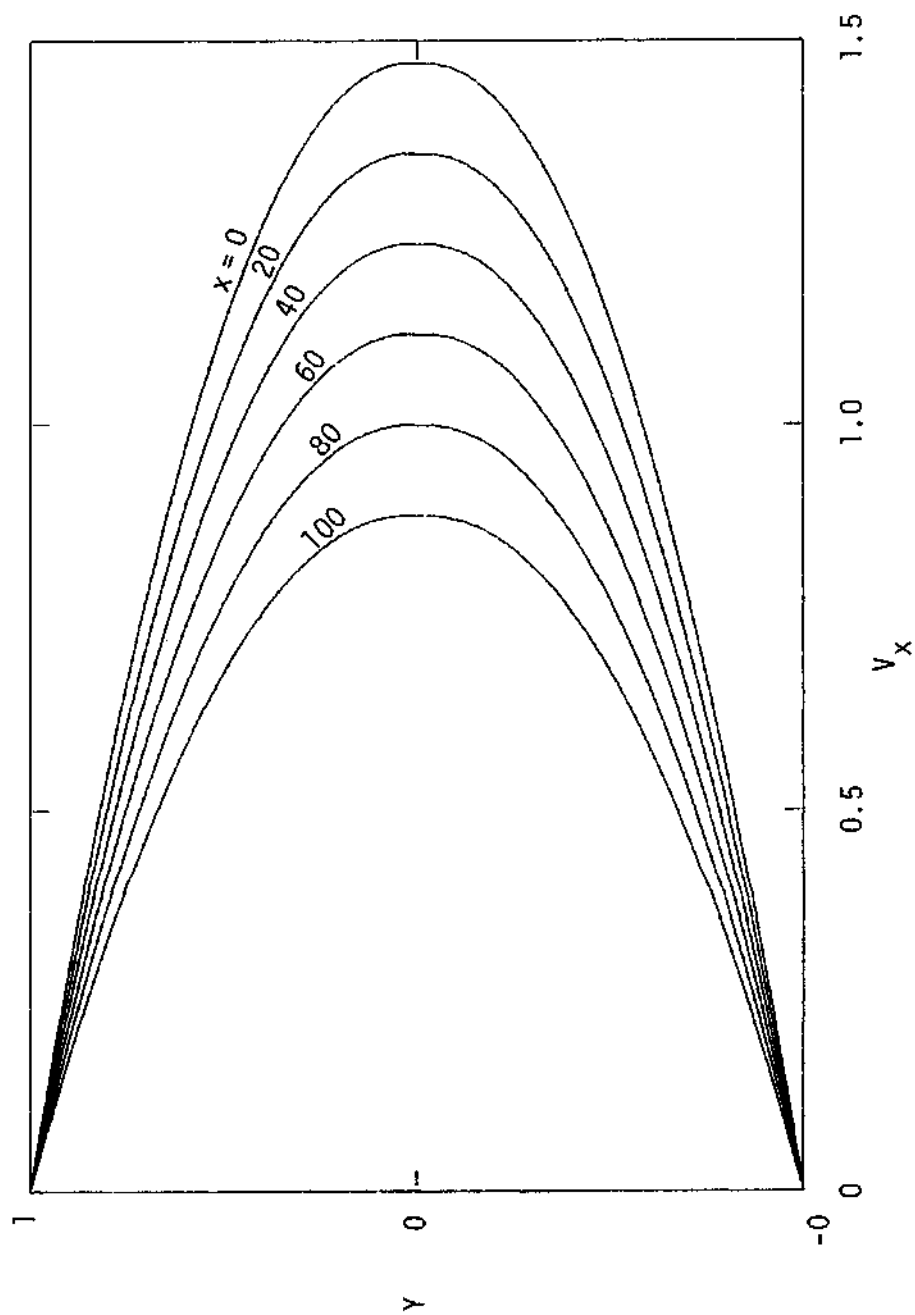


Figure 19. Velocity Profiles (V_x).

Cassonian: $H = 0.01$

$\tau_0 = 0.04$

$R_x = 1.0$

$R_y = 0.001$

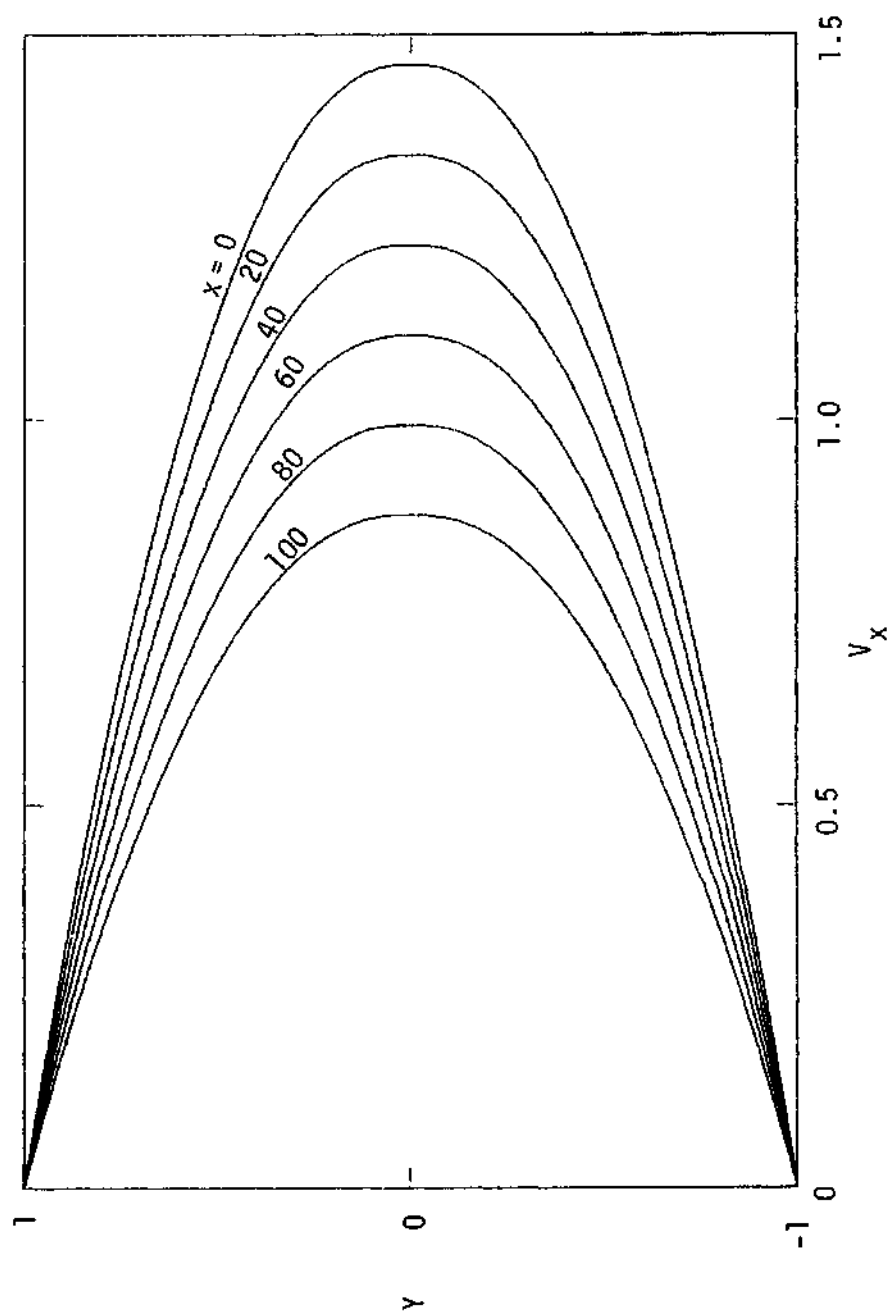


Figure 20. Velocity Profiles (V_x).

Cassonian: $H = 0.01$

$\tau_0 = 0.08$

$R_x = 1.0$

$R_y = 0.001$

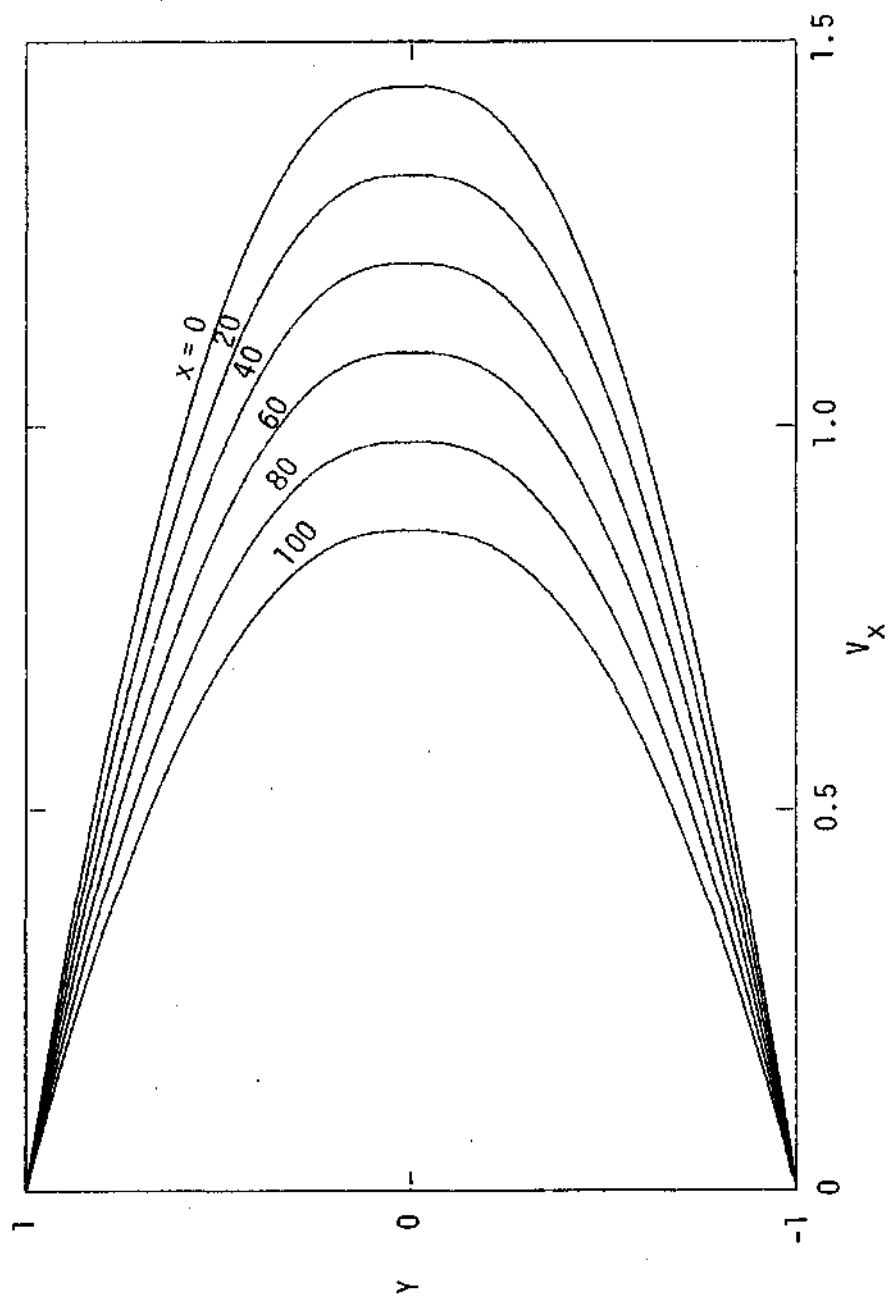


Figure 21. Velocity Profiles (V_x).

Cassonian: $H = 0.001$

$\tau_0 = 0.2$

$R_x = 1.0$

$R_y = 0.001$

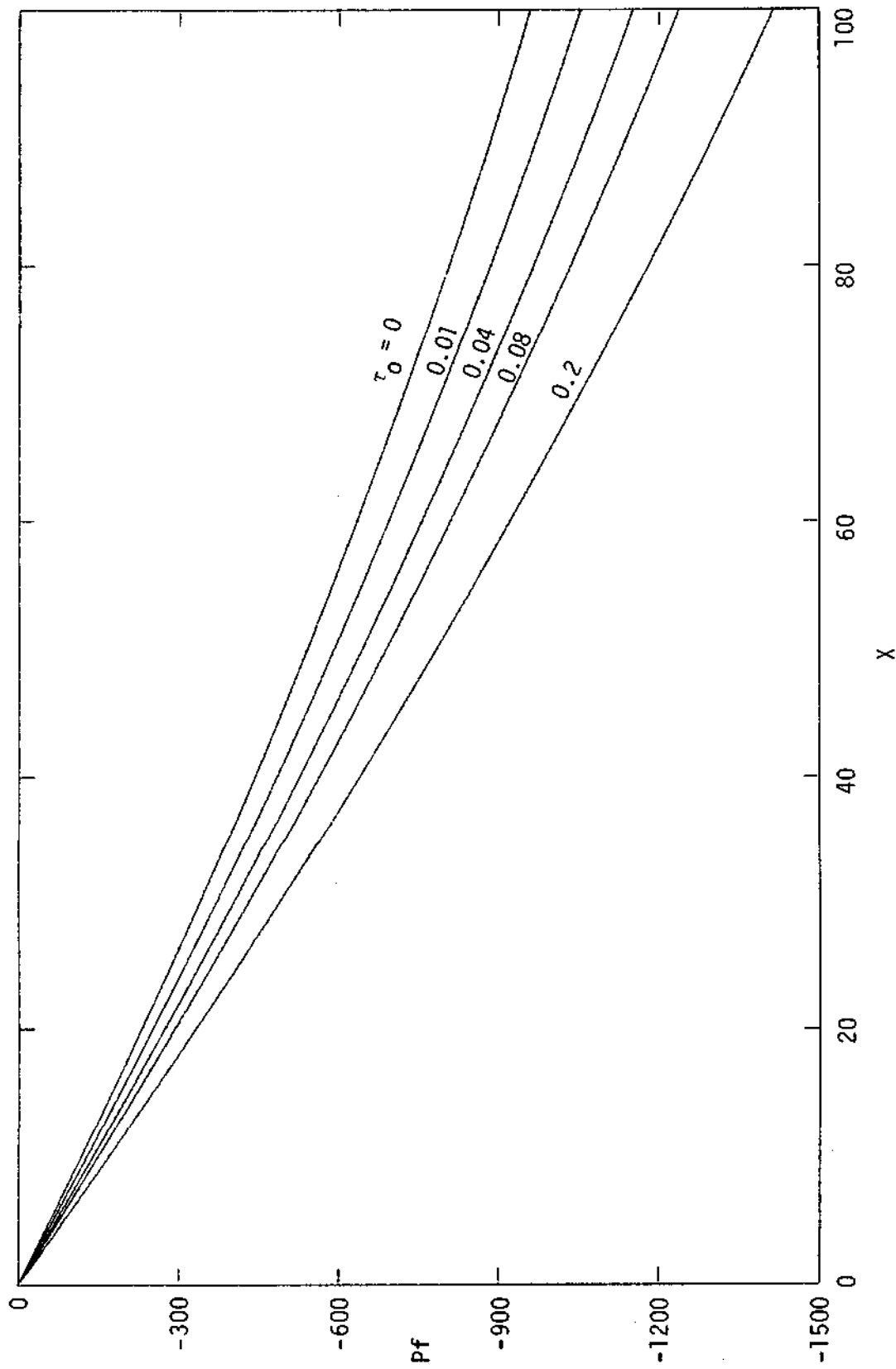


Figure 22. Pressure on the Central Plane vs. X

$$H = 0.01 \quad R_x = 1.0 \quad R_y = 0.001$$

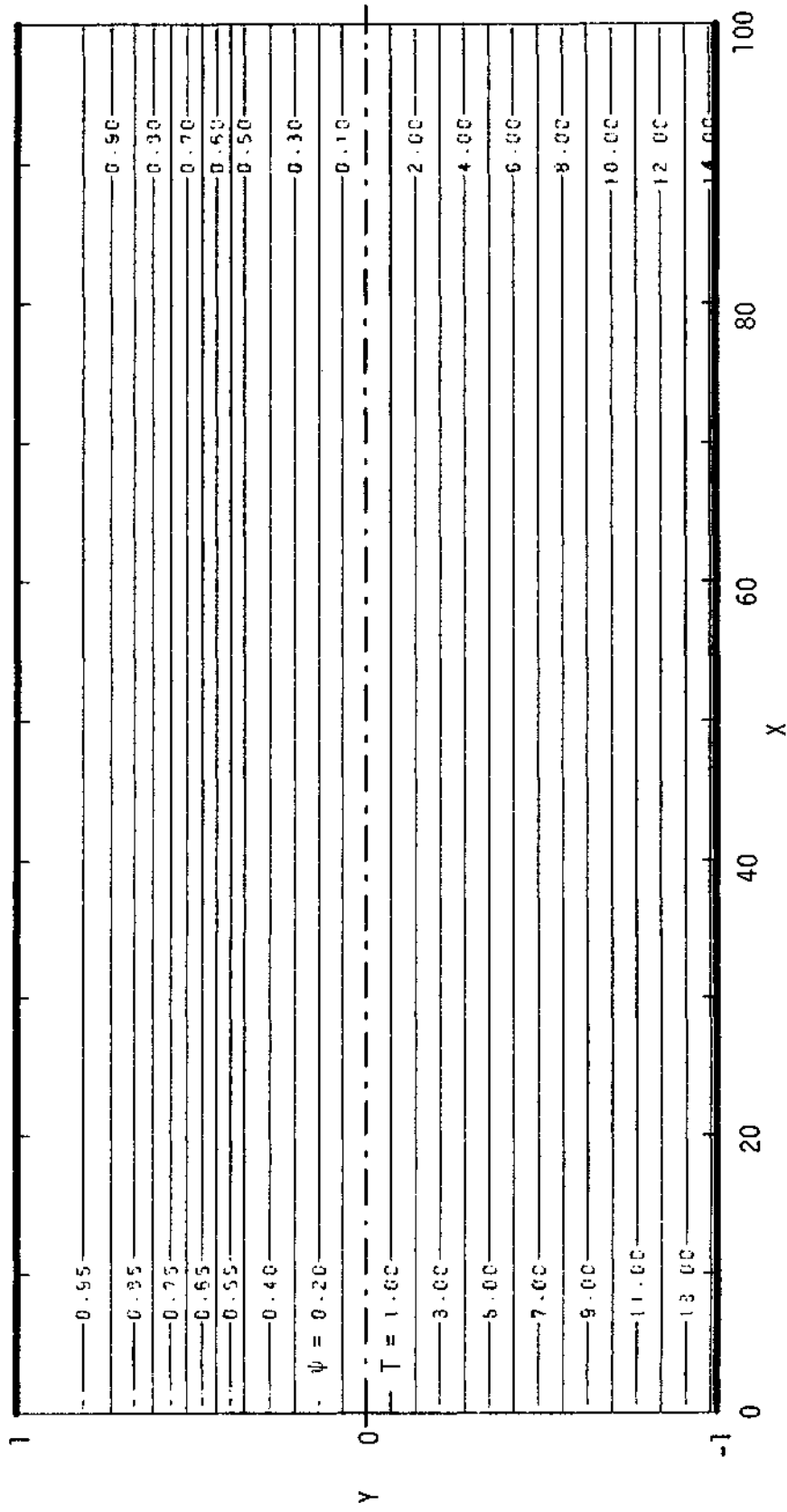


Figure 23. Contours of Stream Function (ψ) and Shear Stress (T_{yx})

Cassonian: $H = 0.01$ $\tau_0 = 0.04$
 $R_x = 1.0$ $R_y = 0$

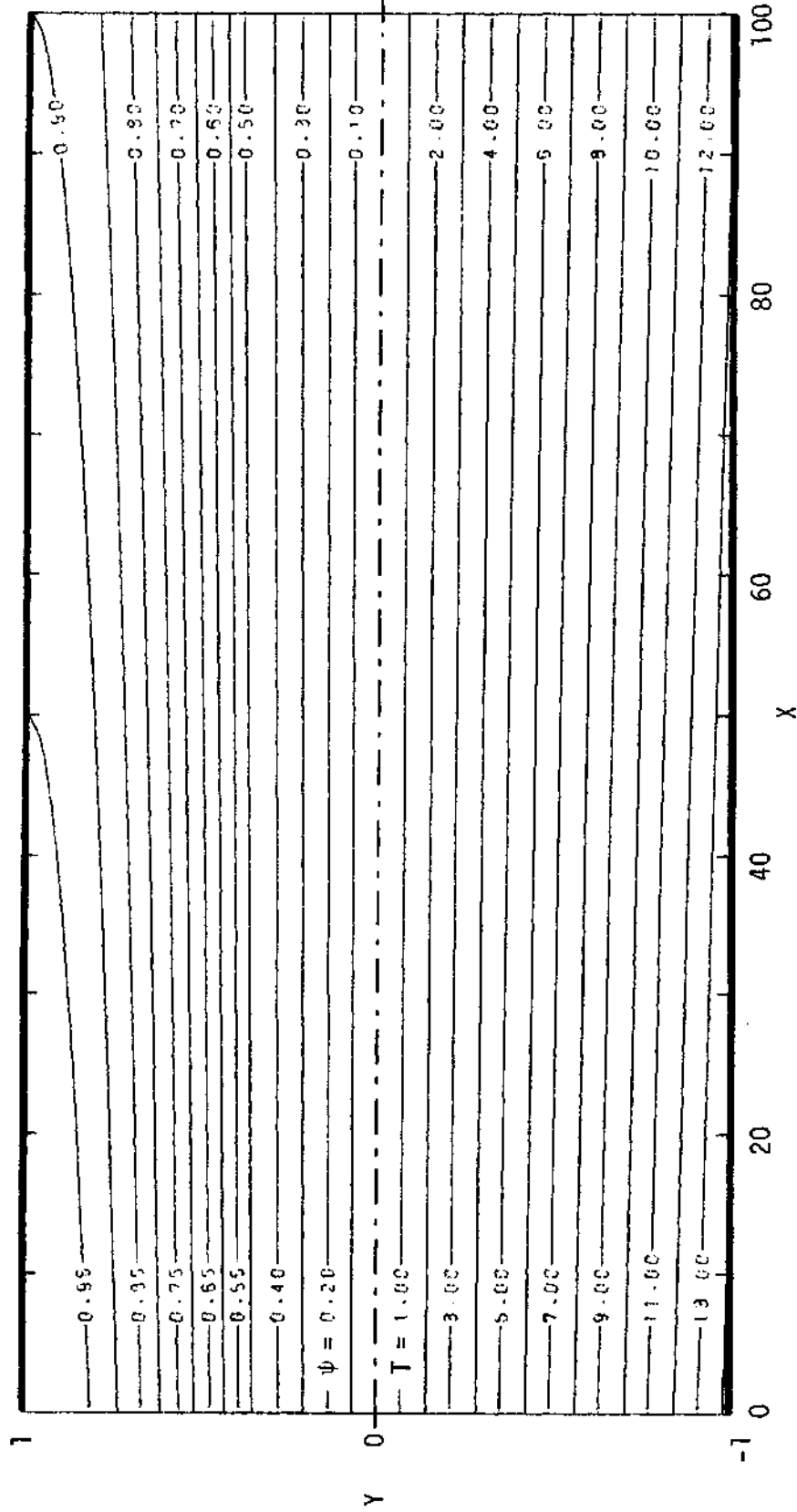


Figure 24. Contours of Stream Function (ψ) and Shear Stress (T_{yx})

Cassonian: $H = 0.01$ $\tau_0 = 0.04$
 $R_x = 1.0$ $R_y = 0.00025$

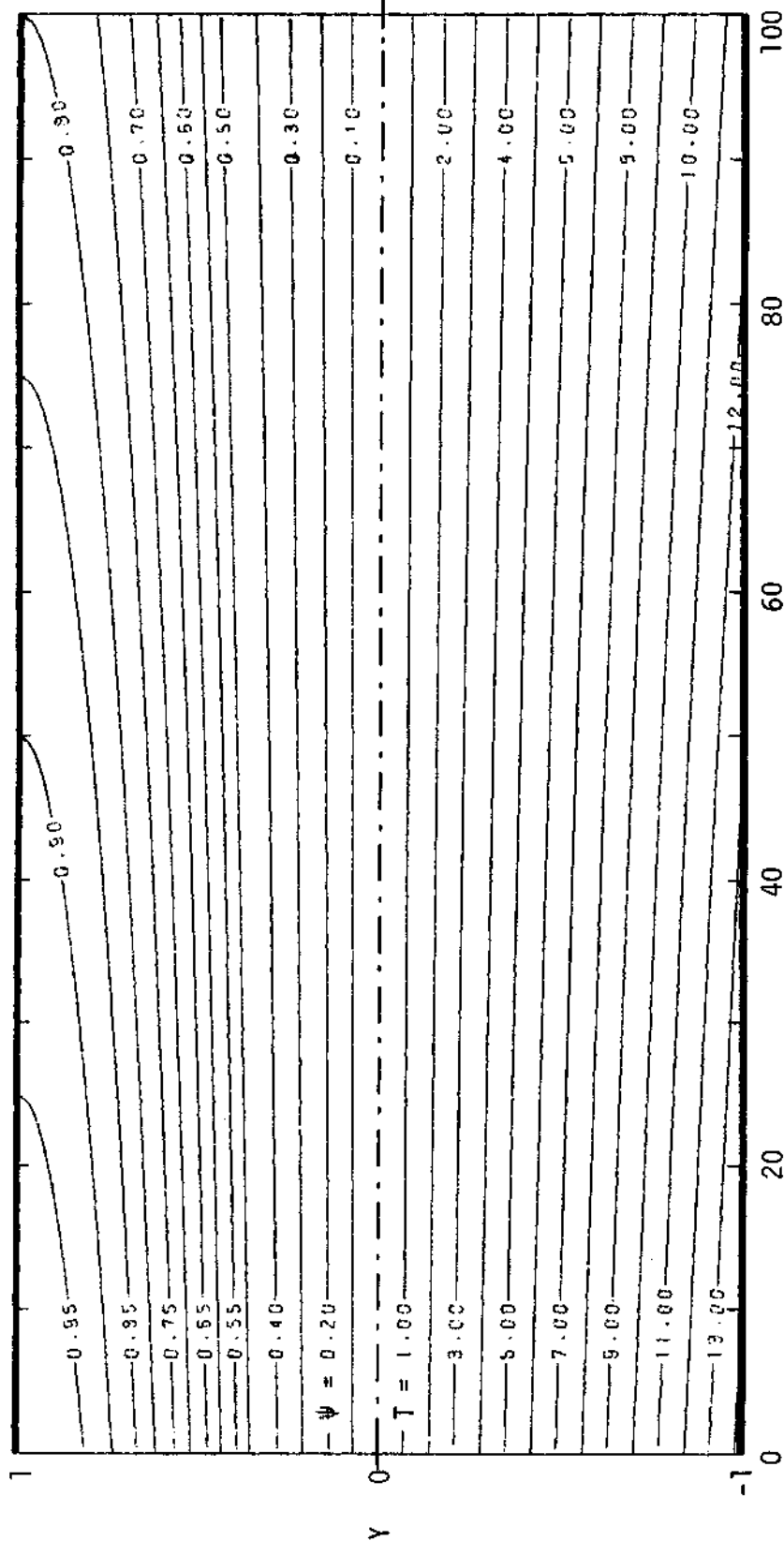


Figure 25. Contours of Stream Function (ψ) and Shear Stress (T_{yx})

Cassonian: $H = 0.01$ $\tau_0 = 0.04$
 $R_x = 1.0$ $R_y = 0.0005$

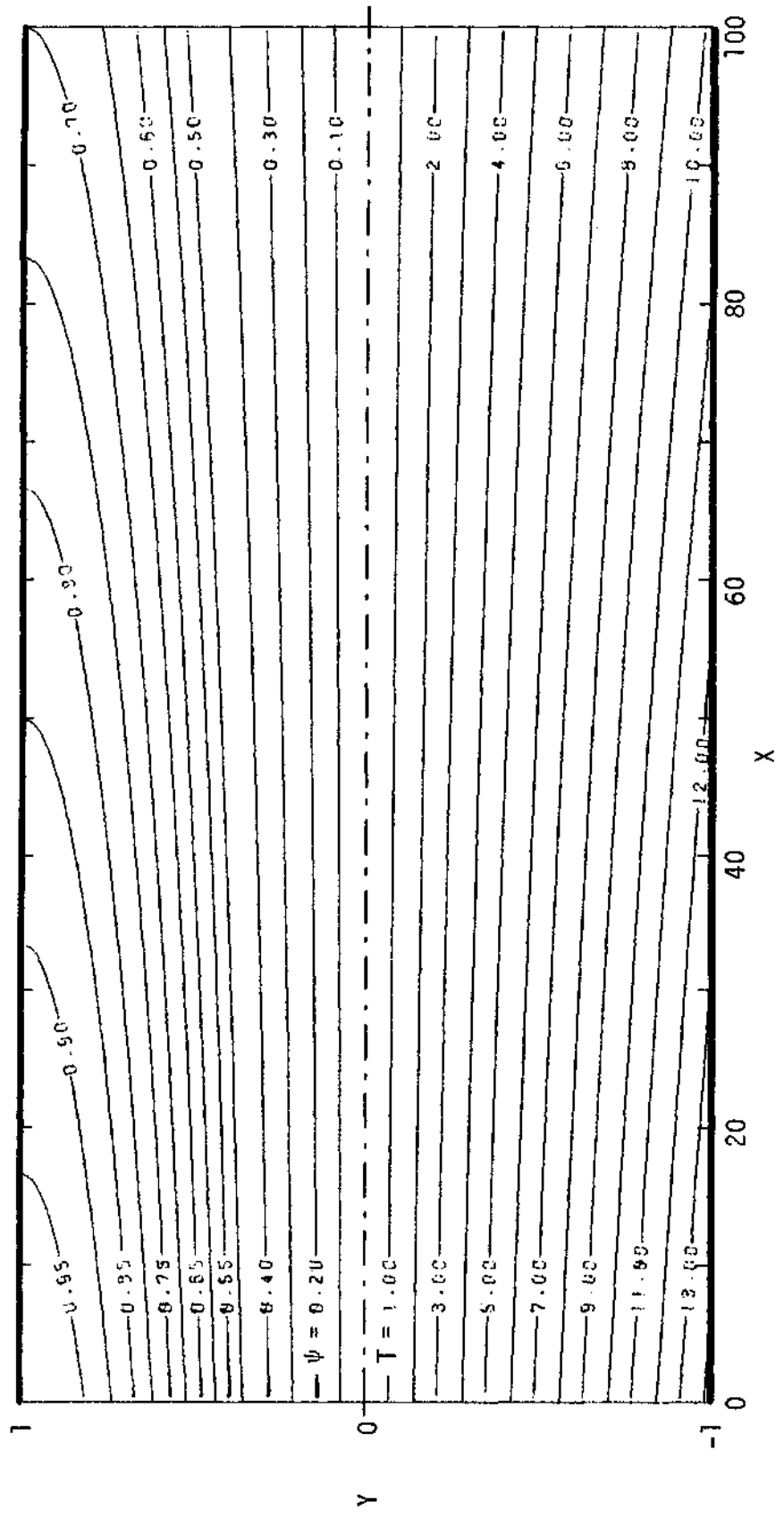


Figure 26. Contours of Stream Function (ψ) and Shear Stress (T_{yx})

Cassonian: $H = 0.01$ $\tau_0 = 0.04$
 $R_x = 1.0$ $R_y = 0.00075$

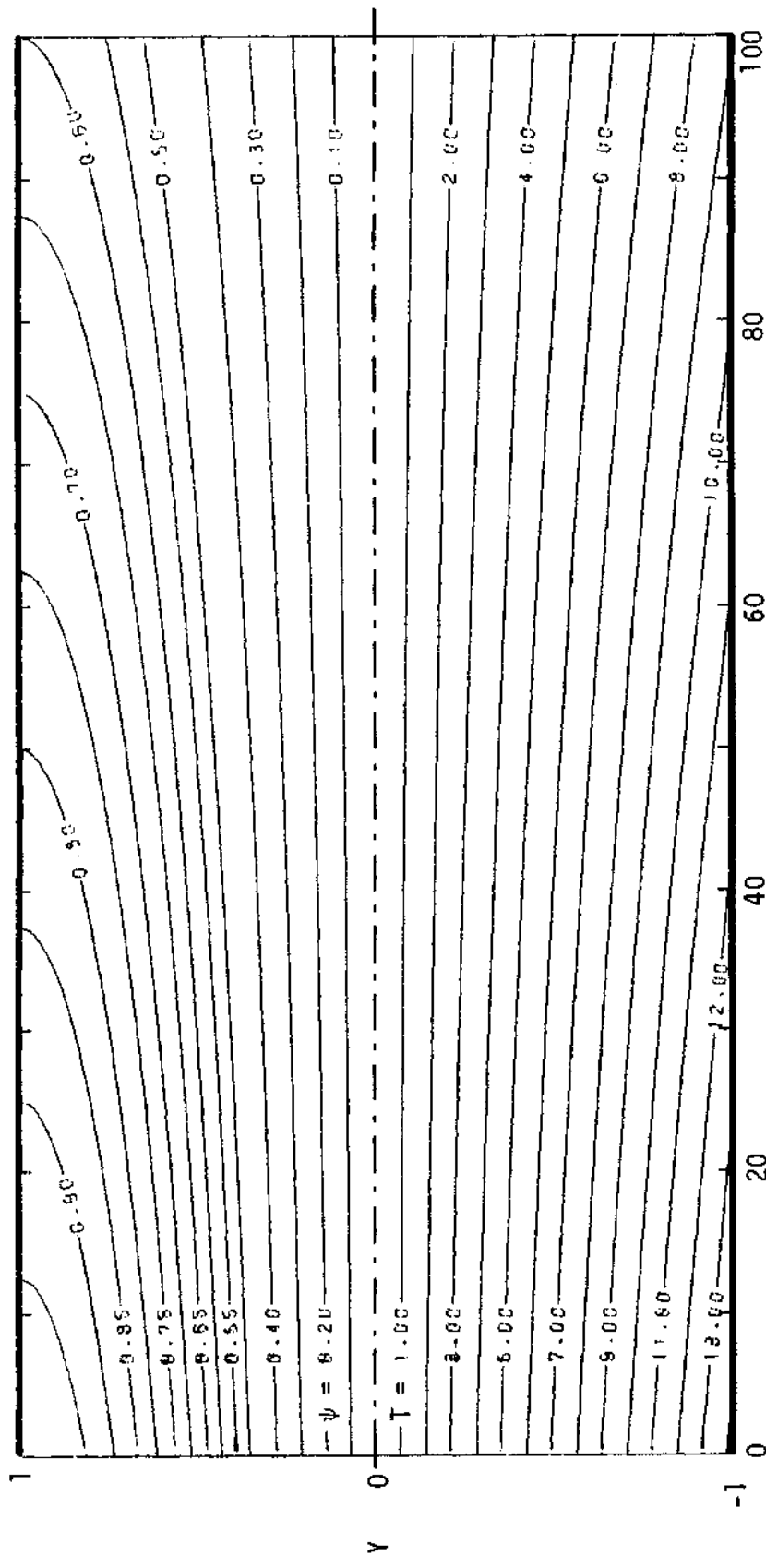


Figure 27. Contours of Stream Function (ψ) and Shear Stress (τ_{yx})

Cassonian: $H = 0.01$ $\tau_0 = 0.04$
 $R_x = 1.0$ $R_y = 0.001$

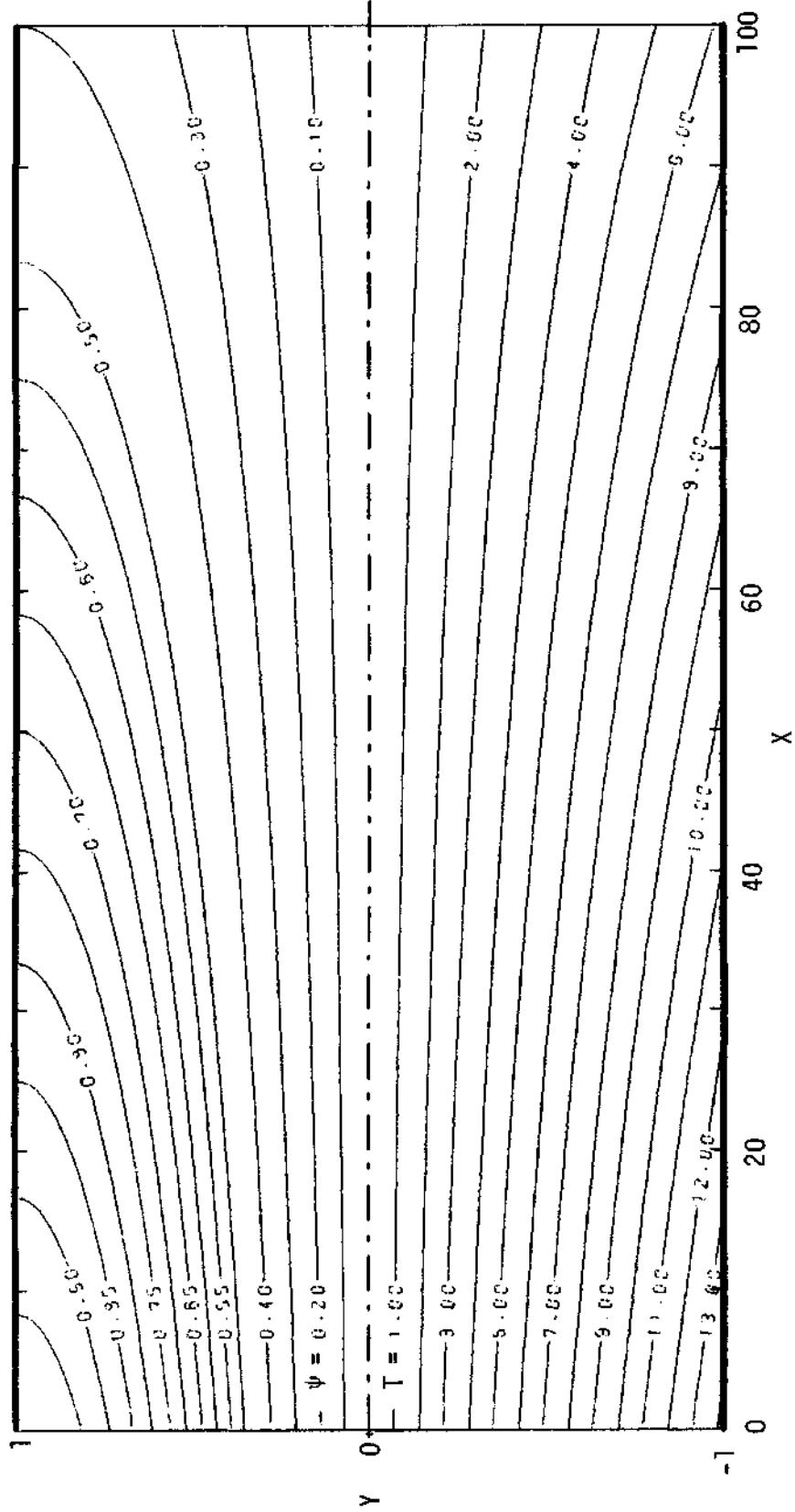


Figure 28. Contours of Stream Function (ψ) and Shear Stress (T_{yx})

Cassonian: $H = 0.01$ $\tau_0 = 0.04$
 $R_x = 1.0$ $R_y = 0.0015$

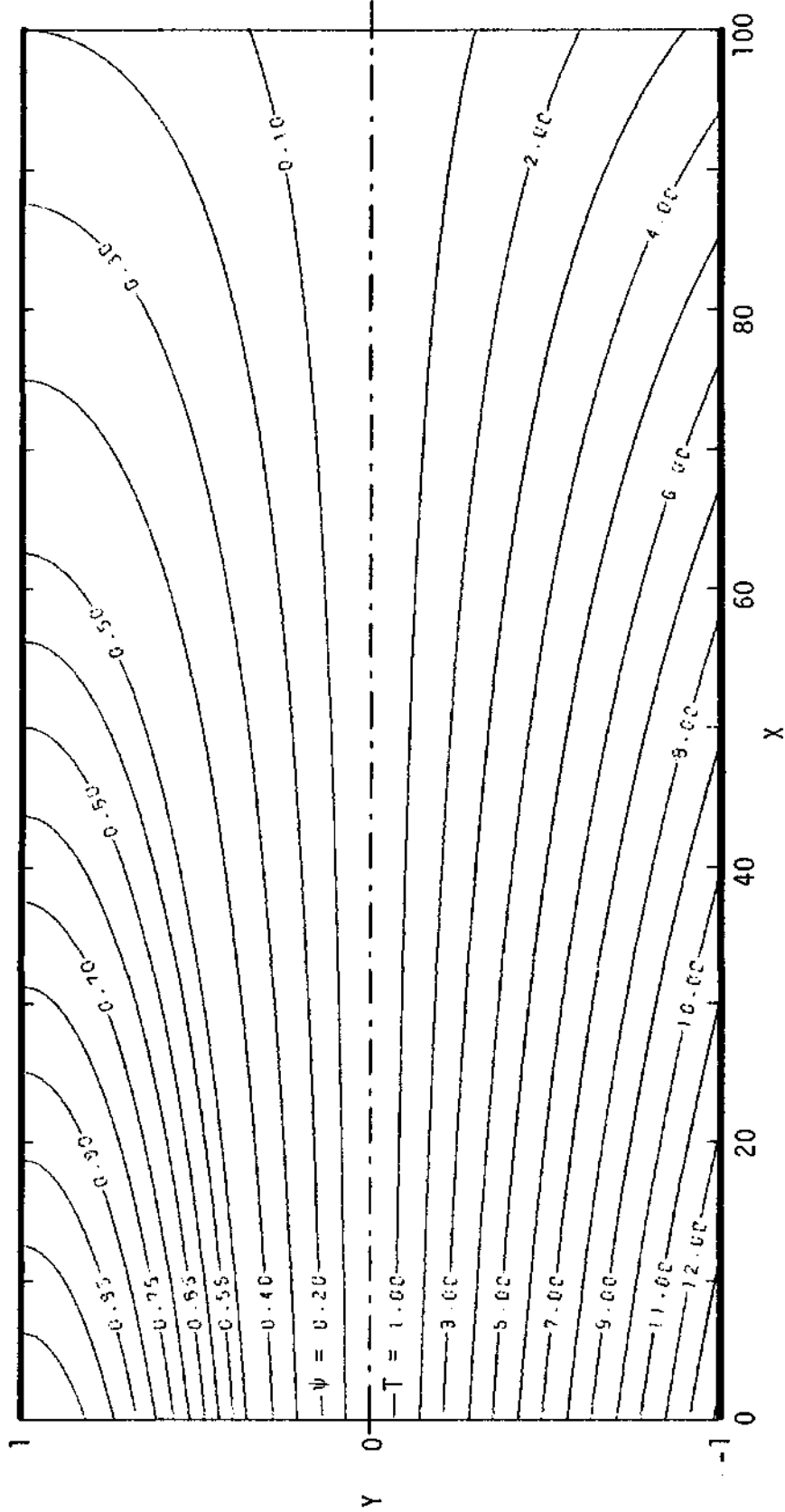


Figure 29. Contours of Stream Function (ψ) and Shear Stress (T_{yx}).

Cassonian: $H = 0.01$ $\tau_0 = 0.04$
 $R_x = 1.0$ $R_y = 0.002$

shear stress decrease with increasing X and the contours start to end into the walls. The larger the wall suction, the faster the stream function and shear stress decrease with increasing X and the greater the number of contours that end into the walls. This agrees with what would have been logically expected.

(2) The stream function (ψ) and shear stress (T_{yx}) vs Y at four suction rates ($R_y = 0, 0.0005, 0.001$ and 0.002) are presented in Figures 30 through 33. Plots of Newtonian flow for the same R_x and R_y values are presented in Figures 34 through 37 for comparison. In Figure 30 when there is no wall suction ($R_y = 0$), the stream functions at different values of X fall on the same curve and so do the shear stress values. When there is wall suction, the stream function and shear stress have different values at different X values. The larger the suction rate, the wider the curves separate from each other because of the decrease in stream function values and shear stress values. The effect of suction rate are similar in Cassonian and Newtonian flow. The only difference is that the Cassonian flow has larger shear stress values than the Newtonian flow with the same R_x and R_y values.

(3) The velocity profiles of V_x at $X = 0, 20, 40, 60, 80, 100$ were calculated from the stream function values and the results are presented in Figures 38 through 41. V_x decreases with increasing X and the rate of decrease is greater with greater wall suction.

(4) The velocity profiles of V_y at $X = 0, 20, 40, 60, 80, 100$ were calculated from the stream function values and the results are presented in Figures 42 through 45. The Y -component of velocity, V_y ,

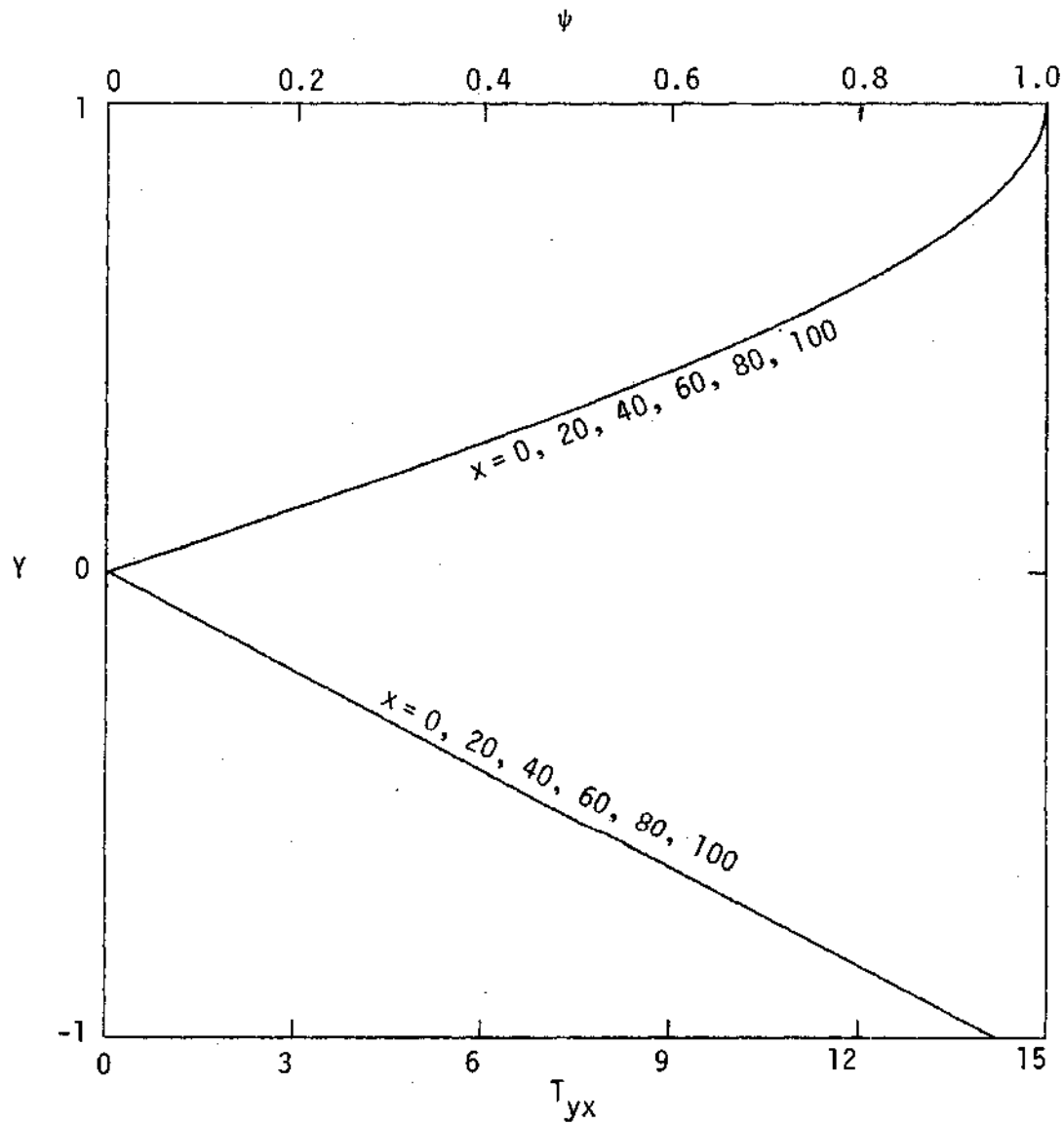


Figure 30. Stream Function (ψ) and Shear Stress (T_{yx}) vs Y.

Cassonian: $H = 0.01$ $\tau_0 = 0.04$

$R_x = 1.0$ $R_y = 0$

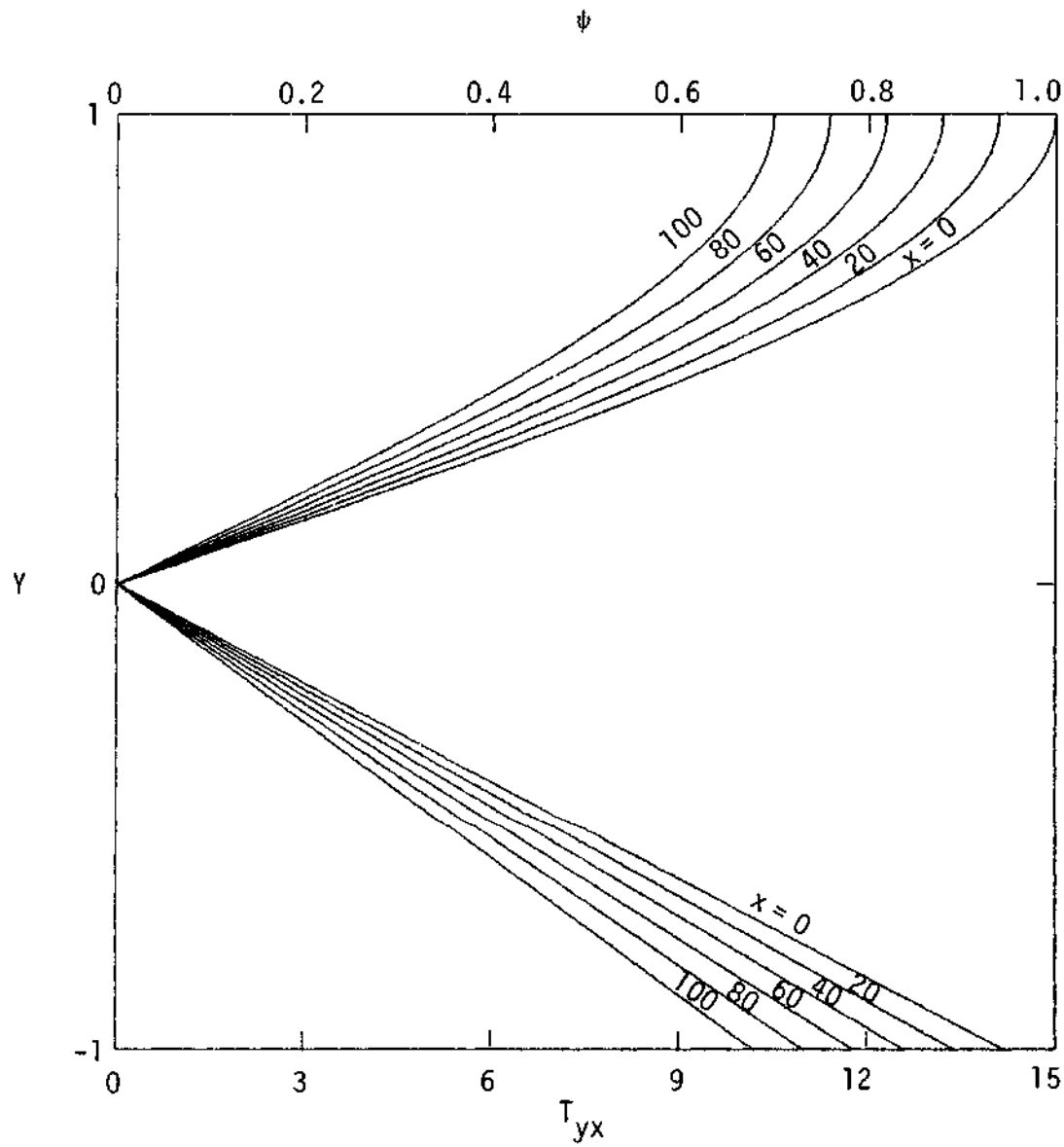


Figure 31. Stream Function (ψ) and Shear Stress (T_{yx}) vs Y .

Cassonian: $H = 0.01$ $\tau_0 = 0.04$

$R_x = 1.0$ $R_y = 0.0005$

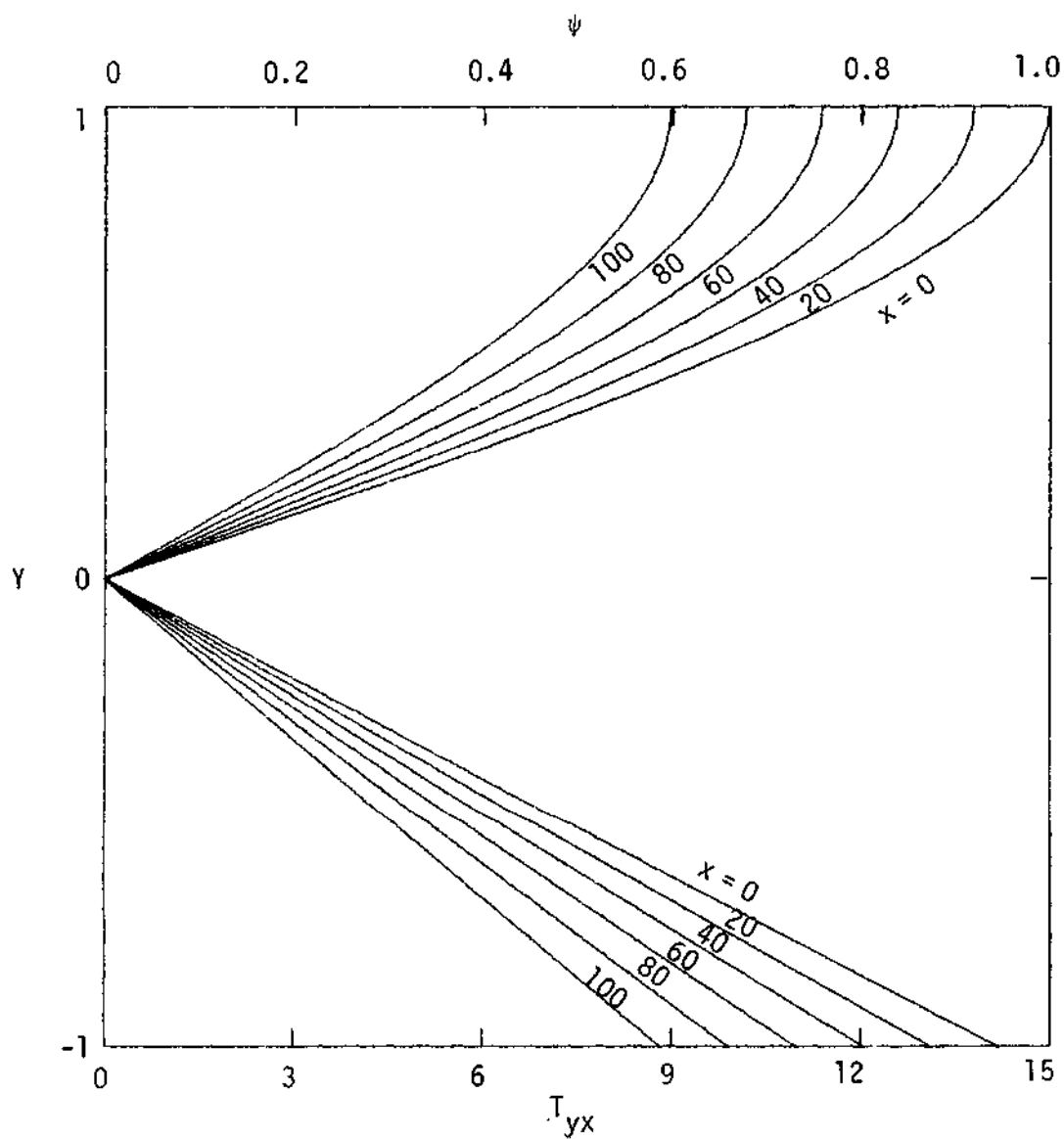


Figure 32. Stream Function (ψ) and Shear Stress (T_{yx}) vs Y .

Cassonian: $H = 0.01$

$T_0 = 0.04$

$R_x = 1.0$

$R_y = 0.001$

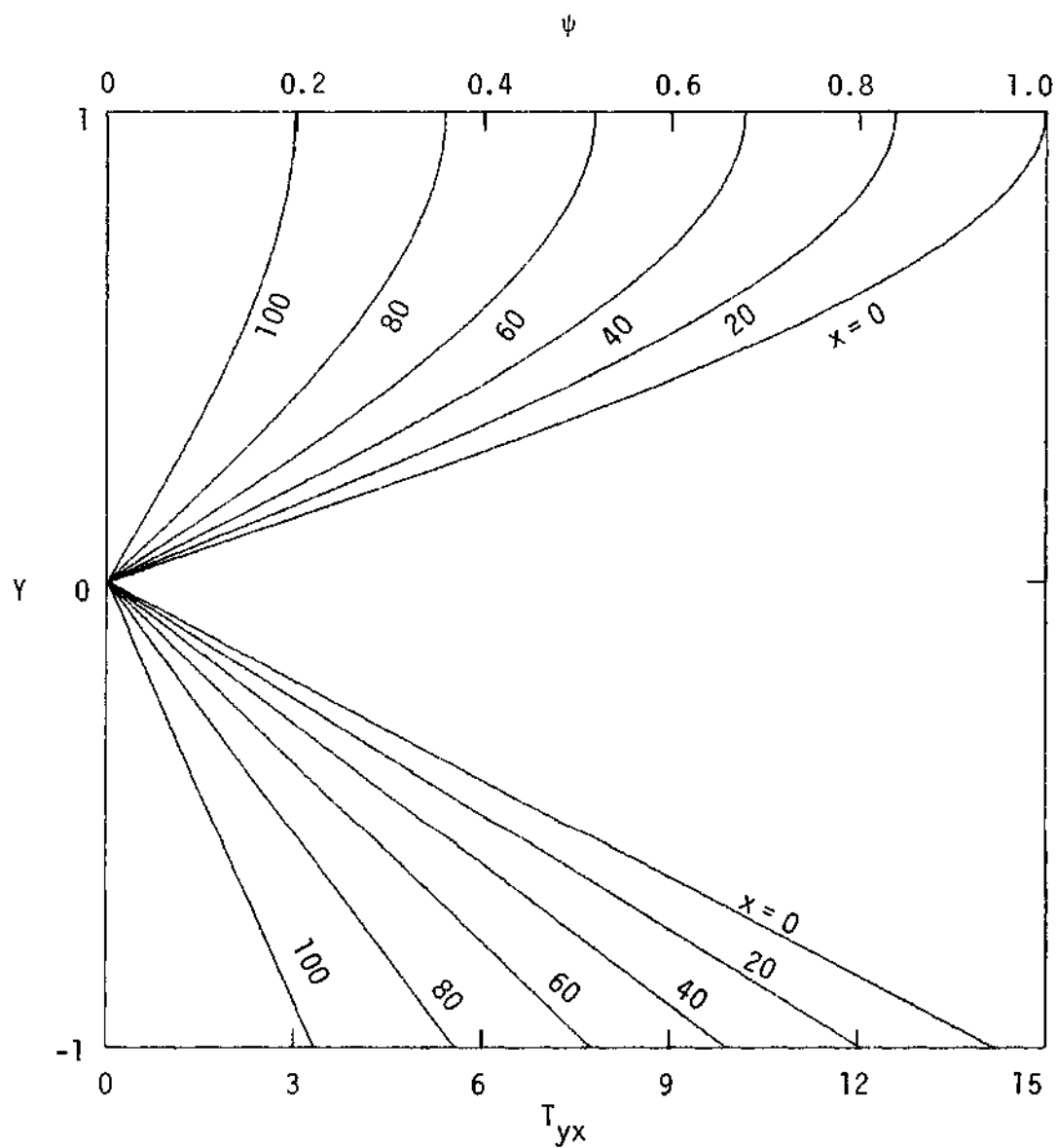


Figure 33. Stream Function (ψ) and Shear Stress (T_{yx}) vs Y .

Cassonian: $H = 0.01$ $\tau_0 = 0.04$

$R_x = 1.0$ $R_y = 0.002$

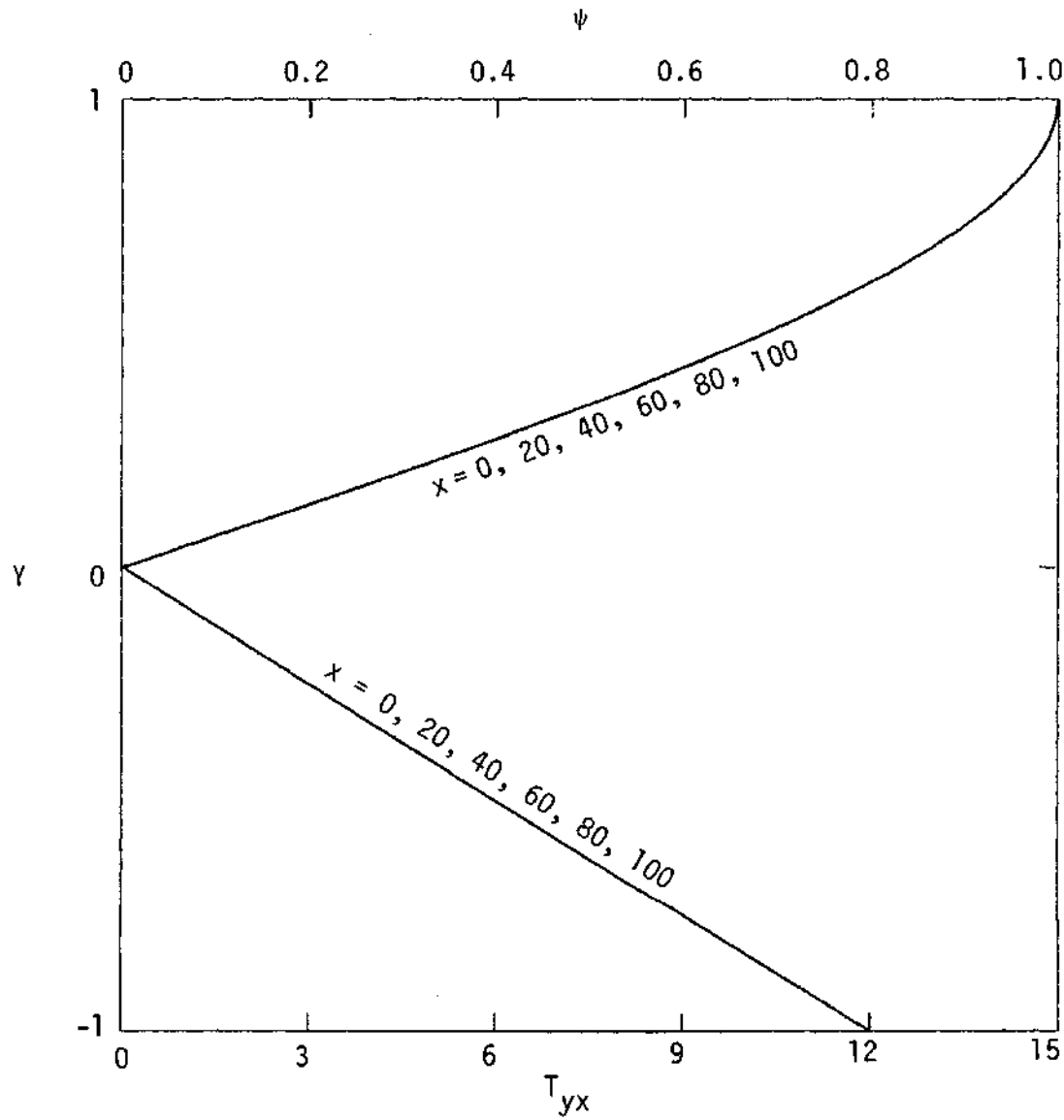


Figure 34. Stream Function (ψ) and Shear Stress (T_{yx}) vs Y .

Newtonian: $H = 0.01$

$R_x = 1.0$

$R_y = 0$

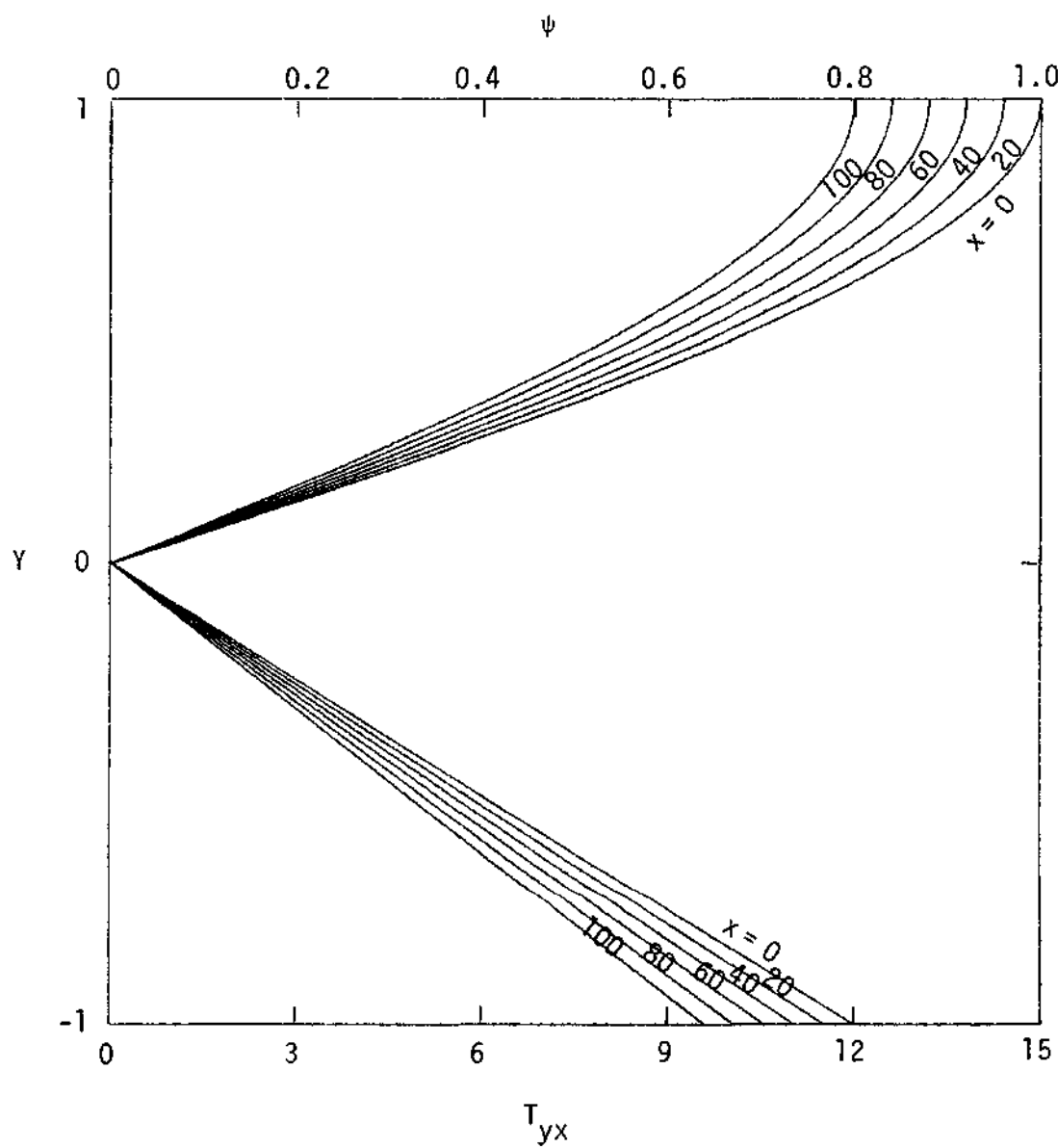


Figure 35. Stream Function (ψ) and Shear Stress (T_{yx}) vs Y .

Newtonian: $H = 0.01$

$$R_x = 1.0$$

$$R_y = 0.0005$$

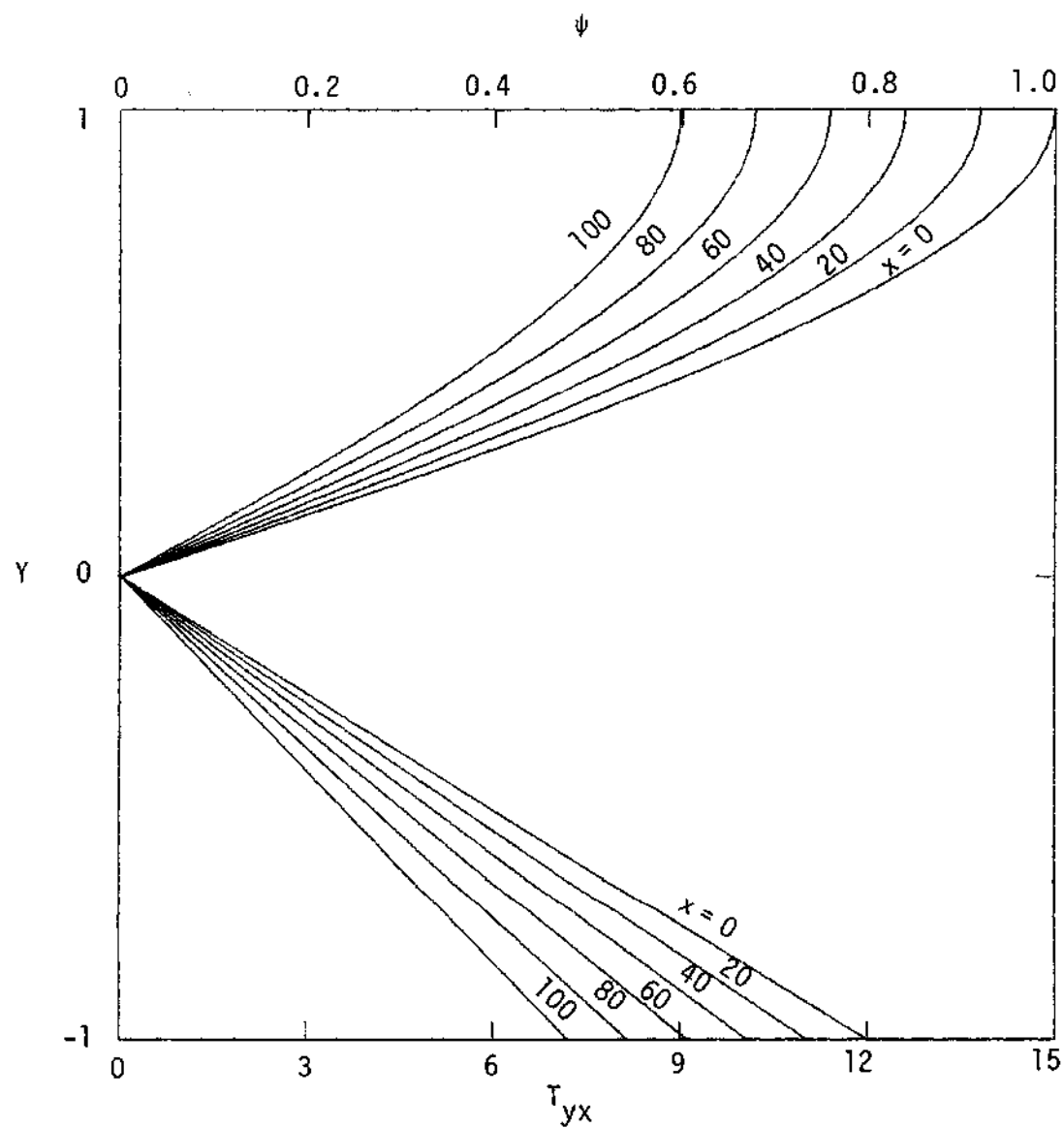


Figure 36. Stream Function (ψ) and Shear Stress (T_{yx}) vs Y.

Newtonian: $H = 0.01$

$R_x = 1.0$

$R_y = 0.001$

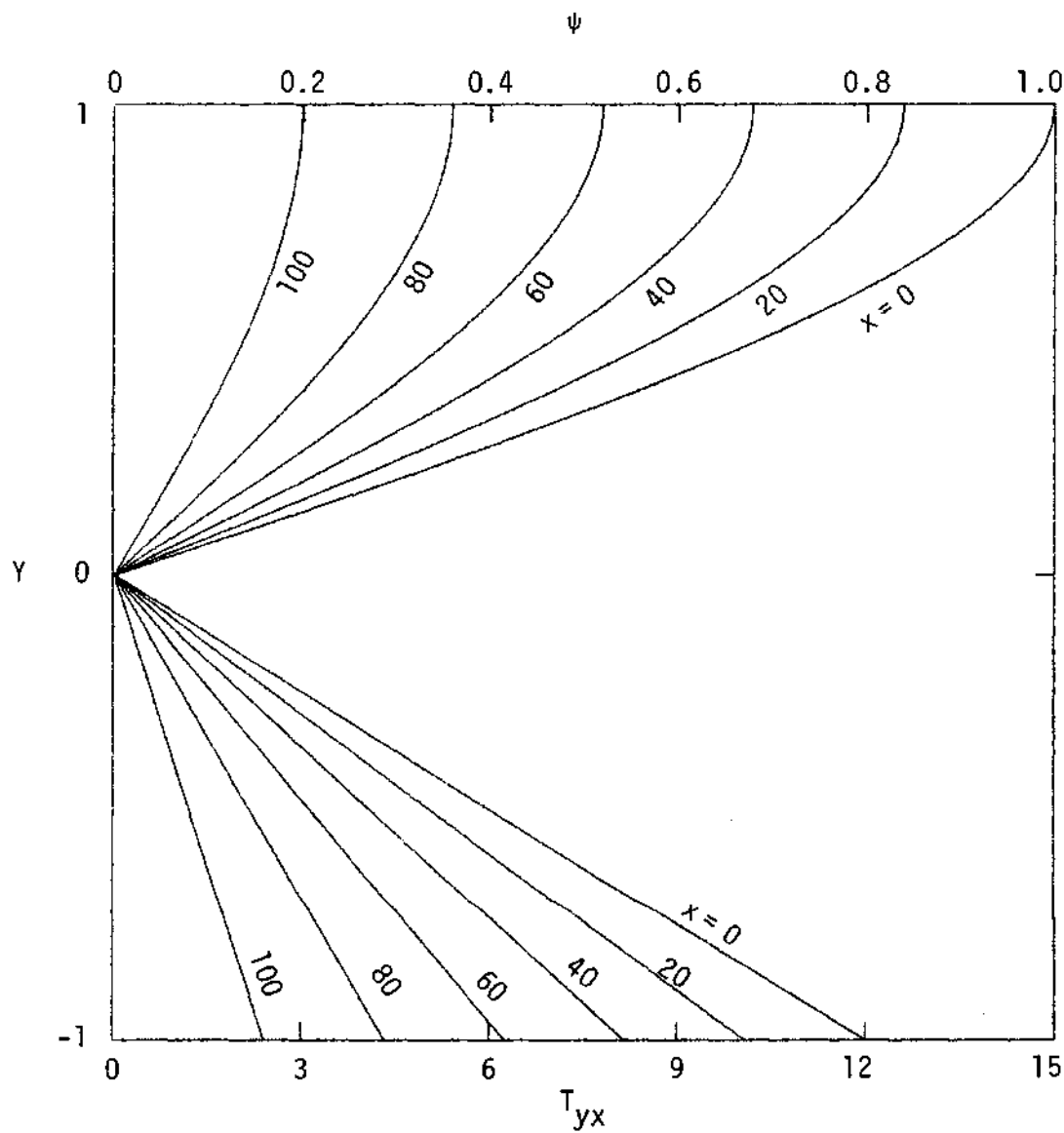


Figure 37. Stream Function (ψ) and Shear Stress (T_{yx}) vs Y .

Newtonian: $H = 0.01$

$R_x = 1.0$

$R_y = 0.002$

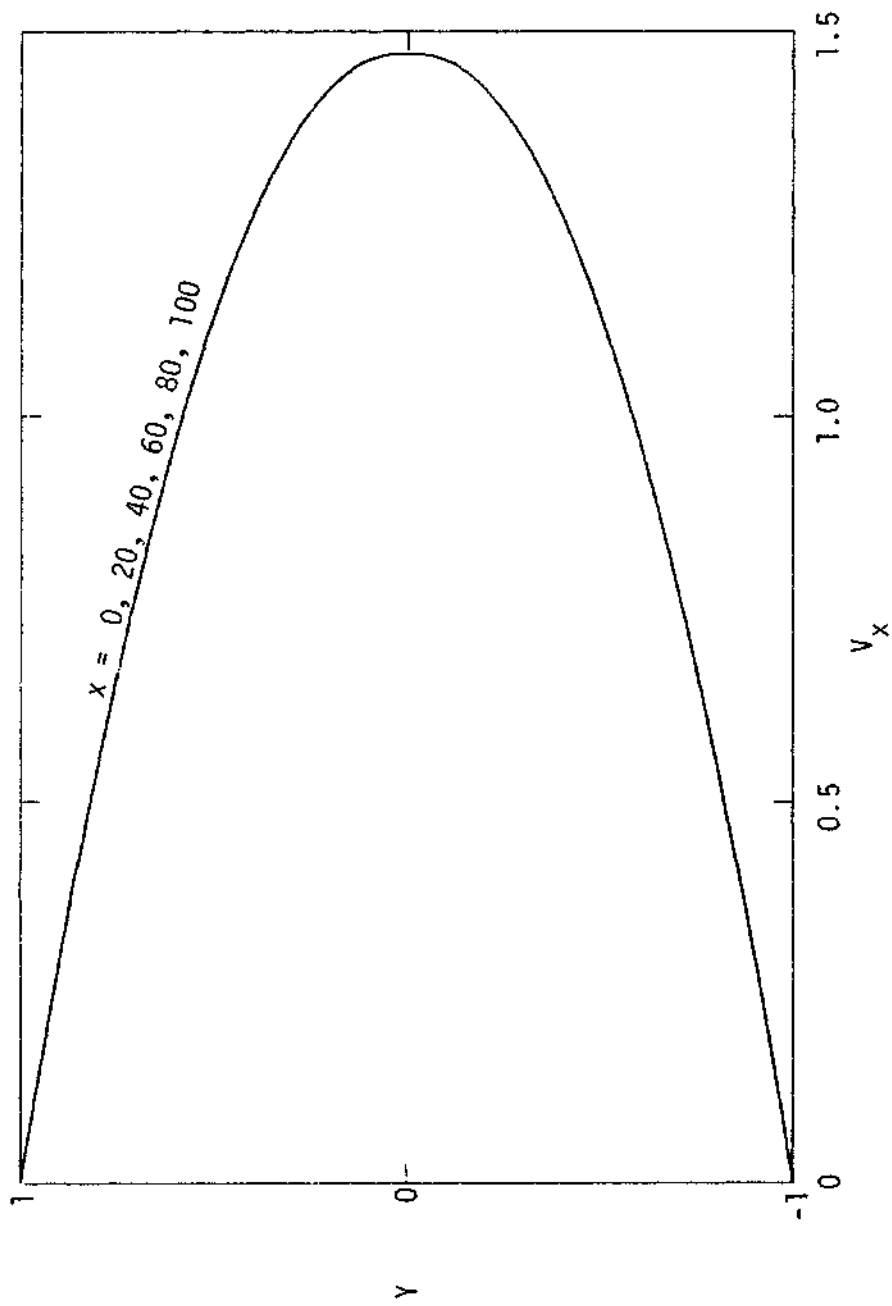


Figure 38. Velocity Profiles (V_x).

Cassonian: $H = 0.01$ $\tau_0 = 0.04$

$R_x = 1.0$ $R_y = 0$

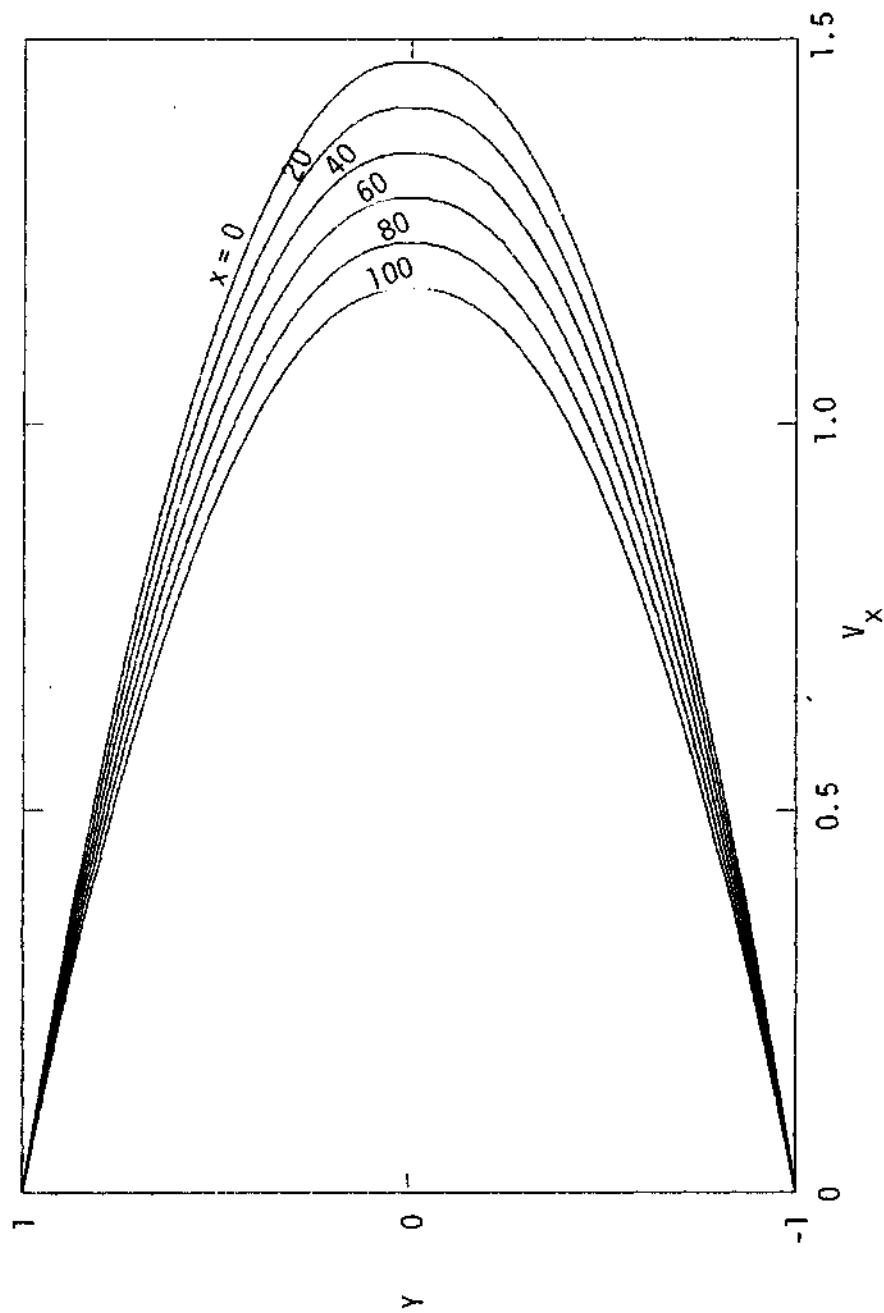


Figure 39. Velocity Profiles (V_x).

Cassonian: $H = 0.01$

$\tau_0 = 0.04$

$R_x = 1.0$

$R_y = 0.0005$

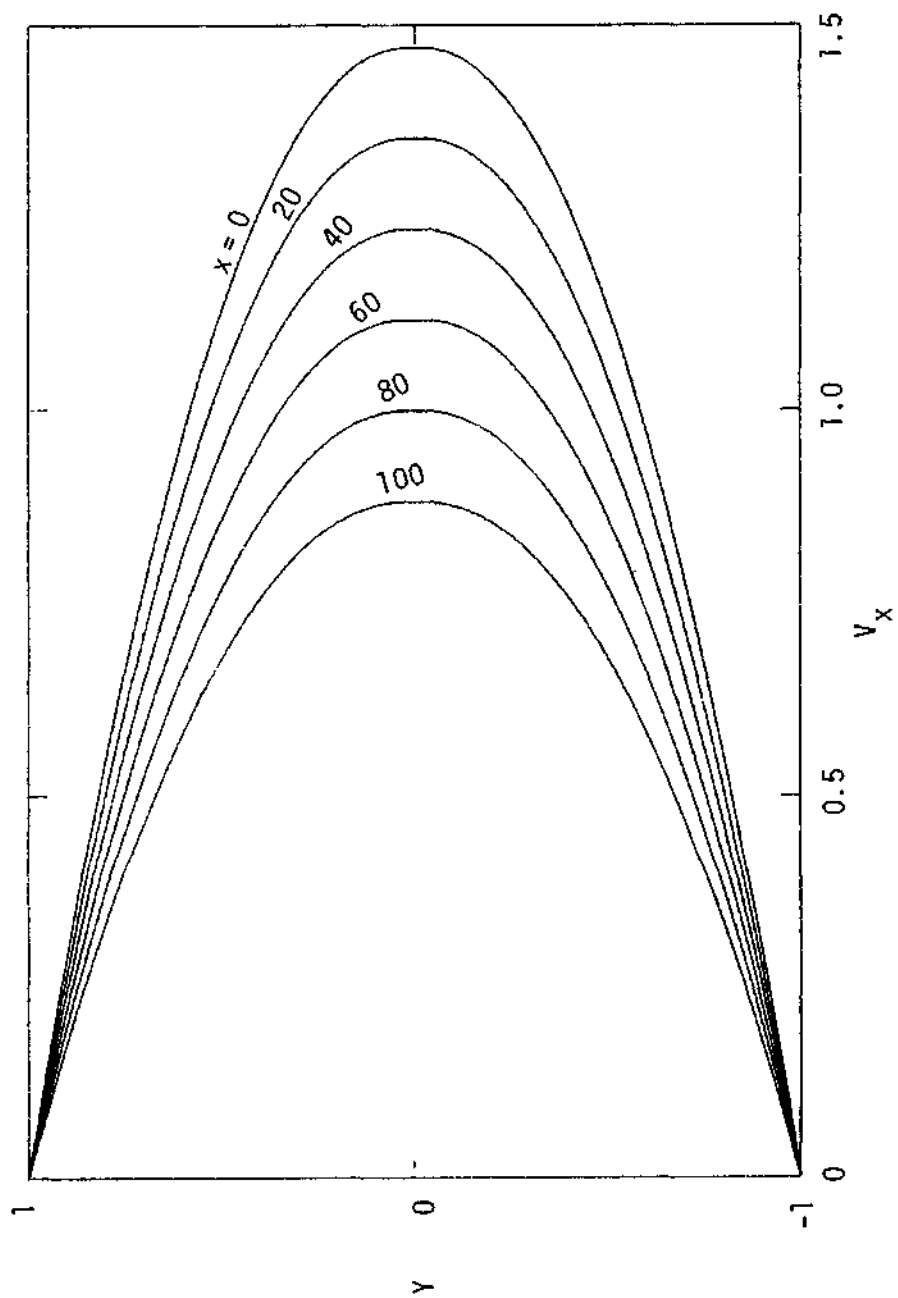


Figure 40. Velocity Profiles (V_x).

Cassonian: $H = 0.001$ $\tau_0 = 0.04$

$R_x = 1.0$ $R_y = 0.001$

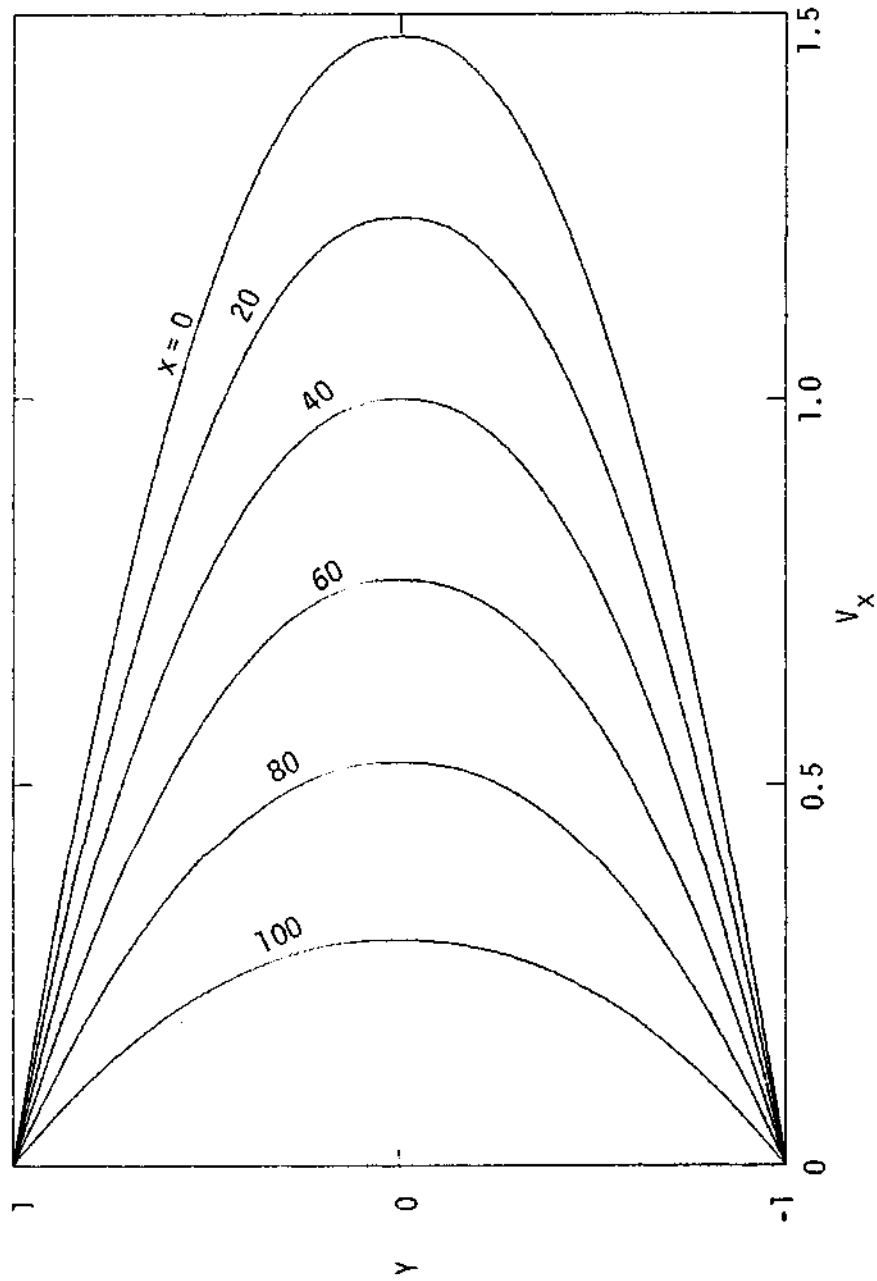


Figure 41. Velocity Profiles (V_x).

Cassonian: $H = 0.01$ $\tau_0 = 0.04$
 $R_x = 1.0$ $R_y = 0.002$

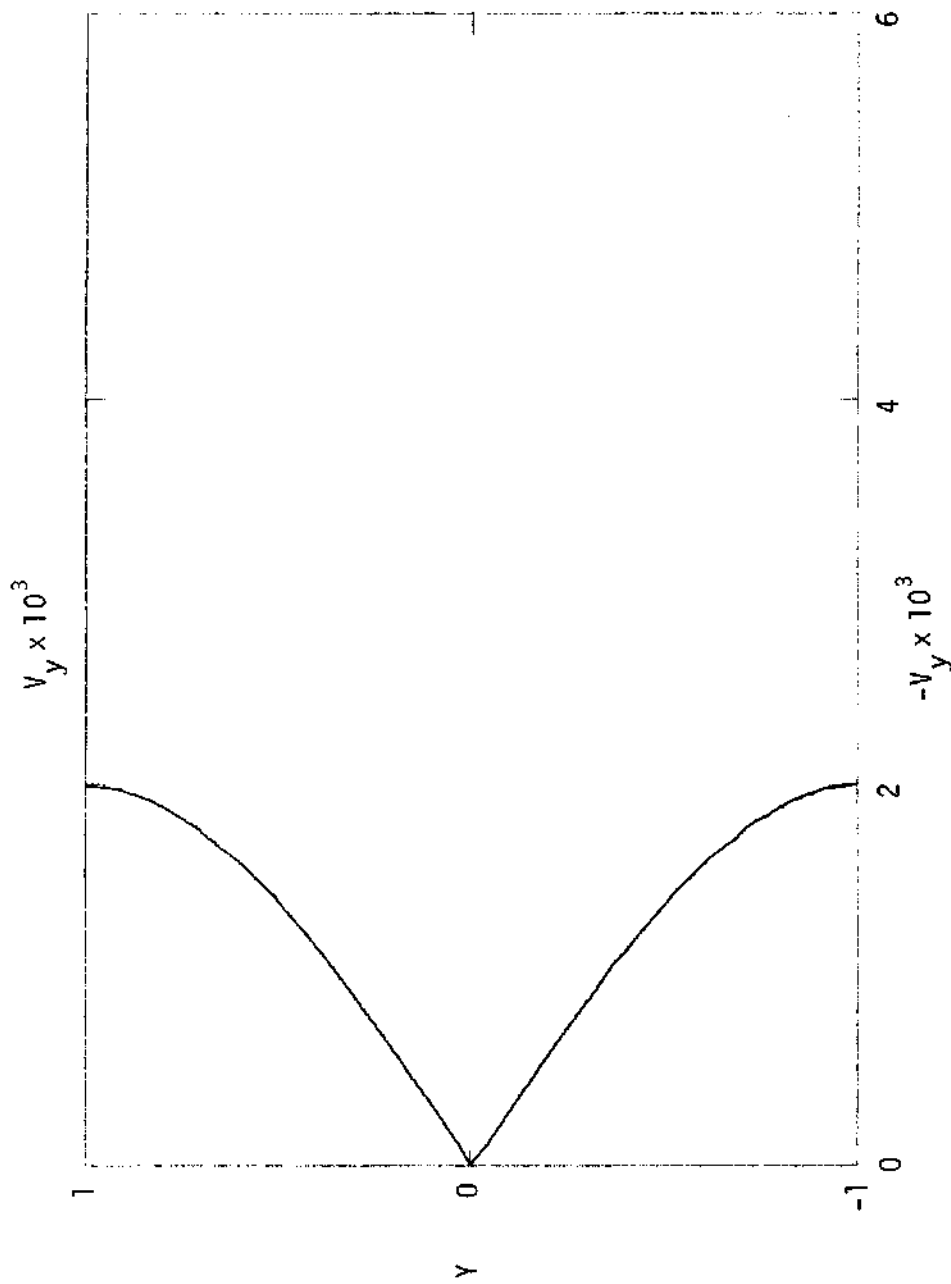


Figure 42. Velocity Profile (V_y).

Cassonian: $H = 0.01$ $\tau_0 = 0.04$
 $R_x = 1.0$ $R_y = 0.0005$

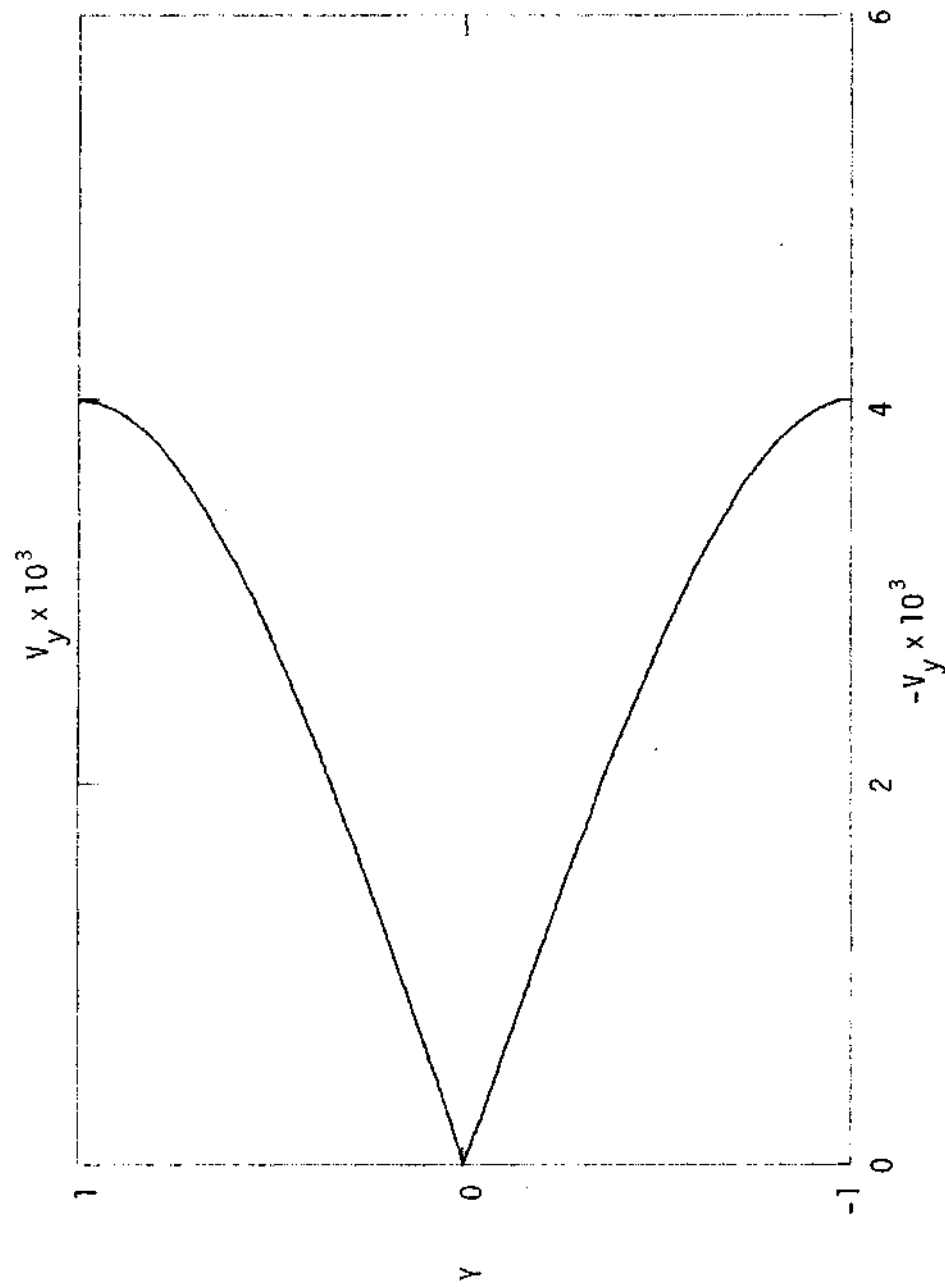


Figure 43. Velocity Profile (V_y).

Cassonian: $H = 0.01$ $\tau_0 = 0.04$

$R_x = 1.0$ $R_y = 0.001$

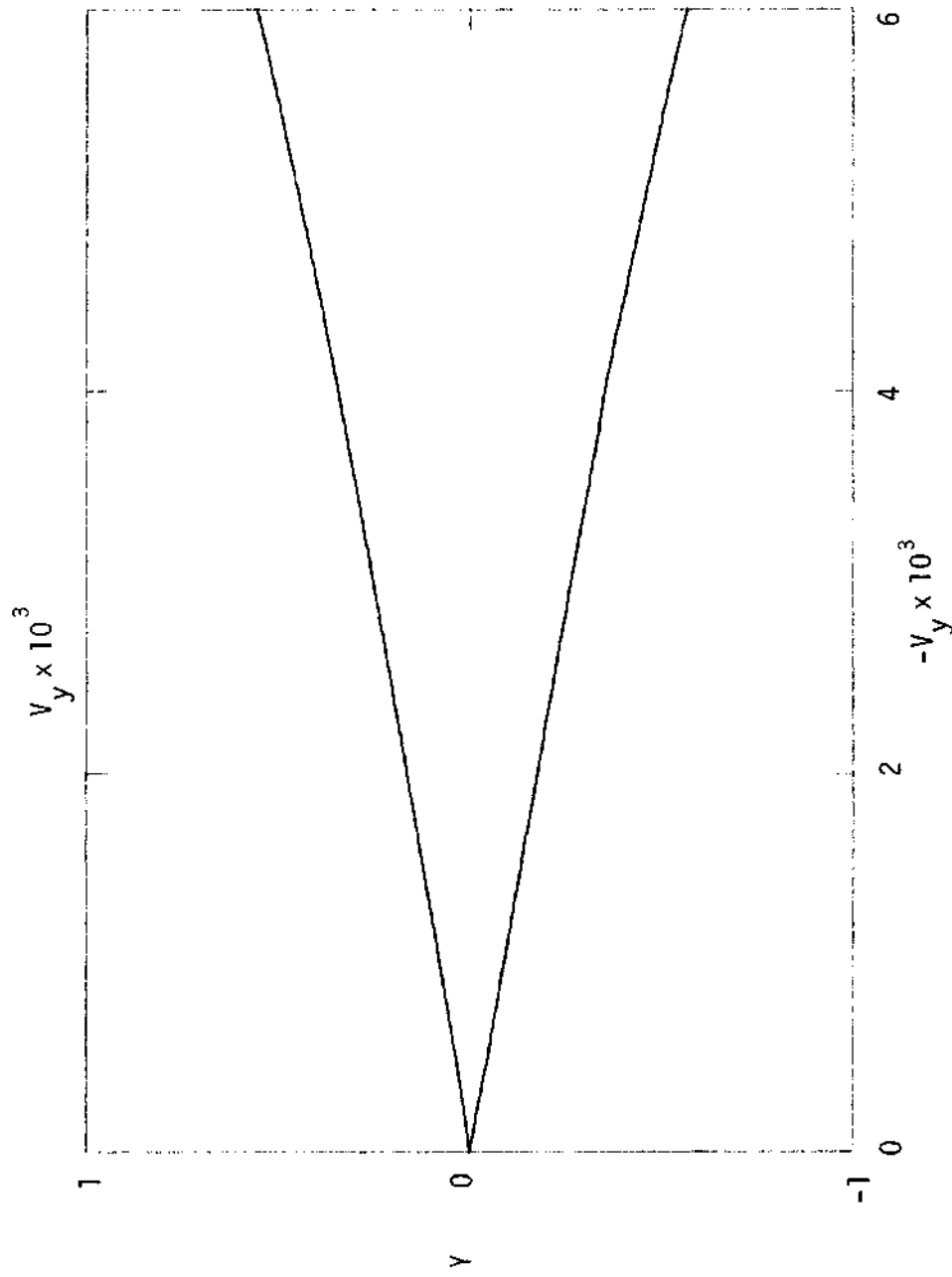


Figure 44. Velocity Profile (V_y).

Cassonian: $H = 0.01$ $\tau_0 = 0.04$
 $R_x = 1.0$ $R_y = 0.002$

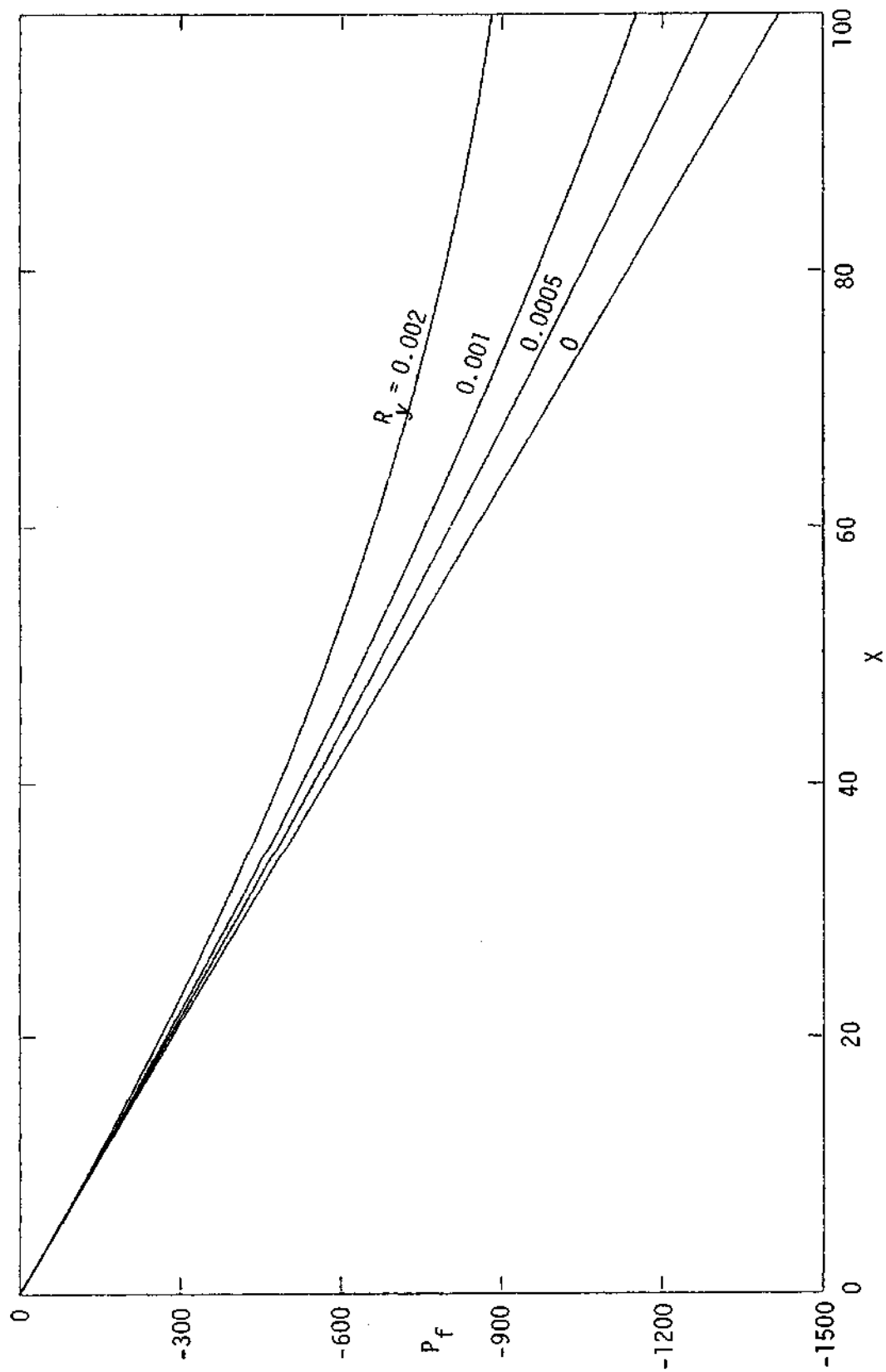


Figure 45. Pressure Drop on the Central Plane vs X .

Cassonian: $H = 0.01$ $\tau_0 = 0.04$ $R_x = 1.0$

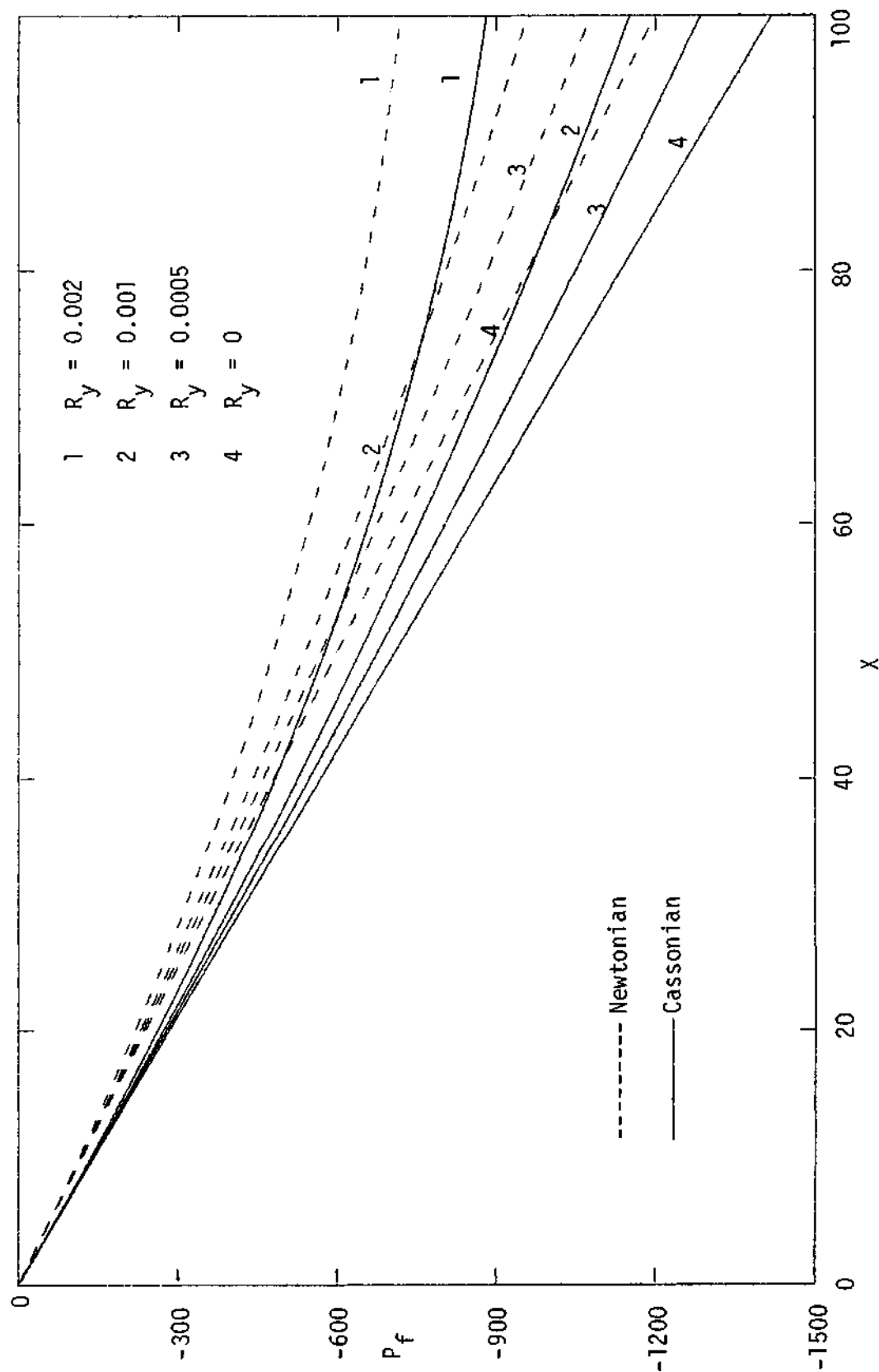


Figure 46. Pressure Drop on the Central Plane vs X.

Comparison: $H = 0.01$ $\tau_0 = 0.04$ $R_x = 1.0$

arises as a result of wall suction. When there is no wall suction, $V_y = 0$ and $R_y = 0$ and there is no velocity profile of V_y . Therefore there is no curve shown in the plot where $R_y = 0$ and this plot is omitted. With constant wall suction, the velocity profiles of V_y are essentially the same at different X values and the computer plotter traced the same curves six times in each plot.

(5) The pressure drop on the central plane is plotted in Figure 45. The pressure drop follows a straight line with no wall suction ($R_y = 0$). The pressure drop becomes smaller and follows a curved line when there is a wall suction. Pressure drops of Newtonian flow with the same R_x and R_y are plotted as dotted lines in Figures 46. Cassonian flow (solid lines) has larger pressure drops than Newtonian flow.

Some Mutually Related Variables

Newtonian Flow:

For Newtonian flow:

$$\psi' = \left[\frac{3}{2} \frac{y}{H} - \frac{1}{2} \left(\frac{y}{H} \right)^3 \right] (v_0 x - \frac{Q_0}{W}) \quad (4-1)$$

where

$$v_x = - \frac{\partial \psi'}{\partial y} \quad v_y = \frac{\partial \psi'}{\partial x}$$

$$\tau_{yx} = \frac{3\mu y}{H^3} \left(\frac{1}{2} \frac{Q_0}{W} - v_0 x \right) \quad (4-2)$$

Let $X = x/H$, $Y = y/H$, $\psi = -\psi' W/Q_0$, $U_0 = Q_0/2WH$

$$R_x = 4U_0 H \rho / \mu, \quad R_y = v_0 H \rho / \mu, \quad T_{yx} = \tau_{yx} / \rho U_0^2$$

then the above equations can be written in the dimensionless form

$$\psi = \left(\frac{3}{2} Y - \frac{1}{2} Y^3\right) \left(1 - 2 \frac{R_y}{R_x} X\right) \quad (4-3)$$

$$T_{yx} = \frac{12}{R_x} Y \left(1 - 4 \frac{R_y}{R_x} X\right) \quad (4-4)$$

From equations (4-3) and (4-4) it can be seen that as long as we keep the ratio of R_y/R_x the same, the dimensionless stream function (ψ) will always stay the same and the dimensionless shear stress will change inversely with R_x . The distance between the membranes has no effect either on the dimensionless stream function (ψ) or on the dimensionless shear stress (T_{yx}). This has been tested numerically and the results are plotted in Figures 47 through 53.

Use Figure 47 as the base case with $H = 0.01$, $R_x = 1.0$ and $R_y = 0.001$. H was changed to 0.05 in Figure 48 and to 0.005 in Figure 49. The plots remain unchanged, proving that the value of H has no effect on ψ or T_{yx} . In Figure 50, R_x and R_y are changed to 25 and 0.025 respectively. The resulting plots have the same ψ values but the T_{yx} values become much smaller. If these T_{yx} values are multiplied by R_x as shown in Figure 51, the plot becomes the same as that in Figure 47 again. In Figure 52, R_x and R_y are changed to 0.25 and 0.00025 respectively. The resulting plot again has the same ψ values but the T_{yx} values become much greater. If these T_{yx} values are multiplied by R_x as in Figure 53, the plot again becomes the same as that in Figure 47.

Cassonian Flow:

The flow equations for a Cassonian flow can be written as:

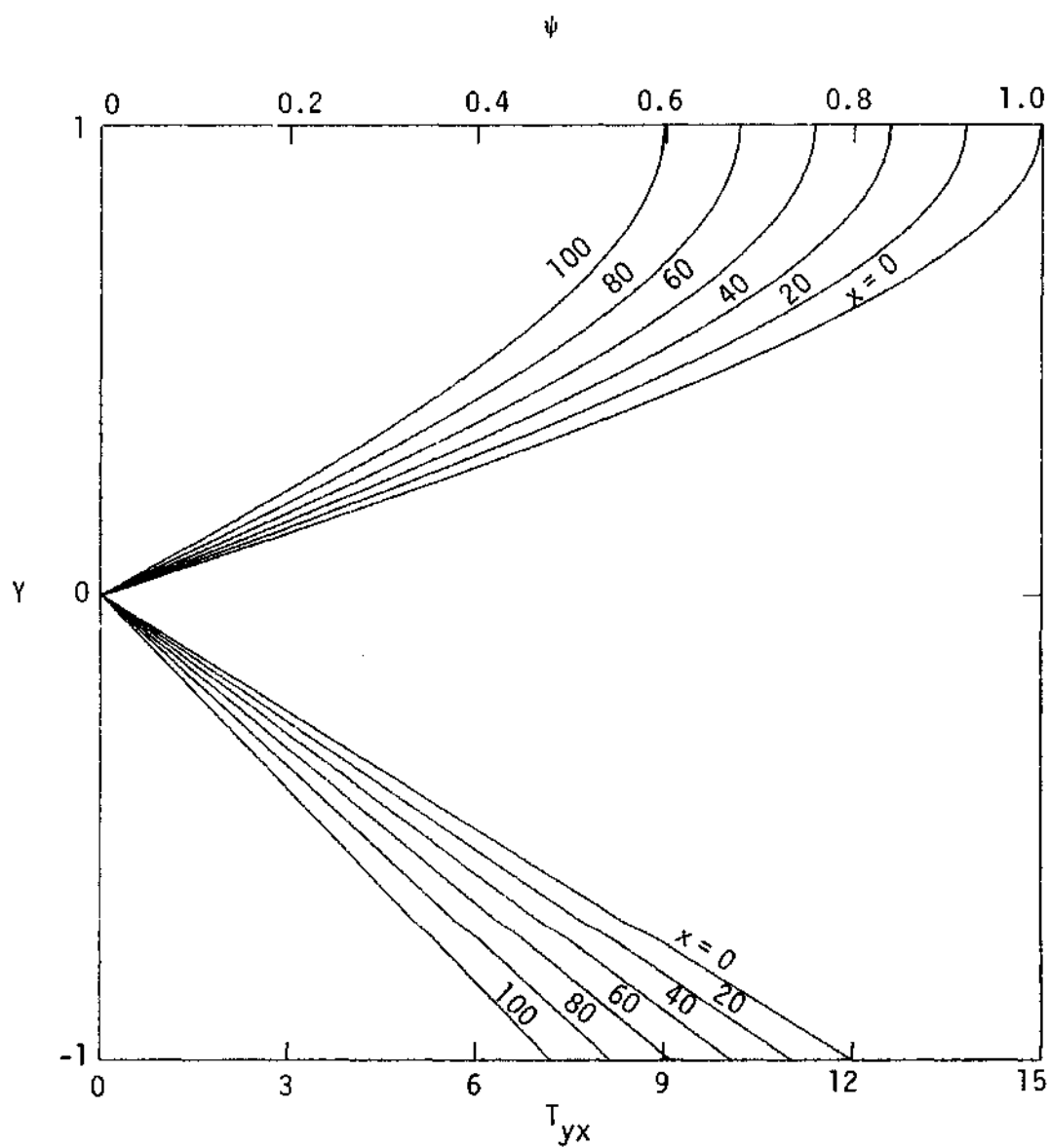


Figure 47. Stream Function (ψ) and Shear Stress (T_{yx}) vs Y.

Newtonian: $H = 0.01$

$R_x = 1.0$

$R_y = .001$

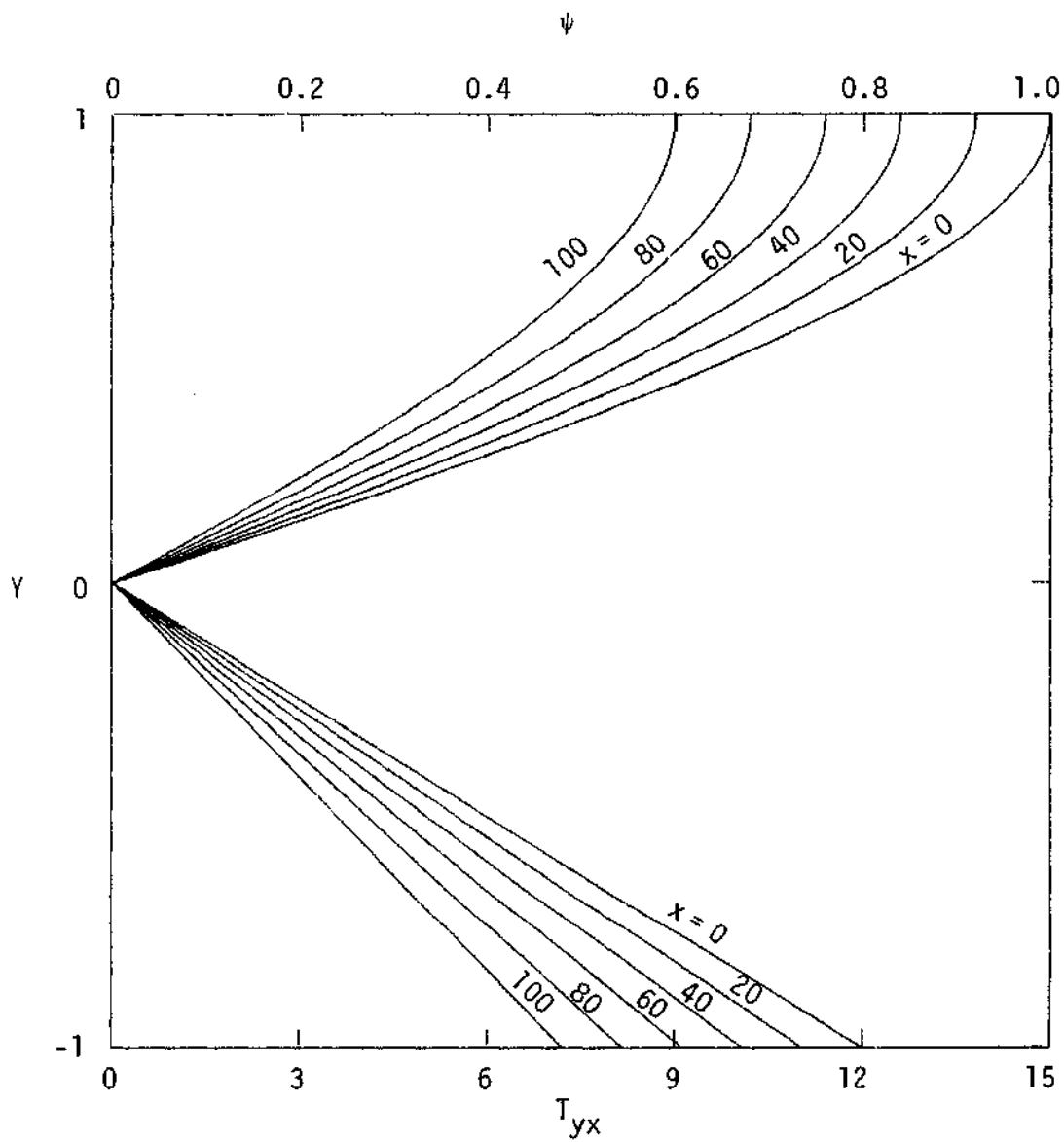


Figure 48. Stream Function (ψ) and Shear Stress (T_{yx}) vs Y

Newtonian: $H = 0.05$

$R_x = 1.0$

$R_y = 0.001$

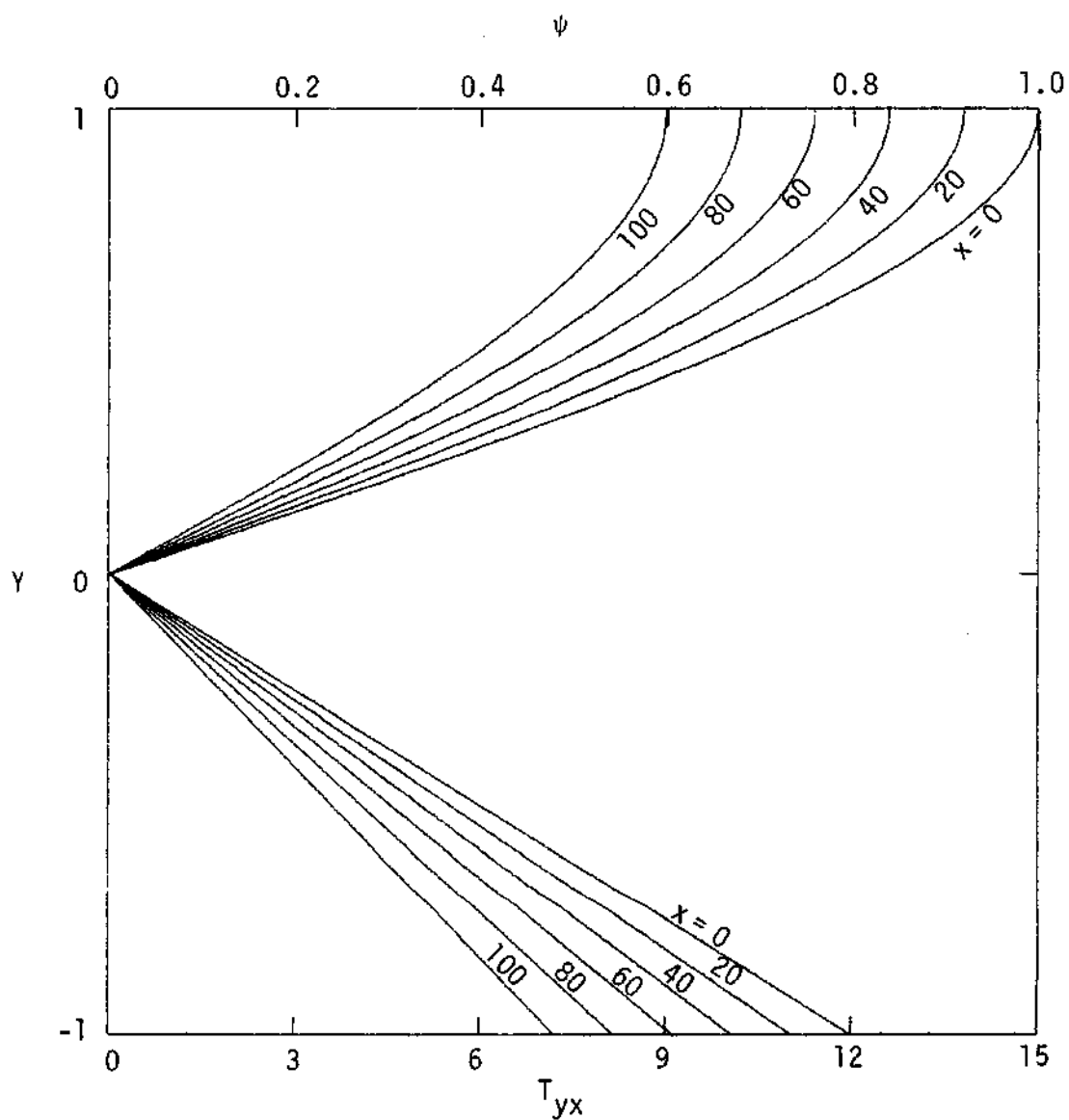


Figure 49. Stream Function (ψ) and Shear Stress (T_{yx}) vs Y .

Newtonian: $H = 0.005$

$R_x = 1.0$

$R_y = 0.001$

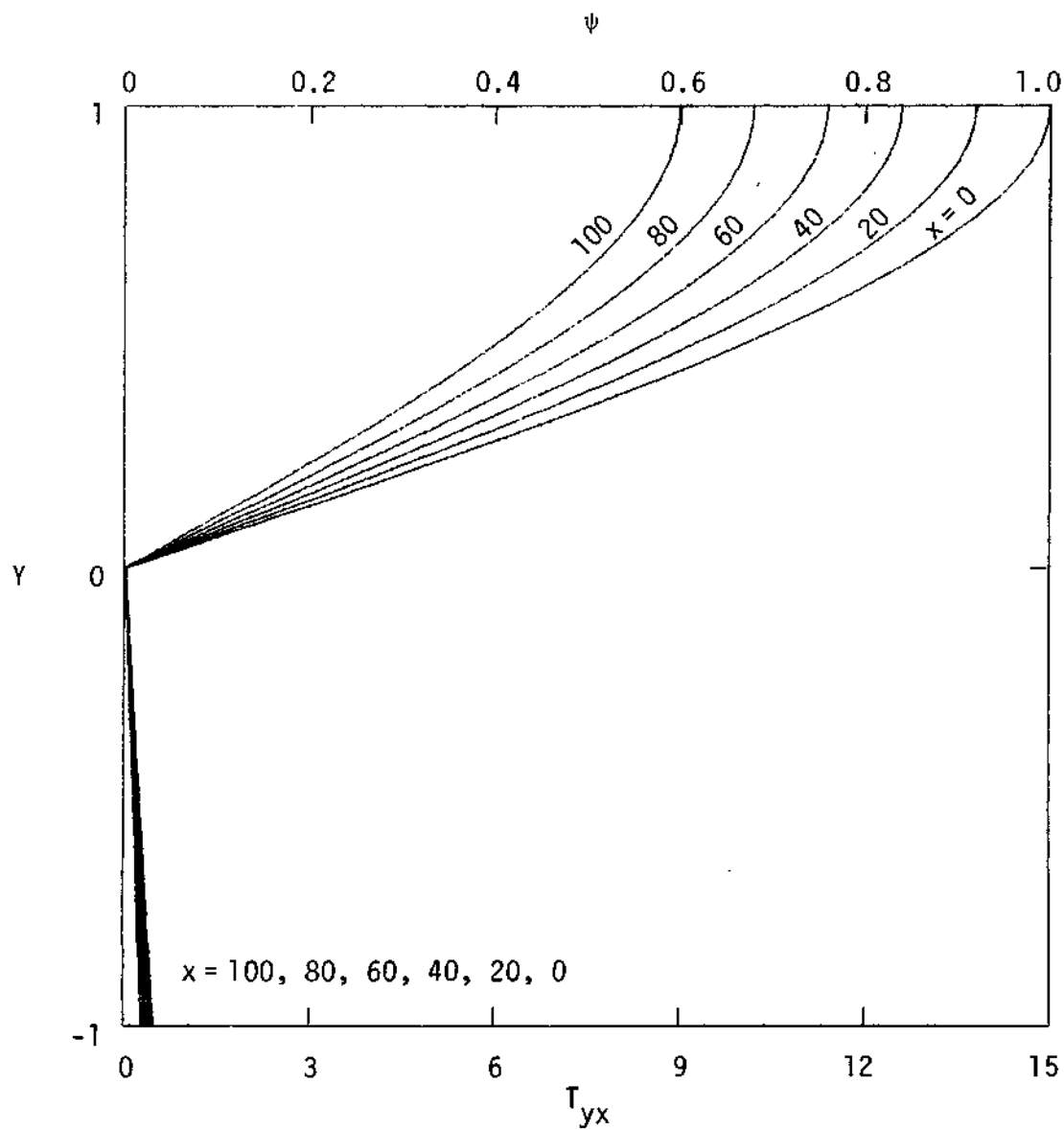


Figure 50. Stream Function (ψ) and Shear Stress (T_{yx}) vs Y

Newtonian: $H = 0.01$

$$R_x = 25$$

$$R_y = 0.025$$

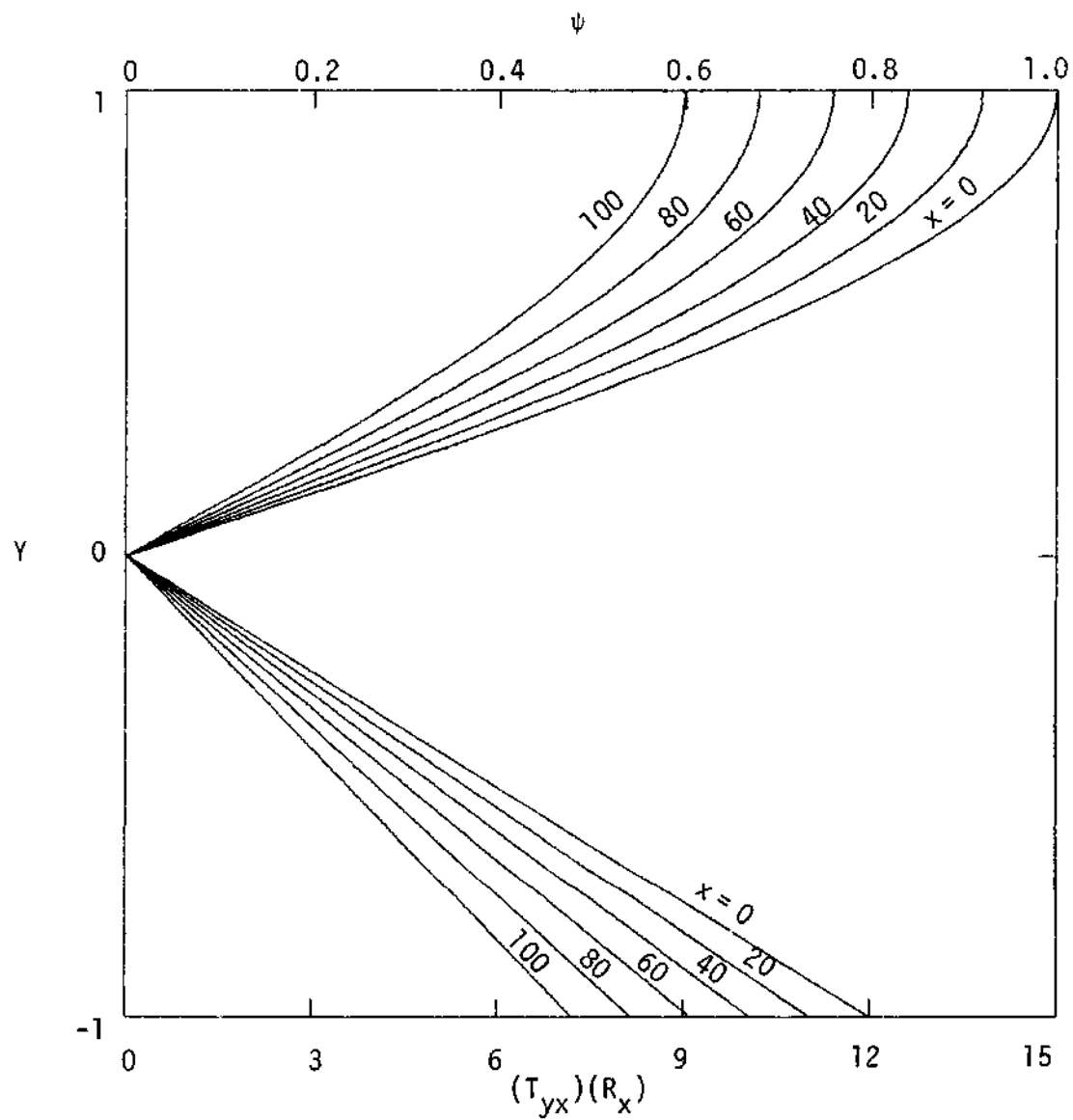


Figure 51. Stream Function (ψ) and Shear Stress $(T_{yx})(R_x)$ vs Y .

Newtonian: $H = 0.01$

$R_x = 25$

$R_y = 0.025$

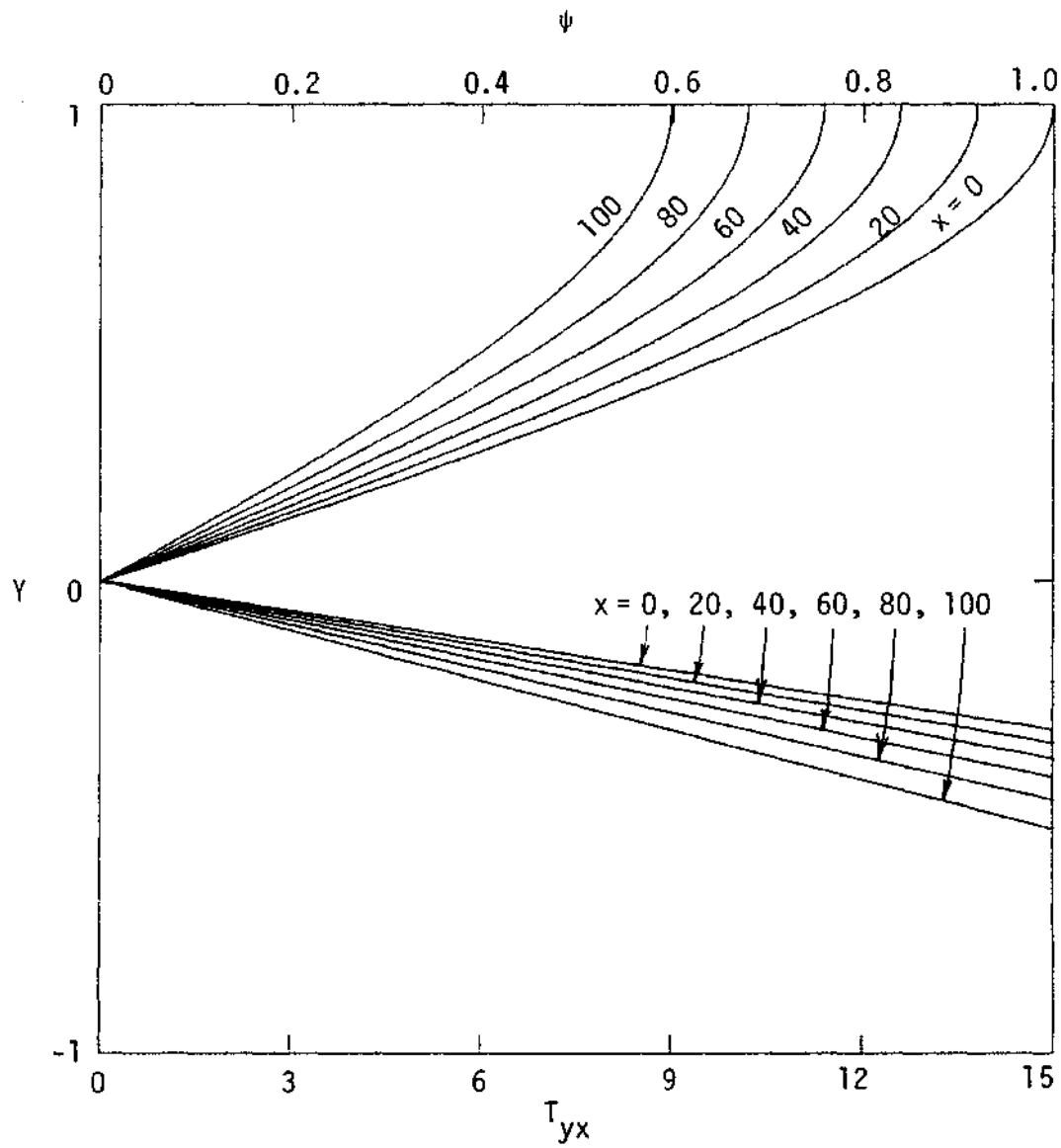


Figure 52. Stream Function (ψ) and Shear Stress (T_{yx}) vs Y .

Newtonian: $H = 0.01$

$$R_x = 0.25$$

$$R_y = 0.00025$$

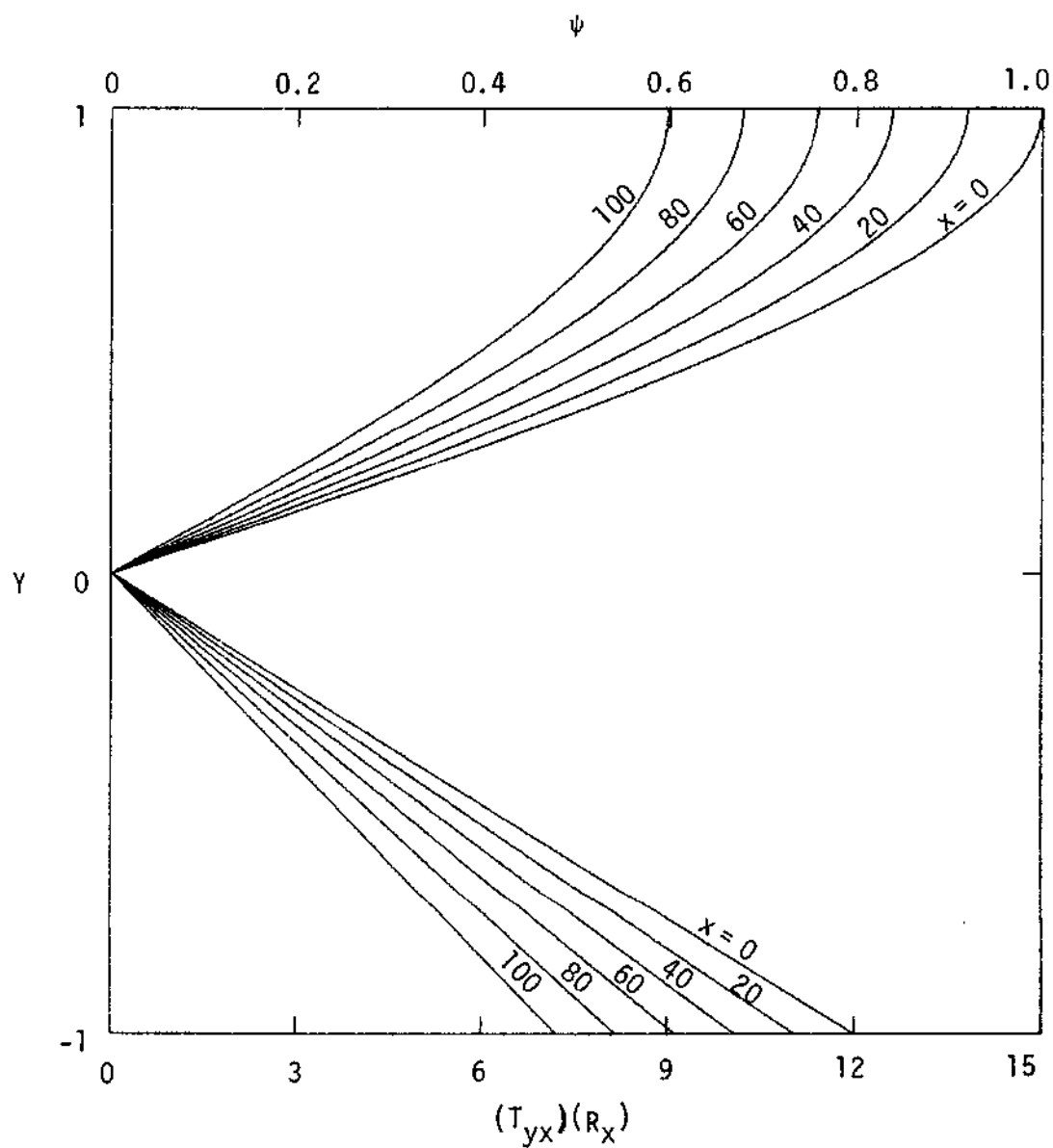


Figure 53. Stream Function (ψ) and Shear Stress $(T_{yx})(R_x)$ vs Y .

Newtonian: $H = 0.01$

$R_x = 0.25$

$R_y = 0.00025$

$$2F^2(\gamma T_{yx}) + D^2 T_{yx} = 0 \quad (4-4)$$

where

$$\begin{aligned} T_{yx} = & -\frac{4}{R_x} \left\{ \frac{4H^2}{k^4} \left(\frac{\tau_0}{R_x} \right) [4(F^2\psi)^2 + (D^2\psi)^2]^{-\frac{1}{2}} \right. \\ & + \frac{4\rho^{\frac{1}{2}}H}{k^2} \left(\frac{\tau_0}{R_x} \right)^{\frac{1}{2}} [4(F^2\psi)^2 + (D^2\psi)^2]^{-\frac{1}{4}} \\ & \left. + 1 \right\} (D^2\psi) \end{aligned} \quad (4-5)$$

$$\text{at } Y = 0, \quad \psi = 0, \quad T_{yx} = 0$$

$$\begin{aligned} \text{at } Y = 1, \quad \psi &= 1 - V_0 X \\ &= 1 - \frac{V_0}{U_0} X \\ &= 1 - \frac{4R_y}{R_x} \end{aligned}$$

From the above equations and boundary conditions it can be observed that if R_x and R_y are kept constant and if the resultant value of the group $(\rho H^2 \tau_0 / k^4)$ remains the same, equations (4-4) and (4-5) should always have the same solution. If (R_y/R_x) and (τ_0/R_x) are kept the same with $(\rho H^2/k^4)$ remaining constant, the value of T_{yx} will change inversely with R_x . These observations are proved numerically and the results are presented in Figures 54 through 59. In Figure 32, Figure 54 and Figure 55 only H and τ_0 have been changed and $(H^2 \tau_0) = 0.000004$

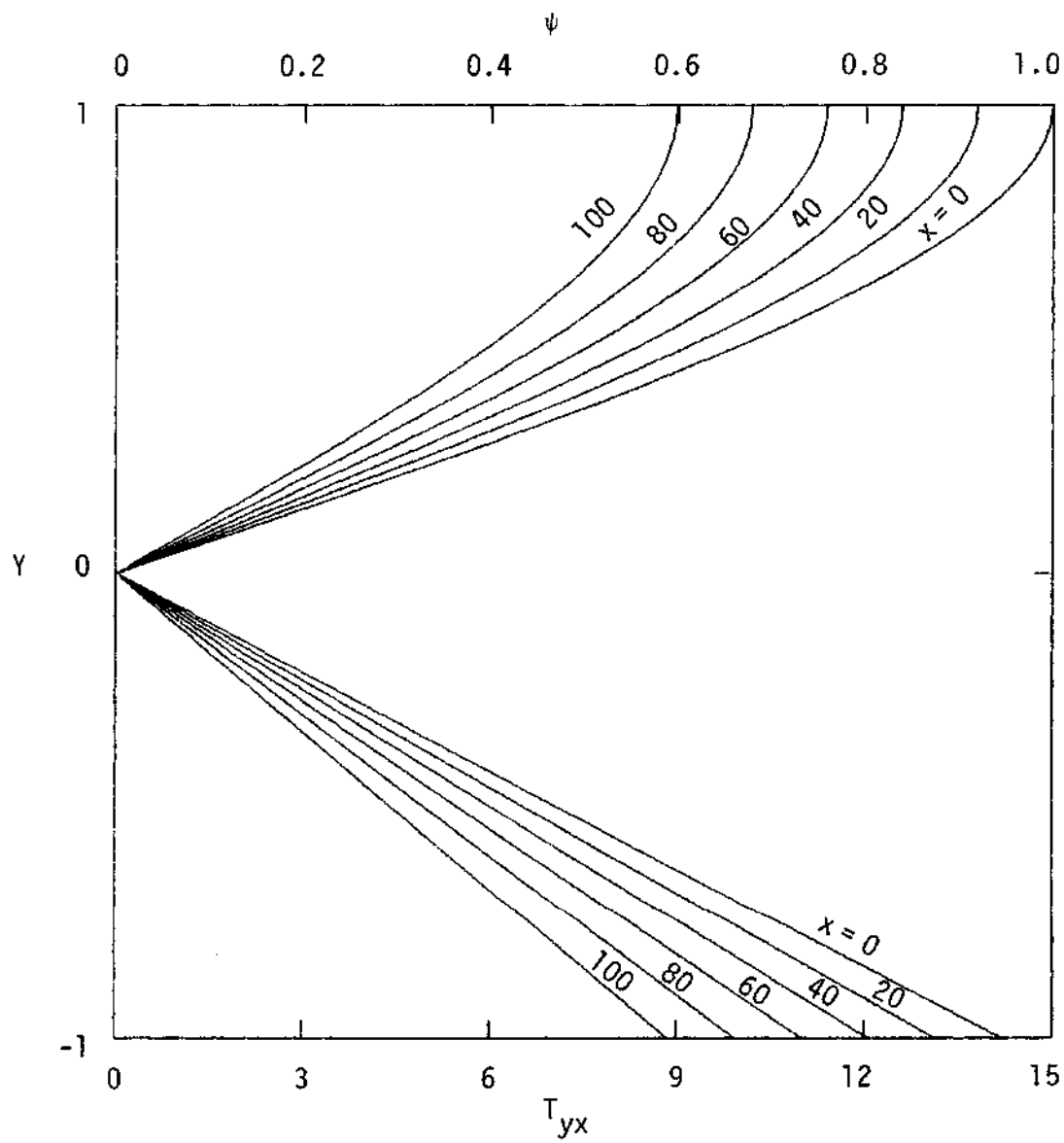


Figure 54. Stream Function (ψ) and Shear Stress (T_{yx}) vs Y .

Cassonian: $H = 0.05$ $\tau_0 = 0.0016$

$R_x = 1.0$ $R_y = 0.001$

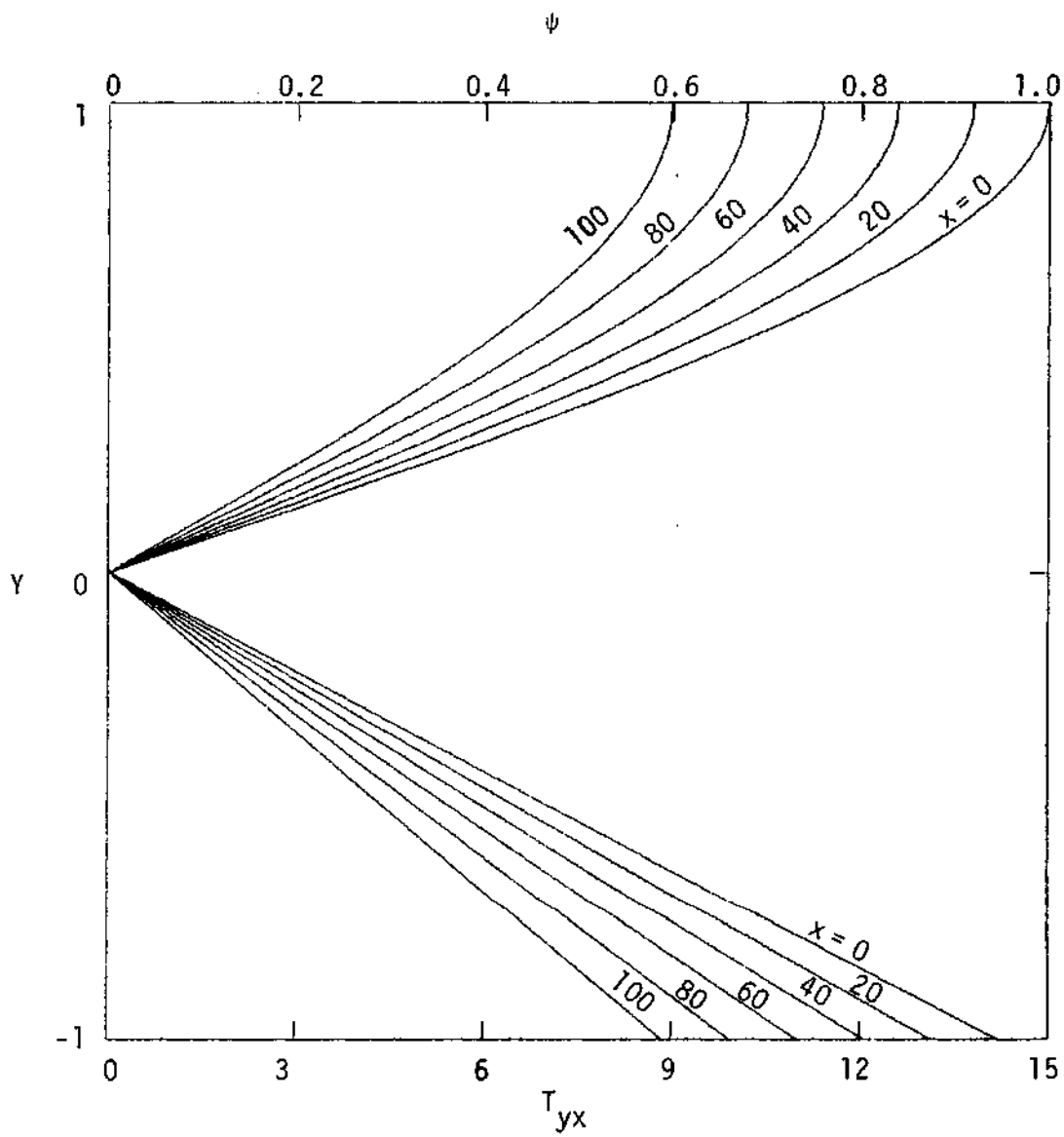


Figure 55. Stream Function (ψ) and Shear Stress (T_{yx}) vs Y .

Cassonian: $H = 0.005$ $\tau_0 = 0.16$
 $R_x = 1.0$ $R_y = 0.001$

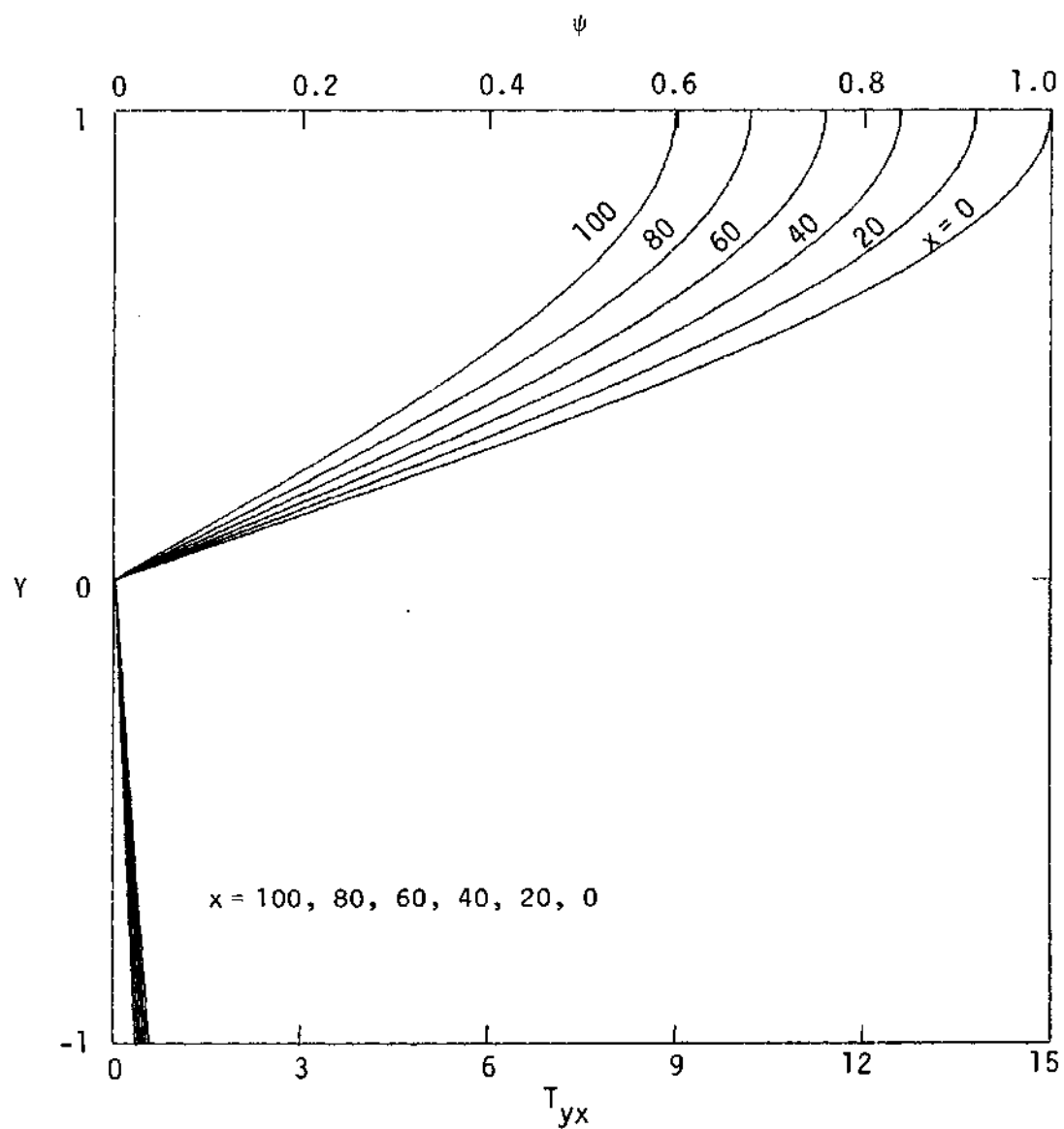


Figure 56. Stream Function (ψ) and Shear Stress (T_{yx}) vs Y .

Cassonian: $H = 0.01$ $\tau_0 = 1.0$
 $R_x = 25$ $R_y = 0.025$

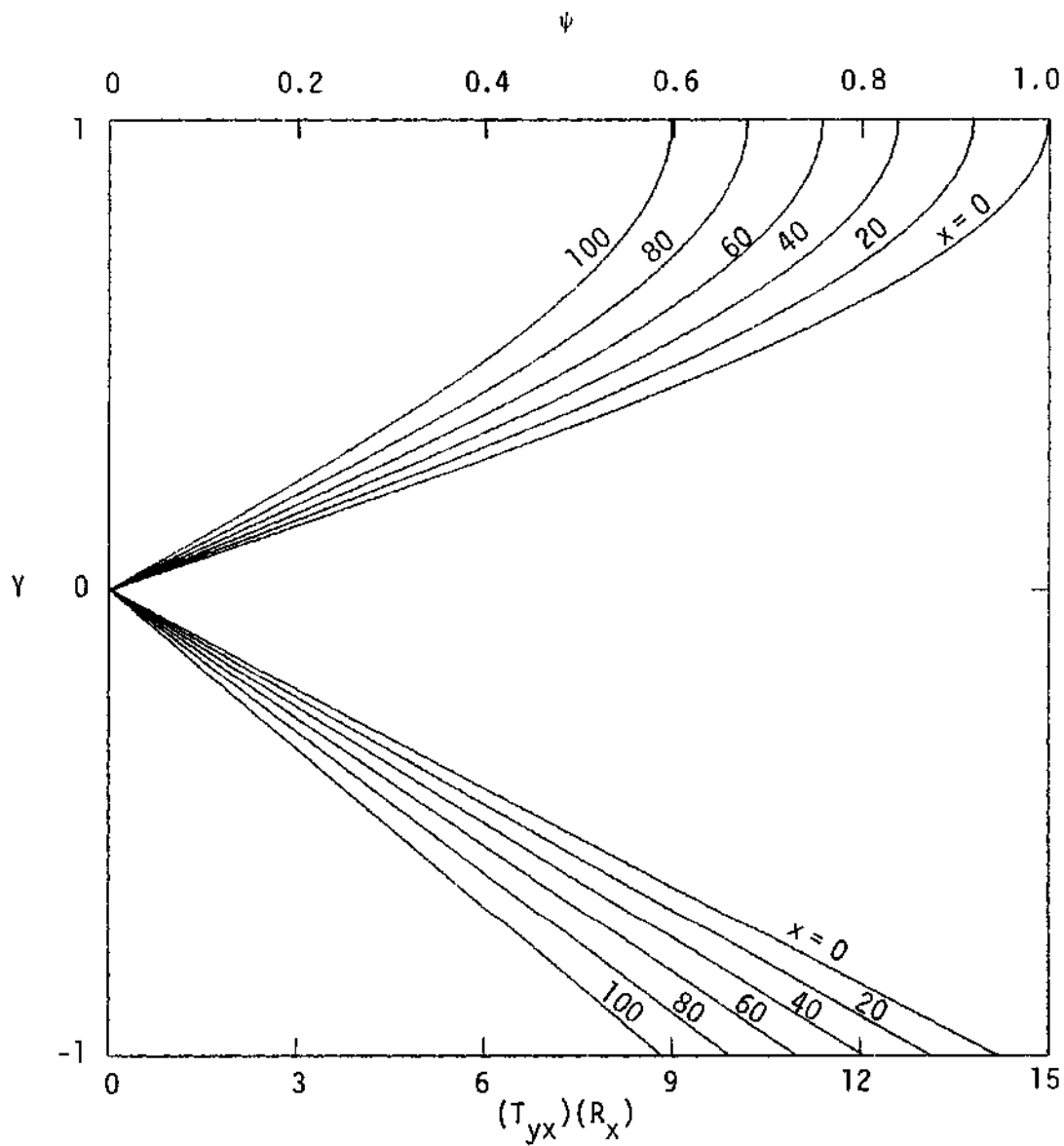


Figure 57. Stream Function (ψ) and Shear Stress $(T_{yx})(R_x)$ vs Y .

Cassonian: $H = 0.01$

$\tau_0 = 1.0$

$R_x = 25.0$

$R_y = 0.025$

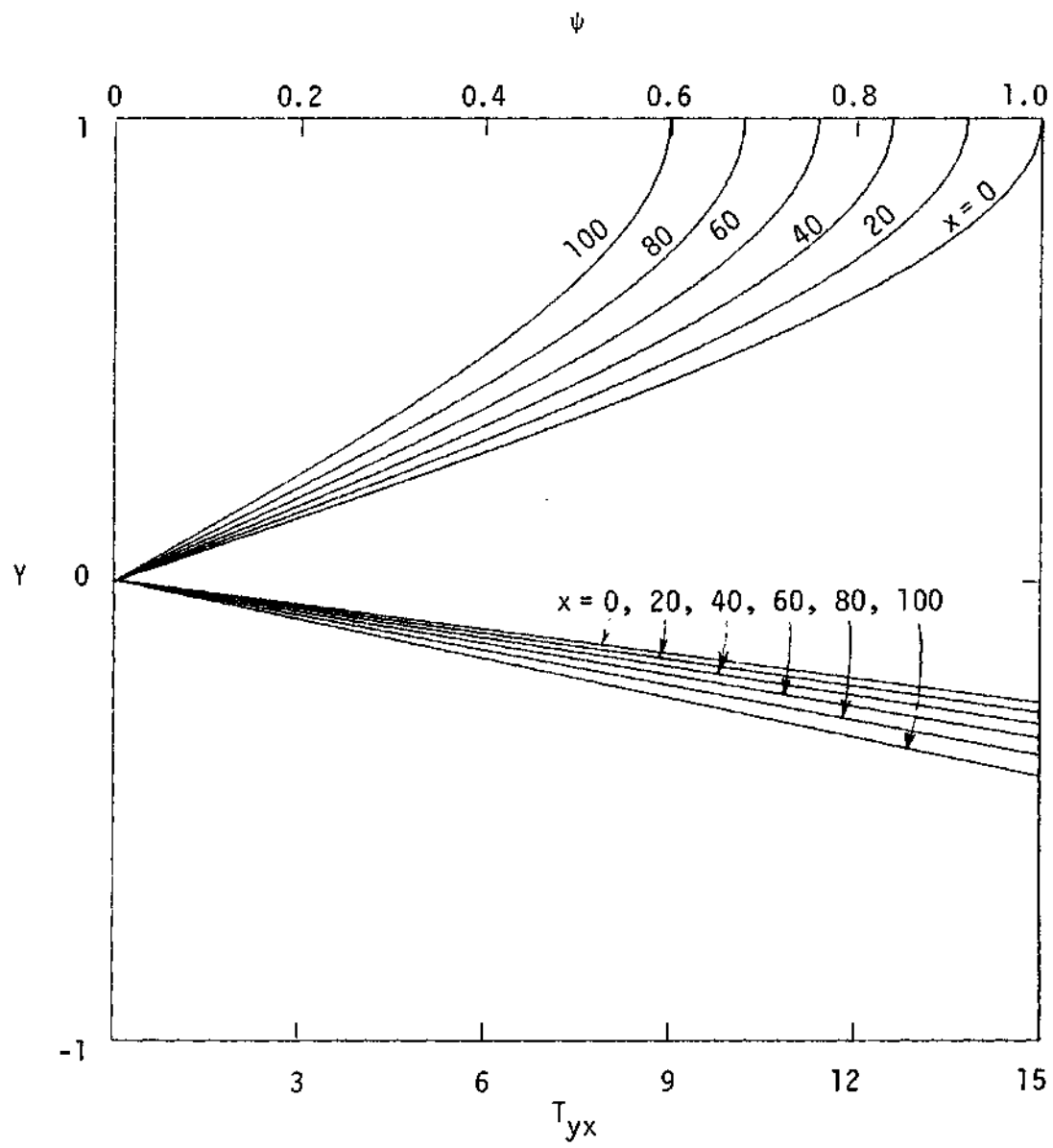


Figure 58. Stream Function (ψ) and Shear Stress (T_{yx}) vs Y .

Cassonian: $H = 0.01$ $\tau_0 = 0.01$
 $R_x = 0.25$ $R_y = 0.00025$

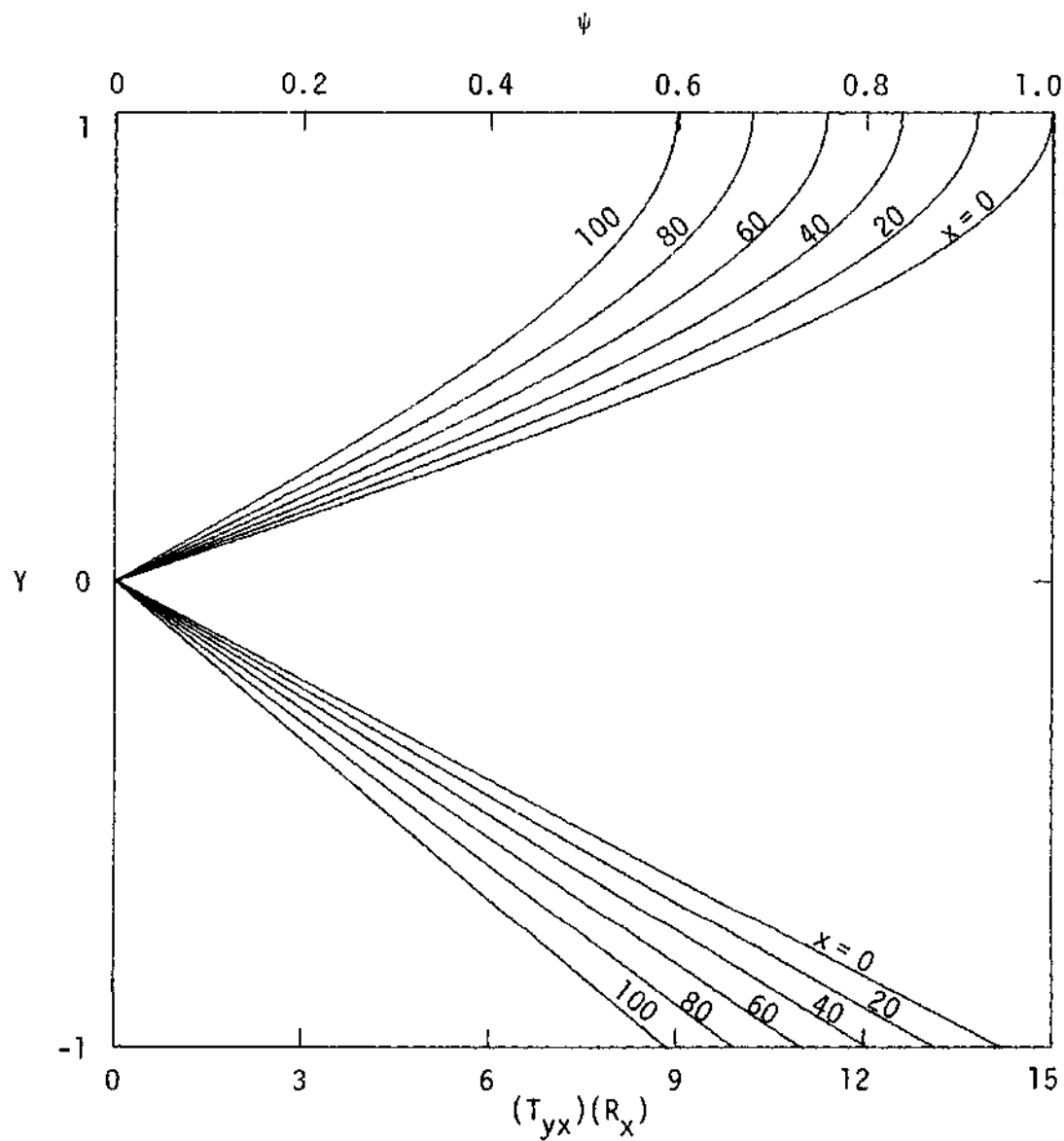


Figure 59. Stream Function (ψ) and Shear Stress $(T_{yx})(R_x)$ vs Y .

Cassonian: $H = 0.01$ $\tau_0 = 0.01$
 $R_x = 0.25$ $R_y = 0.00025$

in all three cases. The plots turn out to be exactly the same. Now compare Figure 32 and Figure 56. The values that are different are τ_0 , R_x and R_y . However the values of the ratio (R_y/R_x) and (τ_0/R_x) remain the same at 0.001 and 40 respectively. The resulting plots have the same stream function values but T_{yx} has much smaller values in Figure 56 than in Figure 32. After multiplying T_{yx} in Figure 57 by R_x as shown in Figure 57, the plot becomes the same as that in Figure 32. In Figure 58, the values of the ratio of (R_y/R_x) and (τ_0/R_x) still remain the same but the values of τ_0 , R_x and R_y are all much smaller than before resulting in large T_{yx} values. After multiplying T_{yx} by R_x as shown in Figure 59, the plot in Figure 59 again becomes the same as that in Figure 32.

The relations derived above can be used to predict the flow behavior at other conditions from the results of a known condition.

CHAPTER V

CONCLUSIONS AND RECOMMENDATIONS

A new method has been developed in this study to solve the two-dimensional Cassonian flow problem between two parallel permeable membranes. The method consists of reducing the four stress components to one stress component and then introducing a stream function in the simplified equation. The results of the numerical solution are (1) the existence of a finite yield stress in the fluid increases the internal stresses and also increases the pressure drop, (2) the increase in wall suction decreases the internal stress and the pressure drop in the x-direction significantly while producing only a slight increase in the pressure drop in the y-direction which is approximately 1/1000 of the magnitude of the pressure drop in the x-direction, (3) the dimensionless stream function ψ and shear stress T_{yx} remain constant with respect to X when there is no wall flux, and decrease with increasing X values when there is a wall suction.

The method developed here is not limited to rectangular coordinates. It can also be applied to cylindrical and spherical coordinates. The correlations between different stress terms can be derived from the equations of continuity. This technique can also be applied to solve two-dimensional flow problems of other non-Newtonian fluids such as Bingham fluids, Ostwald de Waele fluids, etc.

Recommendations for the extension of this study are:

1. Change the constant wall suction rate to variable wall suction rates.

2. Change the geometry from rectangular to cylindrical to simulate blood ultrafiltration in hollow-fiber membranes.

3. Take into consideration the change in fluid rheological properties with the removal of the ultrafiltrate.

A P P E N D I C E S

APPENDIX A

CASSONIAN FLOW BETWEEN TWO PARALLEL
NON-PERMEABLE PLATES

For steady laminar flow of any fluid between two parallel plates, the shear stress equation is

$$\tau_{yx} = \left(\frac{p_0 - p_L}{L} \right) y \quad (\text{A-1})$$

For a Cassonian fluid, the shear stress — shear rate relationship is

$$\tau_{yx} = \tau_0^{1/2} + k \left(- \frac{dv_x}{dy} \right)^{1/2} \quad (\text{A-2})$$

Taking the square root of equation (A-1) gives

$$\tau_{yx}^{1/2} = \left(\frac{p_0 - p_L}{L} \right)^{1/2} y^{1/2} \quad (\text{A-3})$$

Since the flow is symmetrical across the central plane, only the half of the flow field when y is positive is considered. Therefore the negative root has been dropped because τ_{yx} will always be positive when y is positive. Combining equations (A-2) and (A-3) gives

$$\tau_0^{1/2} + k \left(- \frac{dv_x}{dy} \right)^{1/2} = \left(\frac{p_0 - p_L}{L} \right)^{1/2} y^{1/2}$$

Rearranging

$$\left(-\frac{dv_x}{dy}\right)^{1/2} = \frac{1}{k} \left[\left(\frac{p_0 - p_L}{L}\right)^{1/2} y^{1/2} - \tau_0^{1/2} \right]$$

$$-\frac{dv_x}{dy} = \frac{1}{k^2} \left[\left(\frac{p_0 - p_L}{L}\right) y - 2\left(\frac{p_0 - p_L}{L}\right)^{1/2} \tau_0^{1/2} y^{1/2} + \tau_0 \right]$$

Integrating

$$-v_x = \frac{1}{k^2} \left[\left(\frac{p_0 - p_L}{L}\right) \frac{y^2}{2} - \frac{4}{3} \left(\frac{p_0 - p_L}{L}\right)^{1/2} \tau_0^{1/2} y^{3/2} + \tau_0 y \right] + C$$

At $y = H$, $v_x = 0$ $v_x = 0$

$$C = -\frac{1}{k^2} \left[\left(\frac{p_0 - p_L}{L}\right) \frac{H^2}{2} - \frac{4\tau_0^{1/2}}{3} \left(\frac{p_0 - p_L}{L}\right)^{1/2} H^{3/2} + \tau_0 H \right] \quad (\text{A-4})$$

$$v_x = \frac{1}{k^2} \left\{ \frac{H^2}{2} \left(\frac{p_0 - p_L}{L}\right) \left[1 - \left(\frac{y}{H}\right)^2 \right] - \frac{4\tau_0^{1/2}}{3} \left(\frac{p_0 - p_L}{L}\right)^{1/2} H^{3/2} \left[1 - \left(\frac{y}{H}\right)^{3/2} \right] + \tau_0 H \left(1 - \frac{y}{H} \right) \right\} \quad (\text{A-4})$$

$$Q_0 = 2W \int_0^H v_x dy \quad (\text{A-5})$$

$$= \frac{2WH}{k^2} \left[\frac{H^2}{2} \left(\frac{p_0 - p_L}{L}\right) - \frac{4\tau_0^{1/2}}{5} H^{3/2} \left(\frac{p_0 - p_L}{L}\right)^{1/2} + \frac{\tau_0 H}{2} \right]$$

$$= \frac{2WH}{k^2} \left(\frac{H}{2} p_f - \frac{4\tau_0^{1/2}}{5} H^{3/2} p_f^{1/2} + \frac{\tau_0 H}{2} \right)$$

where

$$p_f = \frac{p_0 - p_L}{L} \quad (\text{A-6})$$

Solving equation (A-5) for p_f , we get:

$$p_f = \frac{6}{5} \left(\frac{\tau_0}{H}\right)^{\frac{1}{2}} + \left(\frac{30 \tau_0 k^2}{2WH^3} - \frac{3\tau_0}{50H}\right)^{\frac{1}{2}} \quad (\text{A-7})$$

Equations (A-5) and (A-7) can be written in dimensionless variables as

$$V_x = \frac{1}{K^2} \left[\frac{1}{2} p_f (1 - Y^2) - \frac{4}{3} T_0^{\frac{1}{2}} p_f^{\frac{1}{2}} (1 - Y^{3/2}) + T_0 (1 - Y) \right] \quad (\text{A-8})$$

where

$$p_f = \frac{6}{5} T_0^{\frac{1}{2}} + \left(3K^2 - \frac{3}{50} T_0 \right)^{\frac{1}{2}} \quad (\text{A-9})$$

$$P_f = p_f \left(\frac{H}{\rho U_0^2} \right)$$

$$K^2 = \frac{k^2}{\rho U_0 H}$$

Defining

$$V_x = \frac{\partial \psi}{\partial Y}, \quad V_y = -\frac{\partial \psi}{\partial X}$$

$$\begin{aligned} \psi &= \int V_x dY + C \\ &= \frac{Y}{K^2} \left[\frac{1}{2} P_f \left(1 - \frac{Y^2}{3} \right) - \frac{4}{3} T_0^{\frac{1}{2}} P_f^{\frac{1}{2}} \left(1 - \frac{2}{5} Y^{3/2} \right) \right. \\ &\quad \left. + T_0 \left(1 - \frac{Y}{2} \right) \right] + C \end{aligned}$$

$$\text{At } Y = 0, \quad \psi = 0$$

$$C = 0$$

$$\psi = \frac{Y}{K^2} \left[\frac{1}{2} P_f \left(1 - \frac{Y^2}{3} \right) - \frac{4}{3} T_0^{1/2} P_f^{1/2} \left(1 - \frac{2}{5} Y^{3/2} \right) + T_0 \left(1 - \frac{Y}{2} \right) \right] \quad (\text{A-10})$$

Equation (A-1) can also be written in terms of dimensionless variables as

$$T_{yx} = P_f Y \quad (\text{A-11})$$

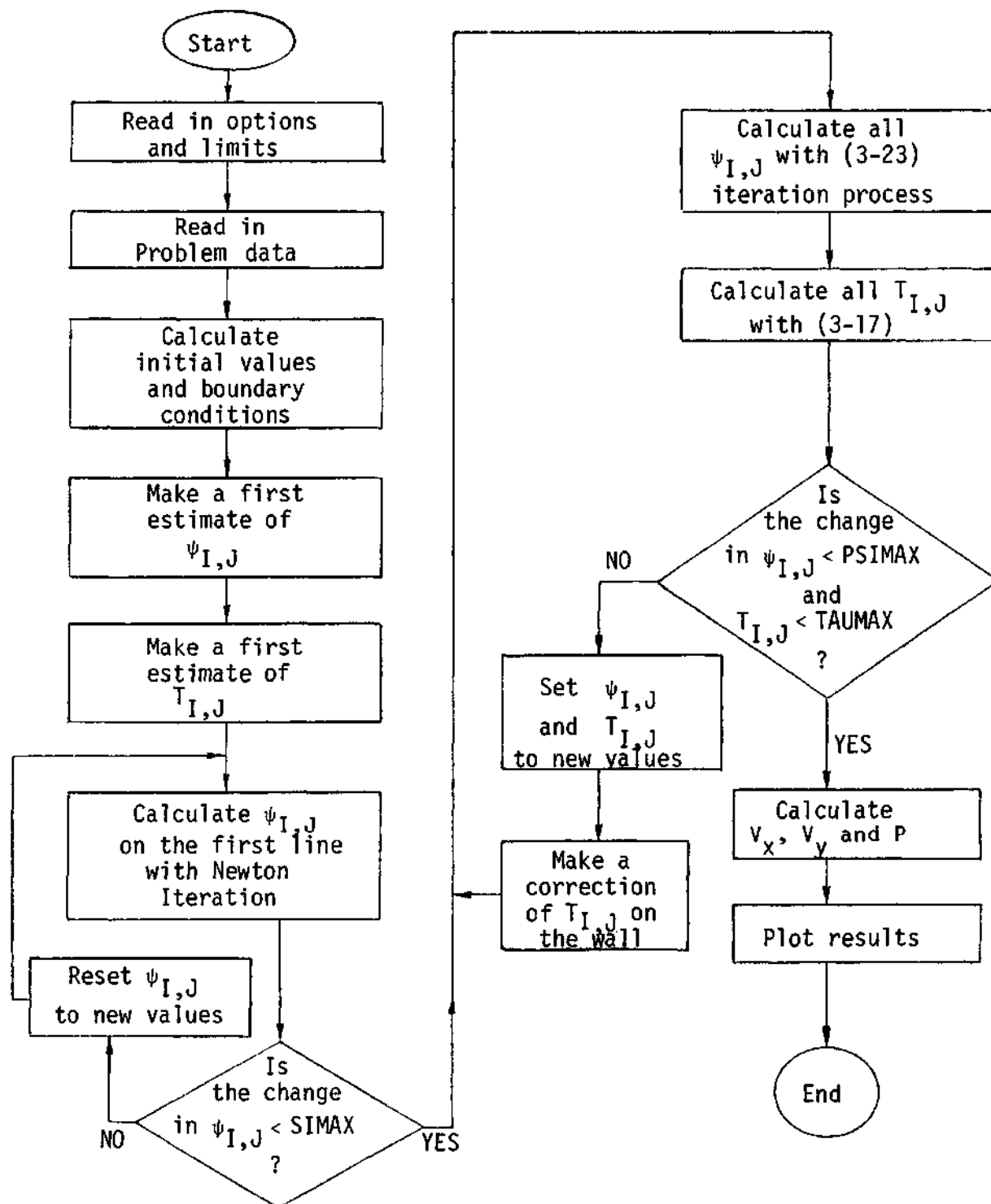
APPENDIX B

COMPUTER PROGRAMS

The computer programs used in this study are presented here together with a simple logic flow diagram of the main program and definitions of some of the more important symbols used. All programs are written in Fortran IV extended language.

<u>Program Symbol</u>	<u>Definition</u>
AN, N	Number of interior grid points in the Y direction.
ALPHA, BETA	Relaxation factors α and β .
AK	Square root of ultimate viscosity coefficient k in Casson equation.
DUMMY	Temporary print out storage.
DY	Step size in Y direction, ΔY .
D2	$D^2\psi, \left(\frac{\partial^2\psi}{\partial Y^2} - \frac{\partial^2\psi}{\partial X^2}\right)$
F	Function used in Newton iteration.
FP	$\frac{\partial F}{\partial \psi_{I+1,J}}$
F2	$F^2\psi, \frac{\partial^2\psi}{\partial X\partial Y}$
GAMMA	$\gamma, F^2\psi/D^2\psi$
GROUP	$4(F^2\psi)^2 + (D^2\psi)^2$.
H	Half distance between the two parallel membranes.
I, J	Grid point subscripts in X- and Y-directions.

L	Number of grids in X-direction.
LOOPM	Maximum number of ψ, τ iteration loops allowed before terminating the run.
MXORLP	Maximum number of loops allowed for the iteration of the first line.
MXSTEP	Maximum number of Newton iteration steps allowed.
P	Fluid pressure factor, P_f .
PSI	Stream function, ψ .
PSIMAX	Convergence criterion for the stream function.
QO	Initial volumetric flowrate, Q_0 .
RENX	Entrance Reynolds number, R_x .
RENY	Wall Reynolds number, R_y .
RHO	Fluid density, ρ .
RV	Dimensionless ultimate viscosity coefficient, K .
S	Grid step size ratio, $\Delta X/\Delta Y$.
SIMAX	Convergence criterion for Newton iteration and False Position iteration.
TAU	Shear stress, T_{yx} .
TAUO	Yield stress of the fluid, τ_0 .
TAUP	Temporarily stored shear stress.
TAUMAX	Convergence criterion for the shear stress.
UO	Average entrance velocity, U_0 .
VO	Wall suction velocity, V_0 .
VX	Velocity component in the X-direction.
VY	Velocity component in the Y-direction.



```

C
C      TWO-DIMENSIONAL CASSONIAN FLOW PROGRAM
C      N. WEI (JULY, 1975)
C
C      DOUBLE PRECISION PSI, TAU, TAU3, F2, D2, PSIN2, PSIN4, PSIP,
1          PSITMP, GROUP, F, FP, PSINN2, PSINN4, PS11,
2          D21, GROUP1, FPSI1, PSI2, D22, GROUP2, FPSI2,
3          PST3, FPSI3, FPSI, GAMMA, TAUP, UO, PF
C      DIMENSION PSI(104,33), TAU(104,33), F2(104,33), TAU3(33),
1          NAME(25), GAMMA(104,33), D2(104,33),
2          YR(33), XR(104), PSTP(104,33), TAUP(104,33),
3          PSINN2(104), PSINN4(104), DUMMY(33)
C
C
C      *****100** READ INPUT INFORMATIONS *****
C      *****READ IN PROBLEM IDENTIFICATION CARD *****
101 READ (5,4001) IEND, (NAME(I), I=1,25)
    IF (IEND .GT. 0) GO TO 103
    WRITE (10,4002)
    WRITE (6,4002)
    WRITE (6,4002)
    WRITE (6,4003)
    WRITE (6,4004)
    GO TO 9999
C
C      ***** READ IN OPTIONS *****
C      103 READ (5,4006) IFTAPE, IFSTEP, ISTEP, INCOLM, INCLIN
C
C      ***** READ IN CONTROL LIMITS *****
C      READ (5,4006) SIMAX, MXSTEP, MXORLP, PSIMAX, TAUMAX, LOOPM
C
C      ***** READ IN PROBLEM DATA *****
C      READ (5,4006) RHO, TAUO, AK, H, RENX, RENY, N, L, S, ALPHA, BETA,
1          LOOPP, LOOPT, ALPHA1, BETA1
C
C      ***** PRINT PROGRAM NAME, PROBLEM NAME, AND INPUT DATA *****
C      WRITE (6,4007)
C      WRITE (6,4002)
C      WRITE (6,4008) (NAME(I), I=1,25)
C      QO = RENX*AK*AK/(2.*RHO)
C      VO = RENY*AK*AK/(H*RHO)
C      UO = QO/(2.*H)
C      WRITE (6,4009) IFTAPE, IFSTEP, ISTEP, INCOLM, INCLIN,
1          SIMAX, MXSTEP, MXORLP, PSIMAX, TAUMAX, LOOPM,
C      WRITE (6,4010) RHO, TAUO, AK, H, QO, VO, RENX, RENY, N, L, S,
1          ALPHA, BETA, LOOPP, LOOPT, ALPHA1, BETA1
C
C      *****200** CALCULATE DIMENSIONLESS VARIABLES *****
C
C      TAUO = TAUO/(RHO*UO*UO)
C      RV = AK/SQRT(RHO*UO*H)
C      VO = VO/UO
C      PF = 1.2*SQRT(TAUO) + SQRT(3.*RV*RV - .06*TAUO)
C      WRITE (6,4045) TAUO, RV, VO, PF, UO

```

```

C
C
C      *****300** CALCULATE INITIAL VALUES *****
C
      L1 = L - 1
      N1 = N + 1
      N2 = N + 2
      N3 = N + 3
      N4 = N + 4
      AN = N
      DY = 1./(AN + 1.)
      DO 310 J = 2, N4
      AJ = J - 2
      Y = DY*AJ
      YR(J) = Y
      PSI(3,J) = Y*(.5*PF*PF*(1. - Y*Y/3.) - 4.*SORT(TAU0)*PF*
1          (1. - .4*Y**1.5)/3. + TAU0*(1. - .5*Y))/(RV*RV)
      TAU3(J) = PF*PF*Y
310 CONTINUE
      PSI(3,1) = - PSI(3,3)
C
C
C      *****400** MAKE A FIRST ESTIMATION OF PSI(I,J) *****
C
      DO 410 I = 1, L
      AI = I - 3
      X = S*DY*AI
      XR(I) = X
      PSI(I,N3) = 1. - V0*X
      DO 410 J = 1, N4
      PSI(I,J) = PSI(3,J)*PSI(I,N3)/PSI(3,N3)
410 CONTINUE
C
C
C      *****500** MAKE A FIRST ESTIMATION OF TAU(I,J) *****
C
      DO 510 I = 2, L1
      F2(I,N3) = (PSI(I+1,N4) + PSI(I-1,N2) - PSI(I+1,N2)
1          - PSI(I-1,N4))/(4.*G*DY*DY)
      D2(I,N3) = (S*S*(PSI(I,N4) + PSI(I,N2)) - 2.*(S*S-1.)*PSI(I,N3)
1          - PSI(I+1,N3) - PSI(I-1,N3))/(S*S*DY*DY)
      GROUP = 4.*F2(I,N3)**2 + D2(I,N3)**2
      IF (GROUP .LT. 1.E-20) GROUP = 1.E-20
      TAU(I,N3) = - (TAU0/SORT(GROUP) + 2.*SORT(TAU0)*RV/GROUP**.25
1          + RV*RV)*D2(I,N3)
      DO 510 J = 2, N3
      TAU(I,J) = TAU3(J)*TAU(I,N3)/TAU3(N3)
510 CONTINUE
      PSIN2 = PSI(4,N2)
      PSIN4 = PSI(4,N4)
C
C
C      *****600** CALCULATE (PSI) ON THE FIRST LINE *****
C
      JORL = 0
      I = 4
602 MARK = 0
      DO 610 J = 3, N2
      JUST = 0
      NSTEP = 0
      MOVE = 1
      SHIFT = 1.
      PSIP(4,J) = PSI(4,J)

```

```

604 PSITMP = PSIP(4,J)
   F2(3,J) = (PSI(4,J+1) + PSI(2,J-1) - PSI(4,J-1)
1         - PSI(2,J+1))/(4.*S*DY*DY)
   D2(3,J) = (S*S*(PSI(3,J+1) + PSI(3,J-1)) - 2.*(S*S-1.)*PSI(3,J)
1         - PSIP(4,J) - PSI(2,J))/(S*S*DY*DY)
   GROUP = 4.*F2(3,J)**2 + D2(3,J)**2

   F = (TAU0/SGRT(GROUP) + 2.*SGRT(TAU0)*RV/GROUP**.25
1     + RV*RV)*D2(3,J) + TAU(3,J)
   FP = (TAU0/GROUP**.5 + SGRT(TAU0)*RV/GROUP**.25)*
1     D2(3,J)**2/(S*S*DY*DY) - (TAU0/SGRT(GROUP)
2     + 2.*SGRT(TAU0)*RV/GROUP**.25 + RV*RV)/(S*S*DY*DY)
   IF (ABS(F) .LT. 15.) GO TO 609
   IF (JUST .EQ. 0) GO TO 605
   WRITE (6,4011) J, JORL, MOVE, NSTEP, PSIP(4,J), F
605 PSIP(4,J) = PSITMP - F/FP
   IF (ABS(PSIP(4,J) - PSITMP) .LT. SIMAX) GO TO 609
   IF (NSTEP .GT. MXSTEP) GO TO 606
   NSTEP = NSTEP + 1
   GO TO 604
606 IF (MOVE .GT. 20) GO TO 607
   MOVE = MOVE + 1
   FN = MOVE/2
   SHIFT = - SHIFT
   PSIP(4,J) = PSI(4,J) + SHIFT*.07*FN*(PSI(3,J) - PSI(4,J))
   NSTEP = 0
   GO TO 604
607 IF (JUST .GT. 0) GO TO 608
   JUST = JUST + 1
   PSIP(4,J) = PSI(4,J)
   MOVE = 1
   SHIFT = 1.
   NSTEP = 0
   GO TO 604
608 WRITE (6,4012) I, J, JORL, PSI(4,J), F
   GO TO 101
609 IF (JORL .GT. LOOP) BETA = BETA1
   PSIP(4,J) = PSI(4,J) + BETA*(PSIP(4,J) - PSI(4,J))
   IF (ABS(PSIP(4,J) - PSI(4,J)) .GT. SIMAX) MARK = MARK + 1
610 CONTINUE
   IF (MARK .EQ. 0) GO TO 621
   IF (JORL .LT. MXORLP) GO TO 612
   WRITE (6,4013) JORL, MARK
   GO TO 101
612 JORL = JORL + 1
   DO 620 J = 3, N2
   PSIP(4,J) = PSIP(4,J)
620 CONTINUE
   GO TO 602
621 DO 625 J = 3, N2
   PSIP(4,J) = PSIP(4,J)
625 CONTINUE
   PSI(4,1) = - PSI(4,3)
   PSI(4,N4) = PSIN4*PSI(4,N2)/PSIN2

```

```

C
C ***** ENTER I: TO BIG LOOP *****
C
C *****700** RELAXATION OF (pSI) *****
C

```

```

      LOOP = 1
701  PSI1 = 0
      TAU1 = 0
      DO 711 I = 4, L1
        I1 = I + 1
        PSINN2(I1) = PSI(I)*N2
        PSINN4(I1) = PSI(I)*N4
      DO 710 J = 3, N2
        JUST = 0
        NSTEP = 1
        MOVE = 0
        PSIP(I1,J) = PSI(I1,J)
7011  PSI1 = PSIP(I1,J)
        F2(I,J) = (PSI(I+1,J+1) + PSI(I-1,J-1) - PSI(I+1,J-1)
          1 - PSI(I-1,J+1))/(4.*S*DY*DY)
        D21 = (S*S*(PSI(I,J+1) + PSI(I,J-1)) - 2.*(S*S - 1.)*PSI(I,J)
          1 - PSI1 - PSI(I-1,J))/(S*S*DY*DY)
        GROUP1 = 4.*F2(I,J)**2 + D21**2
        IF (GROUP1 .LT. 1.E-20) GROUP1 = 1.E-20
        FPSI1 = (TAU0/SQRT(GROUP1) + 2.*SQRT(TAU0)*RV/GROUP1**.25
          1 + RV*RV)*D21 + TAU(I,J)
        IF (ABS(FPSI1) .LT. 1.E-06) GO TO 710
        PSI2 = 0.
702  D22 = (S*S*(PSI(I,J+1) + PSI(I,J-1)) - 2.*(S*S - 1.)*PSI(I,J)
          1 - PSI2 - PSI(I-1,J))/(S*S*DY*DY)
        GROUP2 = 4.*F2(I,J)**2 + D22**2
        IF (GROUP2 .LT. 1.E-20) GROUP2 = 1.E-20
        FPSI2 = (TAU0/SQRT(GROUP2) + 2.*SQRT(TAU0)*RV/GROUP2**.25
          1 + RV*RV)*D22 + TAU(I,J)
        IF (FPSI1*FPSI2 .LT. 0.) GO TO 703
        IF (MOVE .GT. 0) GO TO 7021
        PSI3 = PSI2
        FPSI3 = FPSI2
        PSI2 = 1.
        MOVE = 1
        GO TO 702
7021  FTEST = FPSI3*FPSI3 - FPSI2*FPSI2
        IF (FTEST .GT. 0.) GO TO 703
        PSI2 = PSI3
        FPSI2 = FPSI3
703  PSIP(I1,J) = PSI2 - FPSI2*(PSI2-PSI1)/(FPSI2-FPSI1)
        D2(I,J) = (S*S*(PSI(I,J+1) + PSI(I,J-1)) - 2.*(S*S - 1.)*PSI(I,J)
          1 - PSIP(I1,J) - PSI(I-1,J))/(S*S*DY*DY)
        GROUP = 4.*F2(I,J)**2 + D2(I,J)**2
        IF (GROUP .LT. 1.E-20) GROUP = 1.E-20
        FPSI = (TAU0/SQRT(GROUP) + 2.*SQRT(TAU0)*RV/GROUP**.25
          1 + RV*RV)*D2(I,J) + TAU(I,J)
        IF (JUST .EQ. 0) GO TO 704
        WRITE (6,4011) I1,J, LOOP, NSTEP, PSIP(I1,J), FPSI
704  IF (ABS(PSIP(I1,J) - PSI2) .LT. SIMAX) GO TO 709
        IF (ABS(PSIP(I1,J) - PSI1) .LT. SIMAX) GO TO 709
        IF (FPSI*FPSI2 .LT. 0.) GO TO 705
        IF (FPSI*FPSI1 .GT. 0.) GO TO 705
        PSI2 = PSIP(I1,J)
        FPSI2 = FPSI
        GO TO 706
705  PSI1 = PSI2
        FPSI1 = FPSI2
        PSI2 = PSIP(I1,J)
        FPSI2 = FPSI

```

```

700 IF (NSTEP .GT. MXSTEP) GO TO 707
    NSTEP = NSTEP + 1
    GO TO 703
707 IF (JUST .GT. 0) GO TO 708
    JUST = JUST + 1
    PSIP(I1,J) = PSI(I1,J)
    MOVE = 0
    NSTEP = 1
    GO TO 7011
708 WRITE (6,4012) I1,J, LOOP, PSIP(I1,J), FPSI
    GO TO 101
709 PSIT = PSIT + ABS(PSIP(I1,J) - PSI(I1,J))
710 CONTINUE
711 CONTINUE
    SPSI = 0.
    DO 715 I = 5, L
    SPSI = SPSI + AN*PSI(I,N3)
715 CONTINUE
    PSIT = PSIT/SPSI
    DO 730 I = 4, L1
    I1 = I + 1
    PSIP(I1,2) = 0.
    PSIP(I1,N3) = PSI(I1,N3)
    PSIP(I1,1) = - PSIP(I1,3)
    PSIP(I1,N4) = PSINN4(I1)*PSIP(I1,N2)/PSINN2(I1)
730 CONTINUE

```

C
C
C

```

*****900** RELAXATION OF (TAU) *****

L2 = L - 2
DO 910 I = 2, L1
DO 910 J = 2, N3
F2(I,J) = (PSI(I+1,J+1) + PSI(I-1,J-1) - PSI(I+1,J-1)
           - PSI(I-1,J+1))/(4.*S*DY*DY)
D2(I,J) = (S+S*(PSI(I,J+1) + PSI(I,J-1)) - 2.*(S*S-1.)*PSI(I,J)
           - PSI(I+1,J) - PSI(I-1,J))/(S*S*DY*DY)
IF (ABS(D2(I,J)) .LT. 1.E-20) D2(I,J) = - 1.E-20
GAMMA(I,J) = F2(I,J)/D2(I,J)
910 CONTINUE
DO 920 I = 3, L2
I1 = I + 1
DO 915 J = 3, N2
IF (ABS(D2(I1,J+1)) .LE. 1.E-20) GO TO 913
IF (ABS(D2(I-1,J-1)) .LE. 1.E-20) GO TO 913
IF (ABS(D2(I+1,J-1)) .LE. 1.E-20) GO TO 913
IF (ABS(D2(I-1,J+1)) .LE. 1.E-20) GO TO 913
TAUP(I1,J) = S*S*(TAU(I,J+1) + TAU(I,J-1)) - 2.*(S*S-1)*TAU(I,J)
1           - TAU(I-1,J) - S*(GAMMA(I+1,J+1)*TAU(I+1,J+1)
2           + GAMMA(I-1,J-1)*TAU(I-1,J-1) - GAMMA(I+1,J-1)*
3           TAU(I+1,J-1) - GAMMA(I-1,J+1)*TAU(I-1,J+1))
GO TO 914
913 TAUP(I1,J) = (TAU(I1,J+1) + TAU(I1,J-1))/2.
914 TAUT = TAUT + ABS(TAUP(I1,J) - TAU(I1,J))
915 CONTINUE
TAUP(I1,2) = 0.
TAUP(I1,N3) = TAU(I1,N3)
920 CONTINUE
STAU = 0.
DO 930 I = 4, L1
STAU = STAU + AN*TAU(I,N3)

```

```

930 CONTINUE
    TAUT = TAUT/STAU
    IF (PSIT .LT. PSIMAX .AND. TAUT .LT. TAUMAX) GO TO 982
    IF (LOOP .LT. LOOPM) GO TO 931
    WRITE (6,4014) LOOPM
    GO TO 101
931 IF (LOOP .GT. LOOPM) ALPHA = ALPHA1
    IF (LOOP .GT. LOOPM) BETA = BETA1
    DO 940 I = 4, L1
    I1 = I + 1
    DO 935 J = 3, N2
    PSI(I1,J) = PSI(I1,J) + BETA*(PSIP(I1,J) - PSI(I1,J))
    TAU(I,J) = TAU(I,J) + ALPHA*(TAUP(I,J) - TAU(I,J))
935 CONTINUE
    PSI(I1,1) = PSI(I1,1) + BETA*(PSIP(I1,1) - PSI(I1,1))
    PSI(I1,N4) = PSI(I1,N4) + BETA*(PSIP(I1,N4) - PSI(I1,N4))
940 CONTINUE
C
C
C    *****800** MAKE A FIRST CORRECTION OF (TAU) ON WALL *****
C
    DO 810 I = 4, L1
    F2(I,N3) = (PSI(I+1,N4) + PSI(I-1,N2) - PSI(I+1,N2) - PSI(I-1,N4))
    1 /((4.*S*DY*DY)
    D2(I,N3) = (S*S*(PSI(I,N4) + PSI(I,N2)) - 2.*(S*S-1.)*PSI(I,N3)
    - PSI(I+1,N3) - PSI(I-1,N3))/(S*S*DY*DY)
    1
    GROUP = 4.*F2(I,N3)**2 + D2(I,N3)**2
    IF (GROUP .LT. 1.E-20) GROUP = 1.E-20
    TAU(I,N3) = - (TAUT/SQRT(GROUP) + 2.*SQRT(TAUT)*RV
    1 /GROUP**.25 + RV*RV)*D2(I,N3)
    TAU(I,2) = 0.
810 CONTINUE
C
C
C    ***** END OF WALL (TAU) CORRECTION *****
C
    LAST = 0
    IF (IFSTEP .EQ. 0) GO TO 981
    IF (ISTEP*(LOOP/ISTEP) .NE. LOOP) GO TO 981
    WRITE (6,4020) LOOP
941 DO 945 J = 2, N3
    PSIP(3,J) = PSI(3,J)
    TAUP(3,J) = TAU(3,J)
945 CONTINUE
    PSIP(4,N3) = PSI(4,N3)
    NS = N1/INCOLM + 1
    DO 950 J = 1, NS
    JS = 2 + (J-1)*INCOLM
    DUMMY(J) = YP(JS)
950 CONTINUE
    WRITE (6,4015) (DUMMY(J), J=1,NS)
    DO 980 I = 3, L, INCOLM
    AI = I - 3
    XR(I) = S*DY*AI
    DO 960 J = 1, NS
    JS = 2 + (J-1)*INCOLM
    DUMMY(J) = PSIP(I,JS)
960 CONTINUE
    WRITE (6,4017) XR(I), (DUMMY(J), J=1,NS)
    DO 970 J = 1, NS
    JS = 2 + (J-1)*INCOLM
    DUMMY(J) = TAUP(I,JS)
970 CONTINUE

```

```

WRITE (6,4018) (DUMMY(J), J=1,N5)
980 CONTINUE
IF (IFTAPE .EQ. 3) GO TO 991
WRITE (10,4011) N3, L, S, DY, TAU0, RV, RENX
WRITE (10,4003) (NAME(I), I=1,25)
WRITE (10,4022) (YR(J), J=2,N3)
DO 990 I = 2, L
AI = I - 3
XR(I) = S*DY*AI
WRITE (10,4021) XR(I)
WRITE (10,4044) (PSI (I,J), J=2,N3)
WRITE (10,4022) (TAU (I,J), J=2,N3)
990 CONTINUE
991 IF (LAST .GT. 0) GO TO 101
981 LOOP = LOOP + 1
GO TO 701
982 LAST = 99
WRITE (6,4019)
GO TO 941
C
C ***** FORMAT LIST *****
C
4001 FORMAT (I1, 4X, 15A3, 10A3)
4002 FORMAT (1H0//)
4003 FORMAT (1H0, 48H END OF PROBLEMS, TEAR OFF THIS PAGE, GOOD LUCK. )
4004 FORMAT (1H1)
4006 FORMAT ( )
4007 FORMAT (1H1, 110H TWO DIMENSIONAL CASSONIAN FLOW PROGRAM (II)
JULY, 1975 NAN WEI )
1
4008 FORMAT (1H, 15A3, 10A3)
4009 FORMAT (1H0, 'INPUT DATA (1=YES, 0=NO)'/
1 ' WRITE RESULTS ON TAPE = ', I1/
2 ' LOOP STEP PRINT OUT = ', I1/
3 ' INCREMENTS IN LOOP STEP PRINT OUT = ', I3/
4 ' COLUMN INCREMENTS IN PRINT OUT = ', I3/
5 ' LINE INCREMENTS IN PRINT OUT = ', I3/
6 ' MAX. PSI POINT ITERATIONS = ', 1PE12.6/
7 ' MAX. ITERATION STEPS = ', I3/
8 ' MAX. PSI RELAXATION STEPS ON FIRST LINE = ', I3/
9 ' MAX. PSI TOLERANCE = ', 1PE12.6/
1 ' MAX. TAU TOLERANCE = ', 1PE12.6/
2 ' MAX. PSI-TAU RELAXATION STEPS = ', I4)
4010 FORMAT( ' RHO = ', 1PE12.6/' TAU0 = ', 1PE12.6/' AK = ', 1PE12.6/
1 ' H = ', 1PE12.6/' R0 = ', 1PE12.6/' V0 = ', 1PE12.6/
2 ' RENX = ', 1PE12.6/' RENY = ', 1PE12.6/' N = ', I2/
3 ' L = ', I3/
4 ' S (X/Y GRID RATIO) = ', 0PF8.4/' ALPHA = ', 0PF6.3/
5 ' BETA = ', 0PF6.3/' LOOPP = ', I4/' LOOPT = ', I4/
6 ' ALPHA1 = ', 0PF6.3/' BETA1 = ', 0PF6.3)
4011 FORMAT (1H, 2(I3, 4X), 5(1PE12.6, 3X))
4012 FORMAT (1H0, ' ***** POINT ITERATION FAILED TO CONVERGE ',
1 3(I3, 4X), 2(1PE12.6, 3X))
4013 FORMAT (1H0, 'RELAXATION OF PSI FAILED TO CONVERGE AFTER ',
1 13, ' LOOPS ON THE FIRST LINE AT ', I3, ' POINTS. ')
4014 FORMAT (1H0, 'PSI-TAU SUCCESSIVE RELAXATION FAILED TO CONVERGE ',
1 'AFTER ', I4, ' LOOPS. ')
4015 FORMAT (1H0, '***** Y(J) *****/ 8(3X,1PE12.6))

```

```

4017 FORMAT (1H0, '***** PSI ***** X = ', 1PE12.6/ 8(3X, 1PE12.6))
4018 FORMAT (1H0, '***** TAU *****/ 8(3X, 1PE12.6))
4019 FORMAT (1H1///, 10X, '***** FINAL RESULTS *****')
4020 FORMAT (1H1///, ' LOOP = ', 10)
4021 FORMAT (1H, 1PE12.6)
4022 FORMAT (1H, 3(2X, 1PE12.6))
4044 FORMAT (1H, 4(2X, 1PD20.14))
4045 FORMAT (1H0, 'DIMENSIONLESS QUANTITIES:/'
1      ' TAU0 = ', 1PE12.6/' RV = ', 1PE12.6/' VO = ', 1PE12.6/
2      ' PF = ', 1PE12.6/' U0 = ', 1PE12.6)

C
C      ***** END OF FORMAT LIST *****
C
9999 CONTINUE
      END

C
C      STREAM FUNCTION CHECK OUT PROGRAM
C      N. WEI (APRIL 29, 1975)
C
      DOUBLE PRECISION PSI, FPSI, TPSI, Q
      DIMENSION PSI(104,64), TAU(104,64), TAUP(104,64), NAME(25),
1      Y(64), P(104,33)

C
C      *****100** READ IN DATA CARDS *****
C
101 READ (5,1001) IEND, (NAME(I), I = 1, 25)
      IF (IEND .GT. 0) GO TO 102
      WRITE (6, 1002)
      WRITE (6, 1002)
      WRITE (6, 1003)
      WRITE (6, 1004)
      GO TO 999
102 READ (5, 1007) ISTYPF, IFREAL, RENX, H, RENY, A, TAU0, AK, RHO, S, D,
1      L, N, INCPRT, IPRT1, IFPLOT
      WRITE (6, 1005)
      WRITE (6, 1002)
      WRITE (6, 1006) (NAME(I), I = 1, 25)
      Q = RENX*AK*AK/(2.*RHO)
      VO = RENY*AK*AK/(H*RHO)
      IF (IPRT1 .EQ. 0) GO TO 301
      WRITE (6, 1008) ISTYPE, IFREAL, Q, RENX, H, VO, RENY, A, TAU0,
1      AK, RHO, S, D, L, N, INCPRT, IPRT1, IFPLOT

C
C      *****300** CALCULATE AND PRINT PSI *****
C
301 N4 = N + 4
      N3 = N + 3
      U0 = Q/(2.*H)
      RV = AK/SQRT(RHO*U0*H)
      AN = N
      DY = H/(AN+1.)
      DO 310 J = 2, N4
      AJM = J - 2
      Y(J) = DY*AJM
310 CONTINUE
      DO 330 I = 2, L
      AI = I - 3
      X = S*DY*D*AI

```

```

DO 320 J = 2, N4
  AY = Y(J)
  TPST = FPSI(X, AY, Q, H, VO, A, TAUO, AK, S, I, ITYPE)
  TTAH = FTAU(X, AY, Q, H, VO, A, TAUO, AK, I, ITYPE)
  PSI(I, J) = TPST*2./Q
  TAU(I, J) = TTAU/(RHO*UO*UO)
  IF (ISTYPE .EQ. 2) GO TO 320
  P(I, J) = (VO*(X*X - AY*AY) - Q*X)*1.5*AK*AK/(H**3*RHO*UO*UO)
320 CONTINUE
  PSI(I, 1) = - PSI(I, 3)
330 CONTINUE
  L1 = L - 1
  CY = DY/H
  TAUO = TAUO/(RHO*UO*UO)
  DO 340 I = 2, L1
  DO 340 J = 2, N3
  F2 = (PSI(I+1, J+1) + PSI(I-1, J-1) - PSI(I+1, J-1) - PSI(I-1, J+1))
  1 / (4.*S*CY*CY)
  D2 = (S*S*(PSI(I, J+1) + PSI(I, J-1)) - 2.*(S*S-1.)*PSI(I, J)
  1 - PSI(I+1, J) - PSI(I-1, J))/(S*S*CY*CY)
  GROUP = 4.*F2*F2 + D2*D2
  IF (GROUP .LT. 1.E-20) GROUP = 1.E-20
  TAUP(I, J) = - (TAUO/SQRT(GROUP) + 2.*SQRT(TAUO)*RV/GROUP**.25
  1 + RV*RV)*D2
340 CONTINUE
  YD = H
  PD = 1.
  TD = 1.
  IF (IFREAL .EQ. 0) GO TO 341
  YD = 1.
  PD = Q/2.
  TD = RHO*UO*UO
341 NS = (N + 1)/INCPRT + 1
  DO 345 J = 1, NS
  JS = 2 + (J-1)*INCPRT
  Y(J) = Y(JS)/YD
345 CONTINUE
  DO 350 I = 2, L
  DO 350 J = 1, NS
  JS = 2 + (J-1)*INCPRT
  PSI(I, J) = PSI(I, JS)*Pn
  TAU(I, J) = TAU(I, JS)*Tn
  TAUP(I, J) = TAUP(I, JS)*TD
  P(I, J) = P(I, JS)
350 CONTINUE
  WRITE (6, 1009) IFREAL, (Y(J), J = 1, NS)
  DO 360 I = 2, L
  AI = I - 3
  X = S*DY*D*AI
  IF (IFREAL .EQ. 1) GO TO 353
  X = X/H
353 WRITE (6, 1010) X, (PSI(I, J), J = 1, NS)
  WRITE (6, 1011) (TAU(I, J), J = 1, NS)
  WRITE (6, 1012) (P(I, J), J = 1, NS)
  WRITE (6, 1013) (TAUP(I, J), J = 1, NS)
360 CONTINUE
  IF (IFPLOT .EQ. 0) GO TO 101
  WRITE (9, 4011) N3, L, S, DY, TAUO, RV, RENX
  WRITE (9, 4008) (NAME(I), I=1, 25)
  WRITE (9, 4022) (Y(J), J=1, NS)

```

```

WRITE (10,4011) N3, L, S, DY, TAUO, RV, RENX
WRITE (10,4008) (NAME(I), I=1,25)
WRITE (10,4022) (Y(J), J=1,NS)
DO 990 I = 2, L
  AI = I - 3
  X = S*DY*D*AI/H
  WRITE (9,4021) X
  WRITE (9,4022) (p(I,J), J=1,NS)
  WRITE (10,4021) X
  WRITE (10,4044) (PSI (I,J), J=1,NS)
  WRITE (10,4022) (TAU (I,J), J=1,NS)
990 CONTINUE
C
C ***** FORMAT LIST *****
C
1001 FORMAT (I2, 3X, 15A3, 10A3)
1002 FORMAT (1H0//)
1003 FORVAT (1H0, 'END OF PROBLEMS, TEAR OFF THIS PAGE, GOOD LUCK.')
```

1004 FORMAT (1H1)

1006 FORMAT (1H0, 15A3, 10A3)

1007 FORMAT ()

1008 FORMAT (1H0, 'INPUT DATA (1=YES, 0=NO)'/

1 TYPE OF CALCULATION = ', I1/

2 DIMENSIONAL PSI = ', I1/

3 Q = ', 1PE12.6/ ' RENX = ', 1PE12.6/

4 H = ', 1PE12.6/ ' VO = ', 1PE12.6/

5 RENY = ', 1PE12.6/ ' A = ', 1PE12.6/

6 TAUO = ', 1PE12.6/ ' AK = ', 1PE12.6/ ' RHO = ', 1PE12.6/

7 S = ', 1PE12.6/ ' D = ', 1PE12.6/

8 L = ', I3/ ' N = ', I2/ ' INCPRT = ', I1/

9 IPRT1 = ', I1/ ' IFPLOT = ', I1)

1009 FORMAT (1H0// '** FINAL RESULTS ** (', I1,!)')//

1 SELECTED GRID POINT VALUS Y(J)://

2 8(3X, 1PE12.6))

1010 FORMAT (1H0, '** STREAM FUNCTION **', 5X, 'X = ', 1PE12.6/

1 8(3X, 1PE12.6))

1011 FORMAT (1H0, '** TAU **'/8(3X, 1PE12.6))

1012 FORMAT (1H0, '** P **'/8(3X, 1PE12.6))

1013 FORMAT (1H0, '** TAUP **'/8(3X, 1PE12.6))

4008 FORMAT (1H, 15A3, 10A3)

4011 FORMAT (1H, 2(I3, 4X), 5(1PE12.6, 3X))

4021 FORVAT (1H, 1PE12.6)

4022 FORMAT (1H, 8(2X, 1PE12.6))

4044 FORVAT (1H, 4(2X, 1PD20.14))

C ***** END OF FORMAT LIST *****

GO TO 101

999 CONTINUE

END

FUNCTION FPSI(X,Y,Q,H,VO,A,TAUO,AK,S,ISTYPE)

DOUBLE PRECISION FPSI, Q

C *****200** DECIDE TYPE OF CALCULATION *****

GO TO (201, 202), ISTYPE

C *** 1. NEWTONIAN FLUID WITH CONSTANT WALL FLUX ***

201 FPSI = (.5*Q - VO*X)*(3. - (Y/H)**2)*Y/(2.*H)

GO TO 99

```

C      *** 2. CASSONIAN FLUID WITH NO WALL FLUX ***
202 PF = 1.2*SQRT(TAU0/H) + SQRT(1.5*Q*AK**2/H**3 - .06*TAU0/H)
      IF (Y .LT. 0.) Y = 0.
      FPSI = (Y/AK**2)*(.5*PF**2*(1. - (Y/H)**2/3.)*H**2
1         - 1.333333*SQRT(TAU0)*H**1.5*PF*(1. - 0.4*(Y/H)**1.5)
2         + TAU0*H*(1. - .5*Y/H))
99 RETURN
      END

      FUNCTION FTAU(X,Y,Q,H,VO,A,TAU0,AK,ISTYPE)
      DOUBLE PRECISION Q

C
C      ****400** DECIDE TYPE OF CALCULATION ****
C
      GO TO (401, 402), ISTYPE
C      *** 1. NEWTONIAN, CONSTANT WALL FLUX ***
401 FTAU = (Q/2. - VO*X)*3.*Y*AK**2/H**3
      GO TO 99
C      *** 2. CASSONIAN, NO WALL FLUX ***
402 PF = 1.2*SQRT(TAU0/H) + SQRT(1.5*Q*AK**2/H**3 - .06*TAU0/H)
      FTAU = PF*PF*Y
99 RETURN
      END

C
C      ***** VELOCITY - PRESSURE PROGRAM *****
C
      DOUBLE PRECISION SI
      DIMENSION PSI(104,33), TAU(104,33), TAU0(104,33), VX(104,33),
1         P(104,33), NAME(25), YR(33), XR(104)
      READ (5,4001) ITA E
1 READ (10,4011,END=9) N3, L, S, DY, TAU0, RV, RENX
      IF (N3 .LT. 1) GO TO 99
      READ (10,4008) (N VE(I), I=1,25)
      READ (10,4022) (Y (J), J=2,N3)
      DO 10 I = 2, L
      READ (10,4021) XR(I)
      READ (10,4044) (P(I,J), J=2,N3)
      PSI(I,1) = - PSI(I,3)
      READ (10,4022) (T U(I,J), J=2,N3)
10 CONTINUE
      L1 = L - 1
      N2 = N3 - 1
      N1 = N2 - 1
      DO 20 I = 3, L1
      DO 19 JJ = 2, N3
      J = 2 + N3 - JJ
      F2 = (PSI(I+1,J+1) + PSI(I-1,J-1) - PSI(I+1,J-1) - PSI(I-1,J+1))
1         / (4.*S*DY*DY)
      D2 = (S*S*(PSI(I,J,1) - PSI(I,J-1)) - 2.*(S*S-1.)*PSI(I,J)
1         - PSI(I+1,J) - PSI(I-1,J)) / (S*S*DY*DY)
      GROUP = 4.*F2*F2 + D2*D2
      IF (GROUP .LT. 1.E-20) GROUP = 1.E-20
      TAU(I,J) = - (TAU0/SQRT(GROUP) + 2.*SQRT(TAU0)*RV/GROUP**25
1         + RV.RV)*2.*F2
      IF ((TAU(I,J)**2 + TAU0*TAU0) .LT. TAU0*TAU0) GO TO 18
      VX(I,J) = (PSI(I,J,1) - PSI(I,J-1)) / (2.*DY)
      GO TO 19

```

```

14 VX(I,J) = VX(I,J+1,
19 CONTINUE
20 CONTINUE
   DO 30 I = 3, L1
   VX(I,N3) = 0.
   TAU(I,1) = - TAU(I,3)
   TAUX(I,1) = TAUX(I,3)
   TAUX(I,N3) = 0.
30 CONTINUE
   DO 40 J = 2, N3
   P(3,J) = 0.
40 CONTINUE
   DO 50 I = 4, L1
   DO 50 J = 2, N2
   P(I,J) = P(I-1,J) * (TAUX(I,J) - TAUX(I-1,J))
1     - (TAU(I,J+1) - TAU(I,J-1) + TAU(I-1,J+1) - TAU(I-1,J-1))
2     *5/4.
50 CONTINUE
   TAU(L,N2) = TAU(L-1,N2) - 2.*(TAU(L-2,N2) - TAU(L-1,N2))
   DO 60 I = 4, L1
   P(I,N3) = P(I,N1) * (TAU(I+1,N2) - TAU(I-1,N2))/5
1     + (TAUX(L,N3) - TAUX(I,N1))
60 CONTINUE
   WRITE (6,4023) (N ME(I), I=1,25)
   WRITE (6,4024) (Y (J), J=2,N3)
   DO 70 I = 3, L1
   WRITE (6,4025) XR( ), (VX(I,J), J=2,N3)
   WRITE (6,4026) (P(I,J), J=2,N3)
70 CONTINUE
   IF (ITAPE .EQ. 0) GO TO 1
   WRITE (8,10001) N3, L, S, DY, TAU0, RV, RENX
   WRITE (8,10002) (AME(I), I=1,25)
   WRITE (8,10003) (R(J), J=2,N3)
   DO 80 I = 3, L1
   WRITE (8,10004) X (I)
   WRITE (8,10005) (X(I,J), J=2,N3)
   WRITE (8,10006) (P(I,J), J=2,N3)
80 CONTINUE
   GO TO 1
C ***** FORMAT LIST *****
4001 FORMAT ( )
4006 FORMAT (1X, 15A3, ,0A3)
4011 FORMAT (1X, 2(I3, X), 5(1PE12.6, 3X))
4021 FORMAT (1X, 1PE12.6)
4022 FORMAT (1X, 8(2X, 1PE12.6))
4044 FORMAT (1X, 4(2Y, PD20.14))
4023 FORMAT (1H, 15A3, 10A3)
4024 FORMAT (1H, ***** Y(J) *****/8(2X, 1PE12.6))
4025 FORMAT (1H, ***** VX ***** X = , 1PE12.6/8(2X, 1PE12.6))
4026 FORMAT (1H, ***** P *****/8(2X, 1PE12.6))
10001 FORMAT (1H, 2(I3, 4X), 5(1PE12.6, 3X))
10002 FORMAT (1H, 15A3, 10A3)
10003 FORMAT (1H, 8(2X, 1PE12.6))
10004 FORMAT (1H, 1PE12.6)
C ***** END OF FORMAT LIST *****
99 CONTINUE
   END

```

```

PROGRAM MAIN(INPUT,OUTPUT,CARY,VP1,TAPE5=INPUT,TAPE6=OUTPUT,
1          TAPE10=CARY,TAPE8=VP1)
C
C ***** VELOCITY - PRESSURE PROGRAM *****
C
  DIMENSION PSI(104,33), TAU(104,33), TAUX(104,33), VX(104,33),
1          P(104,33), NAME(25), YR(33), XR(104), VY(104,33)
  READ (5, * ) ITAPE
1  READ (10,4011)          N3, L, S, DY, TAU0, RV, RENX
  IF (N3 .LT. 1) GO TO 99
  READ (10,4002) (NAME(I), I=1,25)
  READ (10,4022) (YR(J), J=2,N3)
  DO 10 I = 2, L
  READ (10,4021) XR(I)
  READ (10,4044) (PSI(I,J), J=2,N3)
  PSI(I,1) = - PSI(I,3)
  READ (10,4022) (TAU(I,J), J=2,N3)
10 CONTINUE
  L1 = L - 1
  N2 = N3 - 1
  N1 = N2 - 1
  DO 20 I = 3, L1
  DO 19 JJ = 2, N3
  J = 2 + N3 - JJ
  VY(I,J) = (PSI(I-1,J) - PSI(I+1,J))/(2.*S*DY)
  F2 = (PSI(I+1,J+1) + PSI(I-1,J-1) - PSI(I+1,J-1) - PSI(I-1,J+1))
1    / (4.*S*DY*DY)
  D2 = (S*S*(PSI(I,J+1) - PSI(I,J-1)) - 2.*(S*S-1.)*PSI(I,J)
1    - PSI(I+1,J) - PSI(I-1,J))/ (S*S*DY*DY)
  GROUP = 4.*F2*F2 + D2*D2
  IF (GROUP .LT. 1.E-20) GROUP = 1.E-20
  TAUX(I,J) = - (TAU0/SQRT(GROUP) + 2.*SQRT(TAU0)*RV/GROUP*.25
1    + RV*RV)*2.*F2
  IF ((TAU(I,J)**2 + TAUX(I,J)**2) .LT. TAU0*TAU0) GO TO 18
  VX(I,J) = (PSI(I,J+1) - PSI(I,J-1))/(2.*DY)
  GO TO 19
19 VX(I,J) = VX(I,J+1)
19 CONTINUE
20 CONTINUE
  DO 30 I = 3, L1
  VX(I,N3) = 0.
  TAU(I,1) = - TAU(I,3)
  TAUX(I,1) = TAUX(I,3)
  TAUX(I,N3) = 0.
30 CONTINUE
  DO 40 J = 2, N3
  P(3,J) = 0.
40 CONTINUE
  DO 50 I = 4, L1
  DO 50 J = 2, N2
  P(I,J) = P(I-1,J) - (TAUX(I,J) - TAUX(I-1,J))
1    - (TAU(I,J+1) - TAU(I,J-1) + TAU(I-1,J+1) - TAU(I-1,J-1))
2    *S/4.
50 CONTINUE
  TAU(L,N2) = TAU(L-2,N2) - 2.*(TAU(L-2,N2) - TAU(L-1,N2))
  DO 60 I = 4, L1
  P(I,N3) = P(I,N1) - (TAU(I+1,N2) - TAU(I-1,N2))/S
1    + (TAUX(I,N3) - TAUX(I,N1))
60 CONTINUE

```

```

WRITE (6,4023) (NAME(I), I=1,25)
WRITE (6,4024) (YR(J), J=2,N3)
DO 70 I = 3, L1
WRITE (6,4025) XR(I), (VX(I,J), J=2,N3)
WRITE (6,4027) (VY(I,J), J=2,N3)
WRITE (6,4026) (P(I,J), J=2,N3)
70 CONTINUE
IF (ITAPE .EQ. 0) GO TO 1
WRITE (8,10001) N3, L, S, DY, TAUO, RV, RENX
WRITE (8,10002) (NAME(I), I=1,25)
WRITE (8,10003) (YR(J), J=2,N3)
DO 80 I = 3, L1
WRITE (8,10004) XR(I)
WRITE (8,10003) (VX(I,J), J=2,N3)
WRITE (8,10003) (VY(I,J), J=2,N3)
WRITE (8,10003) (P(I,J), J=2,N3)
80 CONTINUE
GO TO 1
C ***** FORMAT LIST *****
4000 FORMAT (1X, 15A3, 10A3)
4011 FORMAT (1X, 2(I3, 4X), 5(1PE13.6, 3X))
4021 FORMAT (1X, 1PE13.6)
4022 FORMAT (1X, 8(2X, 1PE13.6))
4044 FORMAT (1X, 4(2X, 1PE21.14))
4023 FORMAT (1H1, 15A3, 10A3)
4024 FORMAT (1H0, "***** Y(J) *****"/8(2X, 1PE13.6))
4025 FORMAT (1H0, "***** VX ***** X = ", 1PE13.6/8(2X, 1PE13.6))
4026 FORMAT (1H0, "***** P *****"/8(2X, 1PE13.6))
4027 FORMAT (1H0, "***** VY *****"/8(2X, 1PE13.6))
10001 FORMAT (1H , 2(I3, 4X), 5(1PE13.6, 3X))
10002 FORMAT (1H , 15A3, 10A3)
10003 FORMAT (1H , 8(2X, 1PE13.6))
10004 FORMAT (1H , 1PE13.6)
C ***** END OF FORMAT LIST *****
99 CONTINUE
END

C ***** GPCP CONTOUR PROGRAM (1) *****
C
C
DOUBLE PRECISION PSI
DIMENSION NAME(25), YR(33), PSI(104,33), TAU(104,33), XR(104)
1 READ(10,4011, END=99) N3, L, S, DY, TAUO, RV
IF (N3 .LT. 1) GO TO 99
DY = 1./(N3-2)
N2 = N3 - 1
READ(10,4008) (NAME(I), I=1,25)
READ(10,4022) (YR(J), J=2,N3)
DO 990 I = 2, L
READ(10,4021) XR(I)
READ(10,4044) (PSI(1,J), J=2,N3)
READ(10,4022) (TAU(1,J), J=2,N3)
990 CONTINUE
WRITE (6,4001) (XR(I), I=3,L)
WRITE (6,4001) (YR(J), J=2,N3)
WRITE (11,10099)
WRITE (11,10001) (NAME(I), I=1,25)
WRITE (11,10008)
WRITE (11,10002) DY

```

```

WRITE (11,10003)
WRITE (11,10014) N2
L1 = 1 - 1
DO 10 J = 2, N3
WRITE (11,10004) (PSI(I,J), I=3,L1)
10 CONTINUE
WRITE (11,10005)
WRITE (11,10006)
WRITE (11,10007)
WRITE (11,10020)
WRITE (11,10021)
WRITE (11,10009)
DY = - DY
LEVT = TAU(3,N3)/8.
TLEV = LEVT
DO 20 J = 2, N3
YR(J) = - YR(J)
20 CONTINUE
WRITE (11,10023)
WRITE (11,10008)
WRITE (11,10024) DY
WRITE (11,10003)
WRITE (11,10014) N2
DO 30 J = 2, N3
WRITE (11,10004) (TAU(I,J), I=3,L1)
30 CONTINUE
WRITE (11,10005)
WRITE (11,10025) TLEV, TLEV, TLEV, TLEV
WRITE (11,10020)
WRITE (11,10021)
WRITE (11,10010)
WRITE (11,10026) (NAME(I), I=1,10)
WRITE (11,10011)
WRITE (11,10012)
WRITE (11,10027)
GO TO 1
4001 FORMAT (1H0, 8(3X, 1PE12.6))
4008 FORMAT (1X, 15A3, 10A3)
4011 FORMAT (1X, 2(I3, 4X), 4(1PE12.6, 3X))
4021 FORMAT (1X, 1PE12.6)
4022 FORMAT (1X, 8(2X, 1PE12.6))
4044 FORMAT (1X, 4(2X, 1PD20.14))
10001 FORMAT ('JOB', 2X, 12A3, 10A3, 2Y, '15.0', 1X, '00')
10002 FORMAT ('SIZE', 1X, '12.50', '0.500', '2.000', '1.000', 5X, '0.000',
1 '1.000', 5X, '100.0', 5X, '0.000', F5.2, 5X, '1.000')
10003 FORMAT ('ARRAY', 1X, '0.000', '0.070', 4X, '2', 4X, '2', 54X, '0')
10004 FORMAT ('ARRAY', 1X, 0PE14.5, 0PF14.5, 0PE14.5, 0PE14.5, 0PE14.5)
10005 FORMAT ('BEND')
10006 FORMAT ('LEVS', 2X, '0.00', 1X, '0.00', 1X, '0.50', 1X, '0.07',
1 2X, '0.0', 2X, '0.0', 2X, '0.0', 2X, '0.0', 4X, '1', 4X,
2 '4', 4X, '2', '0.100', '0.100', 4X, '6', 4X, '1')
10007 FORMAT ('LEVS', 2X, '0.55', 1X, '0.55', 1X, '0.50', 1X, '0.07',
1 2X, '0.0', 2X, '0.0', 2X, '0.0', 2X, '0.0', 4X, '1', 4X,
2 '4', 4X, '2', '0.050', '0.050', 4X, '9', 4X, '1')
10008 FORMAT ('ANGL', 1X, '0.000', '90.00')
10009 FORMAT ('LINE', 5X, '1', '0.000', '1.000', '100.0', '1.000', '0.800',
1 '-0.07', '0.005', 3X, '-2')
10010 FORMAT ('LINE', 5X, '1', '0.000', '-1.00', '100.0', '-1.00', '0.800',
1 '0.070', '0.005', 3X, '-2')
10011 FORMAT ('SYMB', 5X, '1', '-10.0', '0.450', '90.00', 1X, '0.14', 4X,
1 '3', 15X, 'PSI')

```

```

10012 FORMAT ('SYMB',5X,'1','-10.0','-0.55','90.00',1X,'0.14',4X,
1      '3',15X,'TAU')
10014 FORMAT ('ARRAY',5X,'1',2X,'101',4X,'1',3X,I2)
10020 FORMAT ('PLOT')
10021 FORMAT ('QRDR')
10023 FORMAT ('RAS')
10024 FORMAT ('SIZE',1X,'12.50',10.500',2.000',1.000',5X,'0.000',
1      '1.000',5X,'100.0',5X,'0.000',F5.2,5X,'-1.00')
10025 FORMAT ('LEVS',1X,2F5.2,1X,'0.50',1X,'0.07',
1      2X,'0.0',2X,'0.0',2X,'0.0',2X,'0.0',4X,'1',4X,
2      '4',4X,'2',2F5.2,3X,'15',4X,'1')
10026 FORMAT ('SYMB',5X,'1','-10.00','-1.50','90.00',1X,'0.21',
1      3X,'30',15X,'10A3')
10027 FORMAT ('END')
10099 FORMAT ('BXQT GT*GPCP,GPCP')
99 CONTINUE
END

```

```

C
C ***** PLOT (PSI)-(TAU) AT CONSTANT X *****
C
DOUBLE PRECISION PSI
DIMENSION NAME(25), XR(104), YR(33), PSI(104,33), TAU(104,33),
1      IRUF(1400)
CALL PLOTS(IRUF(1),1400,2,30.,00)
CALL PLOT:MX(300.0)
CALL PLOT(2.0,5.5,-3)
1 READ (8,4011,END=999) N3, L, S, DY, TAUO, RV, RENX
IF (N3 .LT. 1) GO TO 999
READ (8,4008) (NAME(I), I=1,12)
READ (8,4022) (YR(J), J=2,N3)
L1 = 1 - 1
DO 10 I = 2, L
READ (8,4021) XR(I)
READ (8,4044) (PSI(I,J), J=2,N3)
READ (8,4022) (TAU(I,J), J=2,N3)
10 CONTINUE
TAUO = TAUO + S*DY*RV*0.
CALL PLOT(0.0, 2.5,3)
CALL PLOT(0.0,-2.5,2)
CALL PLOT(5.0,-2.5,2)
CALL PLOT(5.0, 2.5,2)
CALL PLOT(0.0, 2.5,2)
CALL PLOT(1.0,-2.5,3)
CALL PLOT(1.0,-2.4,2)
CALL PLOT(2.0,-2.5,3)
CALL PLOT(2.0,-2.4,2)
CALL PLOT(3.0,-2.5,3)
CALL PLOT(3.0,-2.4,2)
CALL PLOT(4.0,-2.5,3)
CALL PLOT(4.0,-2.4,2)
CALL PLOT(5.0, 0.0,3)
CALL PLOT(4.9, 0.0,2)
CALL PLOT(4.0, 2.5,3)
CALL PLOT(4.0, 2.4,2)
CALL PLOT(3.0, 2.5,3)
CALL PLOT(3.0, 2.4,2)
CALL PLOT(2.0, 2.5,3)
CALL PLOT(2.0, 2.4,2)

```

```

CALL PLOT(1.0, 2.5, 3)
CALL PLOT(1.0, 2.4, 2)
CALL SYMBOL(2.2, 2.9, 0.14, 3HPSI, 0.0, 3)
CALL SYMBOL(2.2, -3.1, 0.14, 3HTAU, 0.0, 3)
CALL SYMBOL(-.9, -0.1, 0.14, 2HY, 0.0, 2)
CALL SYMBOL(0.0, -4.0, 0.21, 2HVE, 0.0, 3)
DO 15 J = 2, N3
YR(J) = YR(J) * 2.5
15 CONTINUE
DO 40 I = 3, L1, 20
DO 20 J = 2, N3
PSI(I, J) = PSI(I, J) * 5.
20 CONTINUE
CALL PLOT(0.0, 0.0, 3)
DO 30 J = 3, N3
SI = PSI(I, J)
CALL PLOT( SI, YR(J), 2)
30 CONTINUE
40 CONTINUE
DO 50 J = 2, N3
YR(J) = - YR(J)
50 CONTINUE
DO 80 I = 3, L1, 20
DO 60 J = 2, N3
TAU(I, J) = (TAU(I, J) / 3.) * RENX
60 CONTINUE
CALL PLOT(0.0, 0.0, 3)
DO 70 J = 3, N3
CALL PLOT(TAU(I, J), YR(J), 2)
IF (TAU(I, J) .GE. 5.) GO TO 80
70 CONTINUE
80 CONTINUE
CALL PLOT(14.0, 0.0, -3)
GO TO 1
C ***** FORMAT LIST *****
4008 FORMAT (1X, 12A6)
4011 FORMAT (1X, 2(13, 4X), 5(1PE12.6, 3X))
4021 FORMAT (1X, 1PE12.6)
4022 FORMAT (1X, 8(2X, 1PE12.6))
4044 FORMAT (1X, 4(2X, 1PD20.14))
C ***** END OF FORMAT LIST *****
999 CONTINUE
END

C ***** PLOT VELOCITY PROFILES ***** Vx
C
DIMENSION NAME(25), YR(33), VX(104, 33), P(104, 33), IRUF(1400),
1 VP(66), YP(66), XR(104)
CALL PLOTS(IRUF(1), 1400, 2, 30., 50)
CALL PLOTMX(300.0)
CALL PLOT(1.0, 6.0, -3)
1 READ (R, 4011, END=999) N3, L, S, DY, TAU0, RV, RENX
IF (N3 .LT. 1) GO TO 999
READ (R, 4008) (NAME(I), I=1, 12)
READ (R, 4022) (YR(J), J=2, N3)
L1 = 1 - 1
DO 10 I = 3, L1
READ (R, 4021) XR(I)
READ (R, 4022) (VX(I, J), J=2, N3)

```

```

      READ (A,4022) (P(I,J), J=2,N3)
10  CONTINUE
      N1 = N3 - 2
      N4 = N3 + 1
      M2 = N1 + N3
      TAUO = TA,10 + S*DY*RV*0.
      CALL PLOT(0.0, 2.0,3)
      CALL PLOT(0.0,-2.0,2)
      CALL PLOT(6.0,-2.0,2)
      CALL PLOT(6.0, 2.0,2)
      CALL PLOT(0.0, 2.0,2)
      CALL PLOT(0.0, 0.0,3)
      CALL PLOT(0.1, 0.0,2)
      CALL PLOT(2.0,-2.0,3)
      CALL PLOT(2.0,-1.9,2)
      CALL PLOT(4.0,-2.0,3)
      CALL PLOT(4.0,-1.9,2)
      CALL PLOT(6.0, 0.0,3)
      CALL PLOT(5.9, 0.0,2)
      CALL PLOT(4.0, 2.0,3)
      CALL PLOT(4.0, 1.9,2)
      CALL PLOT(2.0, 2.0,3)
      CALL PLOT(2.0, 1.9,2)
      CALL SYMBOL(2.8,-2.8,0.14,PHVX,0.0,2)
      CALL SYMBOL(-.9,-0.1,0.14,PH Y,0.0,2)
      CALL SYMBOL(0.2,-4.5,0.21,NAME,0.0,30)
      DO 50 I = 3, L1, 20
      DO 20 J = 2, N3
      JJ = I + N3 - J
      VP(J) = VX(I,JJ)*4,
      YP(J) = - YR(JJ)*2.
20  CONTINUE
      DO 30 J = N4, M2
      JJ = J - N1
      VP(J) = VX(I,JJ)*4,
      YP(J) = YR(JJ)*2.
30  CONTINUE
      CALL PLOT(VP(2),YP(2),3)
      DO 40 J = 3, M2
      CALL PLOT(VP(J),YP(J),2)
40  CONTINUE
50  CONTINUE
      CALL PLOT(14.0,0.0,-3)
      GO TO 1
C ***** FORMAT LIST *****
4008 FORMAT (1X, 12A6)
4011 FORMAT (1X, 2(I3, 4X), 5(1PE12.6, 3X))
4021 FORMAT (1X, 1PE12.6)
4022 FORMAT (1X, 8(2X, 1PE12.6))
C ***** END OF FORMAT LIST *****
999 CONTINUE
      END

PROGRAM MAIN(INPUT,OUTPUT,VP1,TAPES=INPUT,TAPE6=OUTPUT,TAPE8=VP1)
C ***** FLCT VY PROFILES *****
C
      DIMENSION NAME(25), YR(33), VX(104,33), P(104,33), IBUF(1400),
1 VP(56), YP(56), XR(104), VY(104,33)
      CALL PLOTS(IBUF,512,2,0)

```

```

      CALL FLOTMX(335,3)
      CALL PLOT(1.0,6.0,-3)
1  READ (8,4011)          N3, L, S, DY, TAUO, RV, RENX
      IF (N3 .LT. 1) GO TO 999
      READ (8,4008) (NAME(I), I=1,12)
      READ (8,4022) (YR(J), J=2,N3)
      L1 = L - 1
      DO 10 I = 3, L1
      READ (8,4021) XR(I)
      READ (8,4022) (VX(I,J), J=2,N3)
      READ (8,4022) (VY(I,J), J=2,N3)
      READ (8,4022) (P(I,J), J=2,N3)
2  CONTINUE
      N1 = N3 - 2
      N4 = N3 + 1
      M2 = N1 + N3
      TAUO = TAUO + S*DY*RV*0.
      CALL PLOT(6.0, 2.0,3)
      CALL PLOT(6.0,-2.0,2)
      CALL PLOT(6.0,-2.0,2)
      CALL PLOT(6.0, 2.0,2)
      CALL PLOT(6.0, 2.0,2)
      CALL PLOT(0.0, 0.0,3)
      CALL PLOT(0.0, 0.0,2)
      CALL PLOT(2.0,-2.0,3)
      CALL PLOT(2.0,-1.9,2)
      CALL PLOT(4.0,-2.0,3)
      CALL PLOT(4.0,-1.9,2)
      CALL PLOT(6.0, 3.0,3)
      CALL PLOT(5.9, 3.0,2)
      CALL PLOT(4.0, 2.0,3)
      CALL PLOT(4.0, 1.9,2)
      CALL PLOT(2.0, 2.0,3)
      CALL PLOT(2.0, 1.9,2)
      CALL SYMBCL(2.8,-2.8,0.14,2HVY,0.0,2)
      CALL SYMBCL(-.9,-2.1,0.14,2H Y,0.0,2)
      CALL SYMBCL(0.2,-4.5,0.21,NAME,0.0,30)
      DO 50 I = 3, L1, 20
      DO 20 J = 2, N3
      JJ = 2 + N3 - J
      VP(J) = VY(I, JJ)*1000.
      YP(J) = - YR(JJ)*2.
20  CONTINUE
      DO 30 J = N4, M2
      JJ = J - N1
      VP(J) = VY(I, JJ)*1000.
      YP(J) = YR(JJ)*2.
30  CONTINUE
      CALL PLOT(VP(2), YP(2), 3)
      DO 40 J = 3, M2
      CALL PLOT(VP(J), YP(J), 2)
40  CONTINUE
50  CONTINUE
      CALL PLOT(14.0,0.0,-3)
      GO TO 1
C ***** FORMAT LIST *****
4008 FORMAT (1X, 12A6)
4011 FORMAT (1X, 2(I3, 4X), 5(1PE13.6, 3X))
4021 FORMAT (1X, 1PE13.6)
4022 FORMAT (1X, 8(2X, 1PE13.6))
C ***** END OF FORMAT LIST *****

```

```

999 CONTINUE
  CALL PLOT(14.0,0.0,999)
  END

```

C
C
C

***** PLOT PRESSURE DROP ***** P(X)

```

1 DIMENSION IBUF(1400), NAME(25), XR(104), YR(35), VX(104,35),
  P(104,35), PP(104)
  READ (5,4001) NC1, NC2, NN1, NN2
  CALL PLOTS(IBUF(1),1400,2,30,00)
  CALL PLOTMX(60,0)
  CALL PLOT(1.0,0.0,-3)
  CALL PLOT(0.0,-5.0,2)
  CALL PLOT(8.0,-5.0,2)
  CALL PLOT(8.0, 0.0,2)
  CALL PLOT(0.0, 0.0,2)
  CALL PLOT(0.0,-1.0,3)
  CALL PLOT(0.1,-1.0,2)
  CALL PLOT(0.0,-2.0,3)
  CALL PLOT(0.1,-2.0,2)
  CALL PLOT(0.0,-3.0,3)
  CALL PLOT(0.1,-3.0,2)
  CALL PLOT(0.0,-4.0,3)
  CALL PLOT(0.1,-4.0,2)
  CALL PLOT(1.6,-5.0,3)
  CALL PLOT(1.6,-4.9,2)
  CALL PLOT(3.2,-5.0,3)
  CALL PLOT(3.2,-4.9,2)
  CALL PLOT(4.8,-5.0,3)
  CALL PLOT(4.8,-4.9,2)
  CALL PLOT(6.4,-5.0,3)
  CALL PLOT(6.4,-4.9,2)
  CALL PLOT(8.0,-4.0,3)
  CALL PLOT(7.9,-4.0,2)
  CALL PLOT(8.0,-3.0,3)
  CALL PLOT(7.9,-3.0,2)
  CALL PLOT(8.0,-2.0,3)
  CALL PLOT(7.9,-2.0,2)
  CALL PLOT(8.0,-1.0,3)
  CALL PLOT(7.9,-1.0,2)
  CALL PLOT(6.4, 0.0,3)
  CALL PLOT(6.4,-0.1,2)
  CALL PLOT(4.8, 0.0,3)
  CALL PLOT(4.8,-0.1,2)
  CALL PLOT(3.2, 0.0,3)
  CALL PLOT(3.2,-0.1,2)
  CALL PLOT(1.6, 0.0,3)
  CALL PLOT(1.6,-0.1,2)
  CALL SYMBOL(-0.8,-2.6,0.14,20PF,0.0,2)
  CALL SYMBOL(3.7,-5.8,0.14,3HV/11,0.0,3)
  CALL SYMBOL(1.0,-7.5,0.21,204 AXIAL PRESSURE DROP,0.0,20)
  IF (NC1 .EQ. 0) GO TO 26
  DO 25 K = NC1, NC2
  READ (8,4011,END=999) N3, L, S, DY, TAU0, RV, RENX
  IF (N3 .LT. 1) GO TO 999
  READ (8,4008) (NAME(I), I=1,12)
  READ (8,4022) (YR(J), J=2,N3)

```

```

      L1 = L - 1
      DO 10 I = 3, L1
      READ (8,4021) XR(I)
      READ (8,4022) (VX(I,J), J=2,N3)
      READ (8,4022) (P(I,J), J=2,N3)
10  CONTINUE
      CALL PLOT(0.0,0.0,3)
      DO 20 I = 4, L1
      PP(I) = P(I,2)/300.
      XR(I) = X0(I)/12.5
      CALL PLOT(XR(I),PP(I),2)
20  CONTINUE
      YS = PP(L1)
      CALL SYMBOL(10., YS ,0.07,NA E,0.0,30)
25  CONTINUE
26  IF (NN1 .EQ. 0) GO TO 999
      DO 50 K = NN1, NN2
      READ (9,4011,END=999) N3, L, S, DY, TAU0, RV, RENX
      IF (N3 .LT. 1) GO TO 999
      READ (9,4008) (NAME(I), I=1,12)
      READ (9,4022) (YK(J), J=2,N3)
      L1 = L - 1
      DO 30 I = 2, L
      READ (9,4021) XR(I)
      READ (9,4022) (P(I,J), J=2,N3)
30  CONTINUE
      CALL PLOT(0.0,0.0,3)
      DASH = 1.
      DO 40 I = 4, L1
      PP(I) = P(I,2)/300.
      XR(I) = XP(I)/12.5
      DASH = - DASH
      IF (DASH .GT. 0.) GO TO 39
      CALL PLOT(XR(I), PP(I),2)
      GO TO 40
39  CALL PLOT(XR(I),PP(I),3)
40  CONTINUE
      YS = PP(L1)
      CALL SYMBOL(15., YS ,0.07,NA E,0.0,30)
50  CONTINUE
C ***** FORMAT LIST *****
4001 FORMAT ( )
4008 FORMAT (1X, 12A6)
4011 FORMAT (1Y, 2(13, 4X), 5(1PE12.6, 3X))
4021 FORMAT (1X, 1PE12.6)
4022 FORMAT (1Y, 8(2X, 1PE12.6))
C ***** END OF FORMAT LIST *****
999 CONTINUE
      END

      PROGRAM MAIN(INPUT,OUTPUT,VP1,TAPE5=INPUT,TAPE6=OUTPUT,TAPE8=VP1)
C ***** FLOT P(Y) PROFILES *****
C
      DIMENSION NAME(25), YR(33), VX(104,33), P(104,33), IBUF(1400),
1      VF(66), YP(66), XR(104), VY(104,33)
      CALL FLOTS(IBUF,51,2,0)
      CALL FLOTIX(300.0)
      CALL FLOT(1.0,6.0,-3)

```

```

1 READ (8,4011)          N3, L, S, DY, TAUD, RV, RENX
IF (N3 .LT. 1) GO TO 999
READ (8,4008) (NAME(I), I=1,12)
READ (8,4022) (YR(J), J=2,N3)
L1 = L - 1
DO 10 I = 3, L1
READ (8,4021) XR(I)
READ (8,4022) (VX(I,J), J=2,N3)
READ (8,4022) (VY(I,J), J=2,N3)
READ (8,4022) (P(I,J), J=2,N3)
10 CONTINUE
N1 = N3 - 2
N4 = N3 + 1
M2 = N1 + N3
TAUC = TAUD + S*DY*RV*0.
CALL PLOT(0.0, 2.0,3)
CALL PLOT(0.0,-2.0,2)
CALL PLOT(6.0,-2.0,2)
CALL PLOT(6.0, 2.0,2)
CALL PLOT(0.0, 2.0,2)
CALL PLOT(0.0, 0.0,3)
CALL PLOT(0.0, 0.0,2)
CALL PLOT(2.0,-2.0,3)
CALL PLOT(2.0,-1.9,2)
CALL PLOT(4.0,-2.0,3)
CALL PLOT(4.0,-1.9,2)
CALL PLOT(6.0, 0.0,3)
CALL PLOT(6.0, 0.0,2)
CALL PLOT(4.0, 2.0,3)
CALL PLOT(4.0, 1.9,2)
CALL PLOT(2.0, 2.0,3)
CALL PLOT(2.0, 1.9,2)
CALL SYMBCL(2.8,-2.8,0.14,2H P,0.0,2)
CALL SYMBCL(-.9,-0.1,0.14,2H Y,0.0,2)
CALL SYMBCL(0.2,-4.5,0.21,NAME,0.0,30)
DO 50 I = 1, L1, 20
DO 20 J = 2, N3
JJ = 2 + N3 - J
VP(J) = -P(I,JJ)*4./1000.
YP(J) = - YR(JJ)*2.
20 CONTINUE
DO 30 J = N4, M2
JJ = J - N1
VP(J) = -P(I,JJ)*4./1000.
YP(J) = YR(JJ)*2.
30 CONTINUE
CALL PLOT(VP(2),YP(2),3)
DO 40 J = 3, M2
CALL PLOT(VP(J),YP(J),2)
40 CONTINUE
50 CONTINUE
CALL PLOT(14.0,0.0,-3)
GO TO 1
C ***** FORMAT LIST *****
4008 FORMAT (1X, 12A6)
4011 FORMAT (1X, 2(I3, 4X), 5(1PE13.6, 3X))
4021 FORMAT (1X, 1PE13.6)
4022 FORMAT (1X, 2(2X, 1PE13.6))
C ***** END OF FORMAT LIST *****
999 CONTINUE
CALL PLOT(14.0,0.0,999)
END

```

BIBLIOGRAPHY

1. E. F. Leonard and R. L. Dedrick, "The Artificial Kidney: Problems and Approaches for the Chemical Engineer," AICHE Symposium Series, 64, 15 (1968).
2. W. J. Kolff and H. T. J. Berk, "The Artificial Kidney: A Dialyser with a Great Area," Acta Med. Scand., 117, 121 (1944).
3. R. H. Scribner, W. Quinton and D. Dillard, "Cannulation of Blood Vessels for Prolonged Hemodialysis," Trans. Amer. Soc. Artif. Int. Organs, 6, 104 (1960).
4. A. L. Babb and L. Grimsrud, "A New Concept in Hmodialyzer Membrane Support," ibid, 10, 31 (1964).
5. W. G. Esmond, et al., "Compact Autoclavable Counter-current Hemodialyser with Disposable Components," Biomedical Sci. Instrum., 1, 363 (1963).
6. R. D. Stewart, E. D. Baretta, J. C. Cerney and H. I. Mahon, "An Artificial Kidney Made from Capillary Fibers," Invest. Urol., 3, 614 (1966).
7. P. D. Oja, et al., "The Hollow Fiber Artificial Kidney," Trans. Amer. Soc. Artif. Int. Organs, 13, 200 (1967).
8. L. W. Henderson, A. Besarab and L. W. Bluemle, Jr., "Blood Purification by Ultrafiltration and Fluid Replacement (Diafiltration)," ibid, 12, 216 (1967).
9. L. W. Henderson, et al., "Uremic Blood Cleansing by Diafiltration Using a Hollow Fiber Ultrafilter," ibid, 16, 107 (1970).
10. L. W. Henderson, et al., "Clinical Experience with Intermittent Hemodiafiltration," ibid, 19, 119 (1973).
11. H. I. Bixler, L. M. Nelson and L. W. Bluemle, Jr., "The Development of a Diafiltration System for Blood Purification," ibid, 14, 99 (1968).
12. W. Dorson and M. Markovitz, "A Pulsating Ultrafiltration Artificial Kidney," AICHE Symposium Series, 64, 85 (1968).
13. W. J. Kolff and J. R. Leonard, "Reduction of Otherwise Intractable Edema by Dialysis or Filtration," Cleveland Clin. Quart., 20, 61 (1959).

14. R. L. Barenberg and J. E. Kiley, "Effect of Ultrafiltration on Artificial Kidney Kinetics," Trans. Amer. Soc. Artif. Int. Organs, 7, 9 (1961).
15. L. W. Henderson, C. K. Colton and C. A. Ford, "Kinetics of Hemodiafiltration," J. Lab. Clin. Med., 85, 372 (1975).
16. E. W. Merrill, et al., "Rheology of Human Blood Near and at Zero Flow, Effect of Temp. and Hematocrit Level," Biophys. J., 3, 199 (1963).
17. N. Casson, Rheology of Disperse Systems, (C. C. Mill, editor), London, Pergamon Press, Chapter 5 (1959).
18. H. L. Goldsmith, "Red Cells and Rouleaux in Shear Flow," Science, 153, 1406 (1966).
19. E. W. Merrill, et al., "Rheology of Human Blood, Near and at Zero Flow," Biophys. J., 3, 199 (1963).
20. E. W. Merrill, W. G. Margetts, G. R. Cokelet and E. R. Gilliland, "The Casson Equation and Rheology of Blood Near Zero Shear," Symp. Biorheol., (A. P. Copley, ed.), 135 (1965).
21. A. W. Rahn, C. Tien and L. C. Cerny, "Flow Properties of Blood Under Low Shear Rate," Chemical Engineering in Medicine and Biology, (Daniel Hershey, ed), Plenum Press, N. Y., 45 (1967).
22. E. W. Merrill, "Rheology of Blood," Physiol. Rev., 4, 863 (1969).
23. E. N. Lightfoot, Transport Phenomena and Living System, John Wiley and Sons, New York (1974).
24. E. W. Merrill, et al., "Pressure Flow Relations of Human Blood in Hollow Fibers at Low Flow Rates," J. Appl. Physiol., 20, 954 (1965).
25. L. Grimsrud, and A. L. Babb, "Velocity and Concentration Profiles for Laminar Flow of a Newtonian Fluid in a Dialyzer," AICHE Symposium Series, 62, 20 (1965).
26. A. L. Babb, L. Grimsrud, R. L. Bell and S. B. Layne, "Engineering Aspect of Artificial Kidney Systems," Chemical Engineering in Medicine and Biology, (Daniel Hersley, ed), Plenum Press, NY (1967) p. 45.
27. J. M. Kooijman, "Laminar Heat or Mass Transfer in Rectangular Channels and in Cylindrical Tubes for Fully Developed Flow: Comparison of Solutions Obtained for Various Boundary Conditions," Chem. Eng. Sci., 28, 1149 (1973).

28. J. Aroesty, "Analysis of Pulsatile Flow in Small Blood Vessels—Casson Model," IEEE, Proc. 23rd Annu. Conf. Eng. Med. Biol., 12, 18 (1970).
29. J. M. Kooijman, and D. C. Van Zanten, "The Flow of a Cassonian Fluid through Parallel Plate Channels and through Cylindrical Tubes," Chem. Eng. J., 4, 187 (1972).
30. W. Shay, D. Schultz and V. L. Shah, "Diffusion of Oxygen Through Blood Flowing in a Porous Capillary Tube," Lett. Heat and Mass Trans., 2, 237 (1975).
31. F. M. White, Jr., B. F. Barfield and M. J. Goglia, "Laminar Flow in a Uniformly Porous Channel," J. Appl. Mech., 25, 613 (1958).
32. R. M. Terrill, and P. W. Thomas, "On Laminar Flow through a Uniformly Porous Pipe," Appl. Sci. Res., 21, 37 (1969).
33. A. A. Kozinsky, F. P. Schmidt and E. N. Lightfoot, "Velocity Profiles in Porous-Walled Ducts." Ind. Eng. Chem. Fundam., 9, No. 3, 502 (1970).
34. S. Oka, "Present Status of Hemorheological Theory," Biorheology, 12, 157 (1975).
35. K. Hohenemser, and W. Prager, "Über die Ansätze der Mechanik isotroper Kontinua," z. angew. Math. Mech., 12, 216 (1932).
36. R. B. Bird, W. E. Stewart and E. N. Lightfoot, Transport Phenomena, Wiley, New York, p. 101 (1960).
37. A. S. Popel, S. A. Regierer and P. I. Usick, "A Continuum Model of Blood Flow," Biorheology, 11, 427 (1974).
38. A. A. Kozinski, F. P. Schmidt and E. N. Lightfoot, "Velocity Profiles in Porous-Walled Ducts," Ind. Eng. Chem. Fundam., 9, No. 3, 502 (1970).
39. L. Lapidus, Digital Computation for Chemical Engineers, McGraw-Hill, New York (1962).
40. H. S. Mickley, T. K. Sherwood, C. E. Reed, Applied Mathematics in Chemical Engineering, McGraw-Hill, New York (1957).
41. S. D. Conte, Elementary Numerical Analysis, McGraw-Hill, New York (1965).
42. B. Carnahan, H. A. Luther, J. O. Wilkes, Applied Numerical Methods, John Wiley & Sons, Inc. (1969).
43. "General Purpose Contouring Program," by California Computer Products, Inc., Revised (1973).

VITA

Nan Wei was born on July 29, 1939, in Hupeh, China. His family moved to Taiwan in 1949. He graduated from Chien Kuo High School at Taipei, Taiwan in 1957. He received a Bachelor of Science degree in Chemical Engineering from Cheng Kung University at Tainan, Taiwan in 1961.

He received a Master of Science degree in Chemical Engineering from the Georgia Institute of Technology in 1965. He worked as a research chemical engineer with Swift and Company, Phosphate Center at Bartow, Florida from April 1965 to May 1966. Then he worked at the Research Center of United Gas Corporation in Shreveport, Louisiana from May 1966 to September 1967.

He came back to Georgia Tech in September 1967 and worked on fertilizer research projects for two and a half years before he changed to ultrafiltration work due to a shift of interest. He was employed as a research assistant or a teaching assistant most of the time during his graduate study. He was also a part-time chemical engineer with Vinings Chemical Company where he was involved in equipment design, plant design and start-up activities.

He is an associate member of AIChE and a member of ACS.